ADDIS ABABA UNIVERSITY
SCHOOL OF GRADUATE STUDIES
FACULTY OF TECHNOLOGY
DEPARTMENT OF
ELECTRICAL AND COMPUTER ENGINEERING

INVESTIGATION AND ANALYSIS OF ASHEGODA WIND FARM INTEGRATION IMPACT ON ETHIOPIAN GRID

A thesis submitted to the school of graduate studies of Addis Ababa University
in partial fulfillment of the requirements for the degree of
Masters of Science in Electrical Engineering (Electrical Power Engineering)

By
Hiwot Eshetu

Advisors: Dr-Ing. Getachew Biru
Dr-Ing. Fekadu Shewarega

Oct 2010

ADDIS ABABA UNIVERSITY

SCHOOL OF GRADUATE STUDIES

"INVESTIGATION AND ANALYSIS OF ASHEGODA WIND FARM INTEGRATION IMPACT ON ETHIOPIAN GRID"

By

Hiwot Eshetu

FACULTY OF TECHNOLOGY

APPROVAL BY BOARD OF EXAMINERS

Dr .- Ing Getahun Mekuria	_____
Chairman, Department of Graduate Committee	Signature
__Dr.- Ing Getachew Biru___	_____
Advisor	Signature
__ Prof. Woldeghiorgis W/ Mariam__	_____
Internal Examiner	Signature
_____Prof. N.P Singh_____	_____
External Examiner	Signature

Abstract

Ethiopian electric power corporation is under implementation stage to integrate wind power to exiting grid system which contains mainly hydro generators.

Integration of wind power plant with grid system has many challenges that need to be studied thoroughly to identify major problems. The major problems induced by the wind farm depend on level of penetration.

In this thesis work operational impacts associated with "Ashegoda Wind Farm (AWF)" integration has been studied, mainly variability, predictability and steady state stability impacts. The variability and predictability impacts have been studied using statistical method on the basis of data supplied from wind project office of "Ethiopian Electric Power Corporations".

Ashegoda wind farm increases the variability of the system load characteristics in case of hourly and thirty minute load. As per the result of the stability study, there is a steady state voltage stability impact under contingency cases. However, in base case, there is no any stability impact. Along with the stability analysis, one of possible solutions, that is, managing the transmission line capacity have been suggested and discussed.

In addition to variability impact, predictability impact also studied by developing a wind power forecasting model. Different models have been developed and the one with best forecast accuracy selected on the basis of MAE and compared with persistence model considering as a base model.

Key words: integration,Variability, forecasting, stability, modeling, frequency distribution, Variable speed, Ancillary service.

Acknowledgement

I express my sincere gratitude towards my supervisors Dr Getachew Biru and Dr Fikadu Shewarega for their continual support and enthusiasm for preparing this thesis work.

I would like to thank my colleagues who are working in Ethiopian electric power corporation for their support specially members of power system department allowing me to use PSS/E simulation software and providing and wind project office for providing the necessary data.

Contents

List of Figures

List of Tables

List of Abbreviations

ACF	Autocorrelation function
AR(p)	Autoregressive order p
ARMA (p,q)	Autoregressive moving average
ASWF	Ashegoda wind farm
CFD	Cumulative frequency distribution
EEPCO	Ethiopian electric power corporation
MA(q)	Moving average order q
MAE	Mean absolute error
MD	Mean deviation
PACF	Partial autocorrelation function
PCC	Point of common coupling
PMAE	Percentage means absolute error
PSS/E	Power system simulator for engineer software
PV	Active power transfer against voltage
QV	Reactive power transfer against voltage
RACF	Residual autocorrelation function
RPACF	Residual partial autocorrelation function
SARMA	Seasonal autoregressive moving average
SIL	Surge impedance loading
SPSS	Statistical packaging software for statics
SS	Skill score factor
SSE	Sum of squared error
STR	Single turbine representation

List of Symbols

B	Back shift operator
B_{tot}	Equivalence shunt impedance
C	Scale factor
E_D	Energy density
K	Shape factor
M_D	Mean deviation
$P_L(V)$	Active power load
$Q_L(V)$	Reactive power load
Z_{TS}	Equivalent pad mounted transformer impedance
Z_T	Equivalent collector impedance
r_k	Autocorrelation coefficient at lag k
V_m	Means wind speed
Y_k	Sample data taken at lag k
θ_k	Autoregressive coefficient at lag k
σ_V	Standard deviation
σ^2	Variance
$\emptyset_k$	Auto regressive moving average coefficient at lag k

Chapter 1. Introduction

1.1. Background

A rapid growth in energy demand has increased the available options of energy producing methods in electric industry. As an electric utility company, maintaining supply and demand balance is necessary that need exploiting available energy resources efficiently.

Renewable energies are one of energy sources that have been taped with an increasing trend these days. Wind power has become one of the main renewable energy resources that have been integrated with existing grid system in large scale using suitable technologies.

Currently federal government of Ethiopia has developed policy and strategy aimed at production of electric energy from wind and solar.

Ethiopian electric power corporation (EEPCO) is in charge of studying, building and operating all electric power plants in Ethiopia. EEPCO grid system is highly dependent on electric power generation from hydropower which is affected by rainfalls variation from year to year.

To fulfill demand growth, EEPCO tries at its best to increase power generation capacity of the country by mixing generation from wind power. Ethiopia has a total capacity of ten thousand mega watt from wind generation only. Due to promising wind resource at northern and central parts of the country around Mekele and Nazareth construction of wind farms have already begun. When the projects finalized they can generate more than 200MW.

1.2. Problem Formulations.

Ashegoda wind farm (AWF) is one of the wind farm that is constructed and being operational in two years period. Currently the project is under implementation stage and completed in three phases. The first phase of the project has a capacity of 30 MW, second and third phases have a capacity of 45 MW each.

The project includes the prefeasibility study, manufacturing and construction. However, the project doesn't include impact study on EEPCO's grid when it is operational.

1.3. Objectives

The aim of this thesis work is making impact study, particularly operational impact, due to variability nature of wind power output, predictability and stability impacts and seeing alternative solutions to make integration smooth when it is operational.

The statistical analysis is used for studying the predictability and variability impact. The steady state impacts are studied using voltage stability impacts. The main computer software analysis-tool used in the study is Siemens power system simulator PSS/E, which is renowned in the power industry for its ability to perform complex power system computations with clear and accurate results.

1.4. Thesis Outline

The thesis is structured as follows;

Chapter 1 presents the background, problem statements and objectives of the thesis.

Chapter 2 gives some background and illustration on forecasting method using time series analysis, statistical method of wind energy output estimations, variability study and steady state voltage stability impacts.

Chapter 3 presents methodology used.

Chapter 4 presents the analysis on how Ashegoda wind farm affect EEPCO grid system. It starts by studying variability impact using statistical methods. Next it will study on predictability impact assessment by developing wind power forecasting model using Box-Jenkins method of times series analysis. Energy output from the wind farm is also estimated using statistical methods on the bases sample wind speed data taken from the field. Finally, it deals with steady state voltage stability impacts of Ashegoda wind farm after modeling the wind farm and representing by single turbine equivalent circuit.

Chapter 5 presents conclusions, recommendations and future works.

Chapter 2. Literature Survey

2.1. Wind Power Integration Impact on Power System

Wind power integration influences power system characteristics from economic dispatch to stability and power quality. Wind power impacts depend on the level of penetration to power system. In [1] gives a definition of penetration level in terms of energy penetration rather than power penetration. If energy produced by wind power (annually) as a percentage of the gross electricity consumption is less than 5% of gross demand, it is categorized under low level penetration and if it is greater than 10% it is categorized under high penetration.

In small-scale wind power integration, the installed wind power is relatively small compared to the conventional power generation, the power system is assumed to have enough spinning reserve of active power and the frequency is kept constant. Therefore, voltage problems are only concerned.

In large-scale wind power integration, the installed wind power size is comparable to conventional power generating stations. Therefore, large-scale integration can cause power quality or stability problems and, in some particular cases, the frequency can be affected. Hence, not only the voltage but also frequency problems are concerned [2].

The impacts of wind power on power systems can also be divided into local impacts and system-wide aspects. The local impacts of wind power mainly depend on local grid conditions and the connected wind-turbine type, and the effects become less noticeable with the distance from the source. In such case ,the observed phenomena include changed branch flows, altered voltage levels, increased fault currents and the risk of electrical islanding, which complicate system protection, and possibly power quality problems, such as harmonics and flicker.

System-wide impacts are largely a result of the variability and limited predictability of the wind and mainly depend on a number of factors, including wind power penetration level, geographical dispersion of wind power and the size of the system.

The problem of network stability is often associated with different types of faults in the network, such as tripping of transmission lines (e.g. overload), loss of production capacity, and short circuits. Tripping of transmissions lines due to overload or component failure disrupts the balance of power (active and reactive) flow. Although the capacity of the operating generators may be adequate, large voltage drops may occur suddenly. The reactive power flowing through new paths in a highly loaded transmission grid may force the voltage of the network in the area down beyond the border of stability. Often a period of low voltage is followed by complete loss of power. Loss of production capacity obviously results in a large, momentary, power imbalance.

Unless the remaining operating power plants have enough "spinning reserve," that is, generators are not loaded to their maximum capacity, to replace the loss within very short time, a large frequency and voltage drop will occur, followed by complete loss of power. In all the situations, the result is a short period with low or no voltage followed by a period when the voltage restores. A large wind farm in the vicinity will see this event and may be disconnect from the grid; if no appropriate control has been implemented. This leads to the situation "loss of production capacity." Disconnection of the wind farm will further aggravate the situation and therefore, in some grid codes, wind turbines and wind farms are required to have the ability of fault ride through.

Under steady state condition a voltage stability problems arise when large–scale wind farms are connected to the transmission network ; as the wind farm affects the power flows and hence the node voltages[1],[2]. Voltages are controlled mainly by large scale conventional power plants. If their capability to control voltages within the transmission network is not sufficient to compensate the impact of the wind farm on the node voltages, the voltage at some nodes can no longer be kept within the allowable deviation from its nominal value and which again leads to deviation of voltage at other nodes. Unless appropriate measures have taken, it goes to voltage instability.

The other problem associated with large-scale integration is mainly originate from displacement of large amount of conventional generating unit from the system by wind generators that uses mostly induction generator or grid-coupled synchronous generator via

power electronic converters. As the dynamic behavior of a power system is determined mainly by generators, wind turbines affect the dynamic behavior of the power system in a way that might be different from synchronous generators .As a result it may begin to affect the overall behavior of the power system .

A voltage variation is also caused by fluctuation wind power generation that may cause voltage quality problems. Fluctuations in the system voltage may cause perceptible light flicker depending on the magnitude and frequency of the fluctuation. This type of disturbance is called voltage flicker, commonly known as flicker .Hence integration of wind power impacts needs a thorough understanding and required a study of steady state to dynamic stability and quality issues [1], [2].

Chapter 3. Methodology

3. Introduction

The approached followed and the tools used during this thesis work are explained in detail. Some basic concepts and derivations related to the time series analysis, energy output estimation and voltage stability analysis are discussed.

In the first section general concept and approach used to analyze time series analysis for developing wind power output forecasting model applying using Box-Jenkins method is discussed and the approach of statistical method of energy output estimation has discussed.

In the next sections energy loss is used to drive an equation of equivalence of pad mounted transformer and collector circuits of the wind farm.

3.1. Time Series Analysis and Forecasting

Forecasting is prediction of the future value based on the observed past data with the model developed. Forecasting model performance depends on the forecast horizon. Short-term wind power forecasting is used for wind turbine controls, real-time dispatch or generation scheduling. In general, wind power is forecasted using two methods, physical and statistical time series analysis.

Physical model considers Numerical Weather Prediction (NWP), detailed conditions of wind farms and their surrounding terrain. It reaches the best possible estimation of the local wind speed and reduces the remaining error.

Statistical time-series related methods include Auto-Regressive Moving Average (ARMA), Artificial Neural Networks, Fuzzy Logic, Kalman Filter, and so on. Statistical models catch the relationships between variables including NWP results and online measured data and usually employ recursive techniques. Prediction capabilities and accuracy of the models or their combination are quite different in terms of forecasting interval.

In this thesis work, Box-Jenkins statistical method of forecast model developing procedures has been followed. Forecasting model developed based on Box-Jenkins method of statistical time series analysis basis on past statistical wind speed data gathered from the site.

Forecast model developed by Box-Jenkins method require in depth analysis of statistical time series. The principal objective of next section is to introduce the basic concepts about time series analysis and steps used for developing forecast model using Box-Jenkins method of time series analysis [3].

3.1.1. Box-Jenkins Method of Time Series Analysis

In year 1972, George E. P. Box and Gwilym M. Jenkins developed a method for analyzing stationary univariante time series data.

The model developed serves not only to explain the underlying process generating the series, but as a basis for forecasting. The Box–Jenkins method differences the series to stationary and then combines the moving average (MA) with autoregressive (AR) parameters to yield a comprehensive model amenable to forecasting [4].
Box-Jenkins models have a few limitations. It needs at least 30 to 50 observations, mostly at least 50.

In addition, Box–Jenkins method requires that the discrete time series data be equally spaced over time and that there must be no missing values in the series.
The choice of temporal interval or sample interval is also important in modeling. For example, if the data vary every month but are gathered only once a year, then the monthly or seasonal changes will be lost in the data collection. Therefore, temporal resolution should be designed to focus on the subject or object of analysis as it changes over time. The rate of observation must be synchronized with the rate of change for proper study of the subject matter [5]. Some of the basic tools used by Box-Jenkins to develop a model are

i. Stationary

ii. Autocorrelation functions (ACF)

iii. Partial autocorrelation functions (PACF)

iv. Autoregressive process (AR)

v. Moving average process (MA)

vi. Autoregressive moving average process (ARMA)

i. Stationary

To make statistical inferences about a stochastic process on the basis of an observed sample of a process, some simplifying assumptions about that process is usually taken.
One of the important simplifying assumptions is stationarity. Specifically, a process $\{Y_t\}$ is said to be strictly stationary, the mean and variance values at all choices of time is constant, that is

$$\left.\begin{aligned} E(Yt) &= E(Y_{t-k}) \\ Var(Yt) &= Var(Y_{t-k}) \end{aligned}\right\} \text{for all t and k} \qquad 3.1.$$

ii. Autocorrelation Function (ACF)

An important guide to the properties of a time series is provided by a series of quantities called sample autocorrelation coefficients, which measure the correlation between observations at distance apart. These coefficients often provide insight into the model which generated the data. In ordinary correlation coefficient, mainly given N pairs of observations on two variables x and y, the correlation coefficient is given by [4], [5];

$$r = \frac{\sum(x_i - \bar{x})(y_i - \bar{y})}{\sqrt{[\sum(x_i - \bar{x})^2 \sum(y_i - \bar{y})^2]}} \qquad 3.2.$$

A similar idea can applied to a time series to see if successive observations are correlated. Given N observations $x_1,\ldots,x_N$, on a discrete time series we can form N-1 pairs of observations, namely $(x_1,x_2),(x_2,x_3),\ldots\ldots(x_{N-1},x_N)$. Assuming the first observation in each pair as one variable, and the second variable as a second variable, the correlation coefficient between xt and xt+1 is give by

$$r_1 = \frac{\sum_{t=1}^{N-1}\left(y_t - \bar{y}_{(1)}\right)\left(y_{t+1} - \bar{y}_{(2)}\right)}{\sqrt{\left[\sum_{t=1}^{N-1}\left(y_t - \bar{y}_{(1)}\right)^2 \sum_{t=1}^{N-1}\left(y_t - \bar{y}_{(2)}\right)^2\right]}} \qquad 3.3.$$

$\bar{y}_{(1)}$ is the mean of observation of N-1 the first pairs and $\bar{y}_{(2)}$) is the mean of the first N-1 observations of the second pair and is given by

By similar analogy, a general expression to find the correlation between observations a distance k apart is given as follows

$$r_k = \frac{\sum_{t=1}^{N-1}(y_t - \bar{y})(y_{t+k} - \bar{y})}{\sum_{t=1}^{N}(y_t - \bar{y})^2} \quad 3.4.$$

This is called the autocorrelation coefficient at lag k [3].

iii. Partial Autocorrelation Function (PACF)

The partial correlation between two variables is the correlation that remains if the possible impact of all other random variables has been eliminated [5]. The partial autocorrelation function is a useful tool to identify models in Box-Jenkins method of time series analysis. In conjunction with autocorrelation function, partial autocorrelation function can be used to identify a first-order from a high order autoregressive process.

iv. Autoregressive Process (AR)

Autoregressive models are based on the idea that the current value of the series, Y_t, can be explained as a function of past values, Y_{t-1}, Y_{t-2}, . . , Yt_{-p}, where p determines the number of steps into the past needed to forecast the current value [9-10]. An autoregressive model of order p, abbreviated AR (p), is of the form

$$Y_t = \phi_1 Y_{t-1} + \phi_2 Y_{t-2} + \phi_3 Y_{t-3} + \cdots + \phi_p Y_{t-p} + e_t \quad 3.5.$$

Where Y_t is stationary and mean is zero, Φ_1, Φ_2,. ., Φp are constants. Unless stated, normally it is assumed that e_t is a Gaussian white noise series with mean zero and variance σ^2 .If the mean, μ,is not zero,Y_t replaced by $Y_{t-\mu}$ in equation 3.5.

v. Moving Average Process (MA)

A moving average process is constituted from a weighted sum of the most recent values of the white noise, e_t. Moving average model of order q, abbreviated as MA (q), assumes the

white noise e_t that is linearly combined to form the observed data, Y_t. The moving average model of order q, or MA (q) model, is defined to be

$$Y_t = \Theta_1 e_{t-1} + \Theta_2 e_{t-2} + \Theta_3 e_{t-3} + \cdots + \Theta_q e_{t-q} + e_t \quad 3.6.$$

Where there are q lags in the moving average and θ_1, θ_2... θ_q, constants and et is assumed to be Gaussian white noise [5].

vi. Autoregressive Moving Average Process (ARMA)

A commonly used time series in wind speed forecast modeling is ARMA process. It contains both autoregressive and moving average process together. If we assume that the series is partly autoregressive and partly moving average, we obtain a quite general time series model given as follows [4].

$$Y_t = \phi_1 Y_{t-1} + \phi_2 Y_{t-2} + \ldots + \phi_p Y_{t-p} + e_t - \Theta_1 e_{t-1} - \cdots - \Theta_q e_{t-q} \quad 3.7.$$

Where $\{Y_t\}$ is a mixed autoregressive moving average process of orders p and q, respectively.

3.1.2. Model Identification

The first stage in modeling process using Box-Jenkins method is identification of the order of the model. In addition to preprocessing of input data of the series, finding the magnitude of autocorrelations and partial autocorrelation is performed to determine whether the values are cut-off or tail-off [4]. Preprocessing of data includes replacing missing data, checking the sanity and stationarity of the data. Checking stationary of data will help us to determine the order of differencing.

Modeling is an iterative process until a good model that fits the sample data has found. Therefore, the order of AR and MA of the model identified at this stage is tentative until it is diagnosed and accepted as a final model.

3.1.3. Parameter Estimation

Once the model order identified the parameters of the model is estimated in the third stage of Box Jenkins approach. Some of the methods used are method of moments, least square methods and so on.

In case of Method of moment estimates the unknown parameter first finding the sample moment and equating with the theoretical moments and solving the equations. The idea of least square method is by minimizing the sum of the error between consecutive sample points at t and t-1[4].

3.1.4. Model Diagnosis

In Box –Jenkins modeling strategy the first step is specifying the order of a model. However, this models are normally tentative that needs to be checked for its capacity to fit the actual data. Model diagnostics, or model criticism, is concerned with testing the goodness of fit of a model and, if the fit is poor, suggesting appropriate modifications.

After estimation of the model, the Box–Jenkins model building strategy demands a diagnosis of the model for its adequacy. More specifically, it is necessary to ascertain in what way the model is adequate and in what way it is inadequate. The methods used to quantify the model adequacy are using the residual from the fitted model and over or under fitting of the model.

In general unobserved stochastic process is accounted by the residual terms, that is, a white noise .If the stochastic component is a white noise, the residuals should have roughly like independent normal random variables with zero mean and constant standard deviation at any time t. If the model residual satisfies this condition, that is, zero mean and constant standard deviation; then the model fit well the observed data. Otherwise, the model left some parameters which are not accounted properly during modeling process.

The most frequently used method of checking whether a residual is a white noise or not is the autocorrelation functions of the estimated residuals; as white noise residuals have no significant autocorrelation function magnitude.

The second tool used for model diagnosis is over fitting the model selected. It is more on an iterative process based on some statistical model fitting values as a reference for the next model to be compared with the previous one[3-6].

3.1.5. Forecast Evaluation

Some of statistics used to describe forecast error are

i. Mean Absolute Error (MAE)

ii. Sum of Squared Error (SSE)

iii. Mean Square Error (MSE)

iv. Root Mean Square Errors (RMSE).

3.2. Analysis of Wind Data

Analysis of wind speed variation needs primarily collection, organization and description of collected speed data. Therefore, it goes through under a statistical treatment that can be presented as tabular or graphical forms which give a good understanding about the nature of the sample data.

In order to put primary data into a proper and easy form of presentation, statistical data should be condensed and grouped together into classes called classification. Another method that can be used to arrange systematical the data is representing it in the form of tabular. A graph such as histograms, frequency curves and bar graphs can also be used to represent the data. In many cases, a graphic presentation of a frequency gives more concise and clear information about a frequency distribution.

As wind speed changes continuously, a best approach to determine its behavior is using a statistical method based on the sample data taken at the field. Statistical analyses of wind speed need a critical examination of basic concepts of probability and statistics. One of the basic concepts used to characterize the sample data is by analyzing the dispersion or central tendency.

The measure of central tendency describes where the central region of the data is; but does not show how the positions are spread out, or scattered on each side of the center. This characteristic of a distribution is referred to as the dispersion or variation. This includes the range, mean deviation, standard deviation and variance [7-9].

The mean deviation simply computes the ranges of the magnitude of the deviation from some central values such as mean, mode, and median. Suppose Y_1, Y_2 ...Y_n are the "n" values of the variables Y and $\overline{Y}$ is the mean then mean deviations (Md) is given as

$$MD = \frac{1}{n}\sum_{i=1}^{n}[Y_i - \overline{Y}] \qquad 3.8.$$

The mean of the square deviation of the variable Y from mean value $\overline{Y}$ is known as variance of the data and is given as follows

$$\sigma^2 = \frac{1}{n-1}\sum_{i=1}^{n}[Y_i - \overline{Y}]^2 \qquad 3.9.$$

Because of the squaring, the variance is expressed in square units and not in original unit. The positive square deviation of the variable from the arithmetic mean is called the standard deviation.

One measure for the variability of wind speed in a given set of wind data is the standard deviation. Standard deviation tells us the deviation of individual speed from the mean value and it is calculated as

$$\sigma_v = \sqrt{\frac{\sum_{i=1}^{n} f_i(V_i - V_m)^2}{n}} \qquad 3.10.$$

Thus, lower values of σ_V indicate the uniformity of the data set.

The standard deviation in normally distributed samples tells us about how much of the data is above or below a given point, see figure 3.1. This asserts that:

- 68% of the data is between (mean + σ) and (mean - σ),
- 95% is between (mean + 2σ) and (mean - 2σ), and

- 99.7% of the data is between (mean + 3 σ) and (mean – 3 σ).

This rule allows us to calculate other things as well. For example, we can determine what percentage of the data points are above (mean + σ). Since 68% of the data is between (mean - σ) and (mean +σ), we know that 32% is outside of this range. Since the curve is symmetric, half of this is below (mean -σ) and half is above (mean +σ).Therefore, 16% of the data lies above (mean + σ) [11].

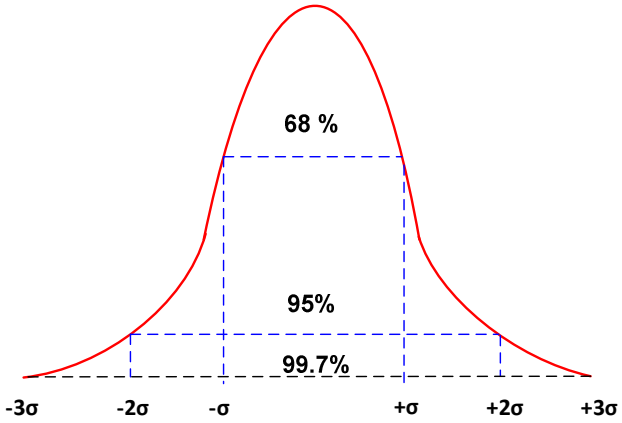

Figure 3.1. Rule of 68-95-99.7 statistics.

3.2.1. Frequency Distribution

The number of occurrences in each class is called the frequency or class frequency. When class frequency is in table form, this table is called frequency table.

The frequency distribution is the basic tool for describing and analyzing the population data or information. This is accomplished by estimating the characteristics of the population frequency distribution from the sample or series. Most frequently, Weibull and Rayleigh distribution are used for analyzing wind speed sample data. In Weibull distribution, the variations in wind speed is characterized by the two functions are the probability density function and cumulative distribution function. The probability density function (f(V)) indicates the fraction of time (or probability) for which the wind is at a given speed V. It is given by [11].

$$f(V) = \frac{K}{C}\left(\frac{V}{C}\right)^{K-1} e^{-(V/C)^{K}} \qquad 3.11.$$

Here, k is the Weibull shape factor and c is scale factor. Weibull curve for different values of shape and scale factors shown in figure 3.2.

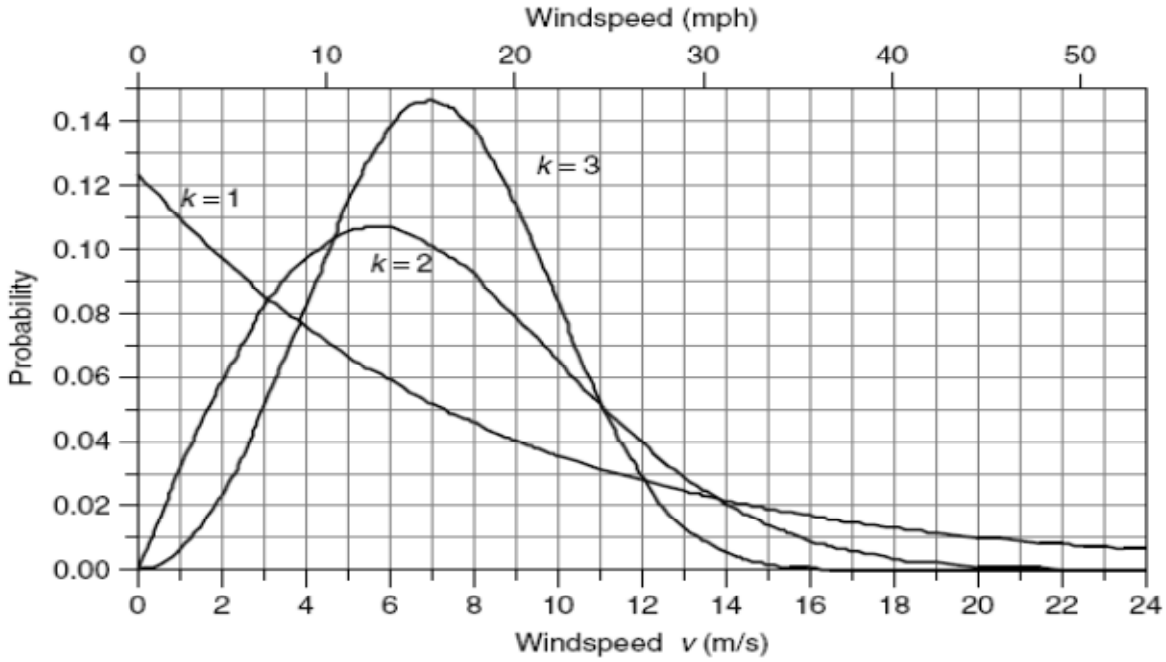

Figure 3.2. Weibull probability density function [10].

The cumulative distribution function of the wind speed V gives us the fraction of time (or probability) that the wind speed is equal or lower than V. The cumulative distribution F(V) is the integral of the probability density function. Thus,

$$F(V) = \int_{0}^{\infty} f(V)dV = 1 - e^{-(V/C)^{K}} \qquad 3.12.$$

The cumulative distribution function can be used for estimating the time for which wind is within a certain speed interval. Probability of wind speed being between V_1 and V_2 is given by the difference of cumulative probabilities corresponding to V_2 and V_1 [11],[12]. Thus

$$P(V_1 < V < V_2) = F(V_2) - F(V_1)$$

That is

$$P(V_1 < V < V_2) = e^{-\left(V_1/C\right)^K} - e^{-\left(V_2/C\right)^K}$$

The reliability of Weibull distribution in wind regime analysis depends on the accuracy in estimating k and C [11]. For the precise calculation of k and C, adequate wind data, collected over a time intervals are essential. In many cases, such information may not be readily available. The existing data may be in the form of the mean wind speed over a given time period (for example daily, monthly or yearly mean wind speed). Under such situations, a simplified case of the Weibull model can be derived, approximating k as 2. This is known as the Rayleigh distribution. The mean is given by

$$V_m = C\,\Gamma\left(\frac{3}{2}\right) \qquad 3.13.$$

Evaluating gamma function of equation 3.13 and rearranging,

$$C = \frac{2V_m}{\sqrt{\pi}} \qquad 3.14.$$

Substituting for C in equation 3.12, we get

$$f(V) = \frac{\pi}{2}\frac{V}{{V_m}^2} e^{-\left[\pi/4\left(V/V_m\right)^2\right]} \qquad 3.15.$$

The form the Rayleigh curve is shown in figure 3.2 (f (V) for K=2).

Similarly, the expression for cumulative distribution can be solved substituting in equation 3.12 the value of C from equation 3.14 and K=2,

$$F(V) = 1 - e^{-\left[\pi/4\left(V/V_m\right)^2\right]} \qquad 3.16.$$

Thus, we can calculate the probability density and cumulative distribution functions of wind on the basis of its average velocity.

In order to analyze the wind speed data using Weibull distribution; the curves parameters, k and C, has to be estimated first from the actual wind speed data. Some of the methods used for determining k and c are Graphical method and Standard deviation method.

i. Graphical Method of Shape and Scale Factor Estimation

In the graphical method, the expression for shape and scale factor can be found by transforming the cumulative distribution function in to a linear form using logarithmic scales [11].The expression for the cumulative distribution of wind speed can be rewritten as

$$1 - F(V) = e^{-(V/C)^K} \quad 3.17.$$

Taking the logarithm twice, we get

$$\ln\{-\ln[1 - F(V)]\} = k\ln(V_i) - k\ln C \quad 3.18.$$

Plotting the above equation with "ln(Vi)" along the X axis and " ln{-ln[1-F(V)]} " along the Y axis, we get nearly a straight line. From equation 3.18, we get "k "as the slope of the line and "–k ln C" as the intercepts of the line.

ii. Standard Deviation Method of Shape and Scale Factor Estimation

The Weibull factors k and C can also be estimated from the mean and standard deviation of wind data as follows,

$$\left(\frac{\sigma_V}{V_m}\right)^2 = \frac{\Gamma\left(1+\frac{2}{K}\right)}{\Gamma^2\left(1+\frac{1}{K}\right)} - 1 \quad 3.19.$$

Once σ_V and V_m are calculated for a given data set, then k can be determined by solving equation 3.19 numerically. Once k is determined, C is given by

$$C = \frac{V_m}{\Gamma\left(1+\frac{1}{K}\right)} \quad 3.20.$$

In a simpler approach, an acceptable approximation for k is given by,

$$K = \left(\frac{\sigma_V}{V_m}\right)^{-1.09} \quad 3.21.$$

Similarly, C can be approximated as

$$C = \frac{2V_m}{\sqrt{\pi}} \quad 3.22.$$

More accurately, C can be found using the expression [16-17]

$$C = \frac{V_m K^{2.6674}}{0.184 + 0.816K^{2.73855}} \quad 3.23.$$

3.3. Energy Output Estimation of Wind Farm

The accuracy of the estimated energy is depends of the geographical distribution of wind and statistical data gathered from the site. The other factor that also affects the estimation is modeling of the wind generating curve that can be used latter to generate the wind speed from measured wind power.

Wind energy density and the energy available in the regime over a period are usually taken for evaluating the energy potential available at the site. The wind energy density (ED) is the energy available in the regime for a unit rotor area and time. Thus, ED is a function of the speed and distribution of wind in the regime. We can arrive at the total energy available in the regime multiplying the wind energy density by the time factor [11], [12].

There are many kinds of probability distributions functions that are applicable for describing the frequency distributions of wind regime at particular site. Some of them which are most frequently used in assessing wind resources are

i. Weibull distribution

ii. Rayleigh distribution

Both Weibull and Rayleigh distributions are used to calculate the monthly energy output of Ashegoda Wind Park.

i. Weibull Based Approach

In Weibull distribution, the variations in wind speeds are characterized by the two functions;

(1) The probability density function and

(2) The cumulative distribution function.

The probability density function (f (V)) indicates the fraction of time (or probability) for which the wind is at a given speed V. It is given by equation 3.12,

$$f(V) = \frac{K}{C}\left(\frac{V}{C}\right)^{K-1} e^{-(V/C)^{K}}$$

Here, k is the Weibull shape factor and C is scale factor. The cumulative distribution function of the speed V gives us the fraction of time (or probability) that the wind speed is equal or lower than V .For a unit area of the rotor, power available (P_V) in the wind stream of speed V is

$$P_V = \frac{1}{2}\rho_a V^3 \qquad 3.24.$$

Thus, the total energy, contributed by all possible speeds in the wind regime, available for unit rotor area and time may be expressed as

$$E_D = \int_0^{\infty} P_V f(V) dV \qquad 3.25.$$

The energy density of the wind farm can be estimated using equation;

$$E_D = \frac{\rho_a C^3}{2}\Gamma\left(\frac{3}{K} + 1\right) \qquad 3.26.$$

And, total energy is the product of the total time and energy density;

$$E_I = E_D T = T\frac{\rho_a C^3}{2}\frac{3}{K}\Gamma\left(\frac{3}{K}\right) \qquad 3.27.$$

Where T is the time period (For example, T is taken as 24 when we calculate the energy on daily basis.

ii. Rayleigh Approach

A simplified case of the Weibull model can be derived, approximating k as 2. This is known as the Rayleigh distribution. The energy density of the wind farm can be estimated as follows [11];

$$E_D = \frac{\rho_a}{2K^{5/2}}\Gamma\left(\frac{5}{2}\right) \quad 3.28.$$

Total energy is the product of the total time and energy density;

$$E_I = E_D T = T\frac{\rho_a}{2K^{5/2}}\Gamma\left(\frac{5}{2}\right) \quad 3.29.$$

Where T is the time period (For example, T is taken as 24 when we calculate the energy on daily basis).

3.4. Modeling of Wind Farm

Although it is very important to understand the dynamics of individual turbines, wind farm characteristics can also be represented by the collective behavior of the wind farm with a single turbine representation (STR).

Among other aspects, the design of collector systems for wind power farm seeks to minimize losses and voltage drops. Within a wind farm, wind turbines are placed optimally to harvest as much wind energy as possible. Some wind farms are built with different types of wind turbines for different reasons. For example,

i. Recent unavailability of new turbines because of wind turbine supply lags behind demand

ii. The economic benefit of mixing wind turbine types within the same wind farm.

iii. Re-powering old wind farm with newer and bigger turbines [13], [14].

3.4.1. General Assumptions for Modelling Wind Farms

Most frequently, the collector system is connected at the 33 kV voltage levels, where the wind turbines are connected to each other in a string using underground cables. Each

cluster may contain one or more groups of wind turbine. Each wind turbine is electrically attached to a pad-mounted transformer that steps up the generator terminal voltage (690 V) to a medium voltage level (33 kV).

The collector system is connected to a central substation transformer which in turn steps up to the transmission voltage level (230 kV).Equivalence of collector circuit is made based on apparent power losses (i.e., real and reactive power losses). In [14] the modeling is made with the following assumptions are considered,

i. The current injection from all wind turbines assumed to be identical in magnitude and angle.

ii. Reactive power generated by the line capacitive shunts is based on the assumption that the voltage at the buses is one per unit.

3.4.2. Equivalence of Collector Circuit

Modeling procedure for collector circuit impedance can be demonstrated considering a cluster which contains only one group with three wind turbine connected as shown in figure 3.3.The voltage drops across the line impedances Z_l can be written as:

$$\Delta V_1 = I_1 Z_1 = \left(\frac{S_1}{V}\right) Z_1 = \left(\frac{P_1}{V}\right) Z_1 \qquad 3.30.$$

The apparent power S_1 can be substituted by active power P_1 assuming that each wind turbine is compensated and have a very close unity power factor. So that, the current injected by wind generator one is given by $I_1=S_1/V$ (where S_1 is the rated apparent power of wind turbine one). The voltage drop across each line impedance Z_2 though Z_3 can also be written as

$$\Delta V_2 = (I_1 + I_2) Z_2 = \left(\frac{S_1}{V} + \frac{S_2}{V}\right) Z_2 = \left(\frac{P_1}{V} + \frac{P_2}{V}\right) Z_2 \qquad 3.31.$$

$$\Delta V_3 = (I_1 + I_2 + I_2) Z_3 = \left(\frac{S_1}{V} + \frac{S_2}{V} + \frac{S_3}{V}\right) Z_3 = \left(\frac{P_1}{V} + \frac{P_2}{V} + \frac{P_3}{V}\right) Z_3 \qquad 3.32.$$

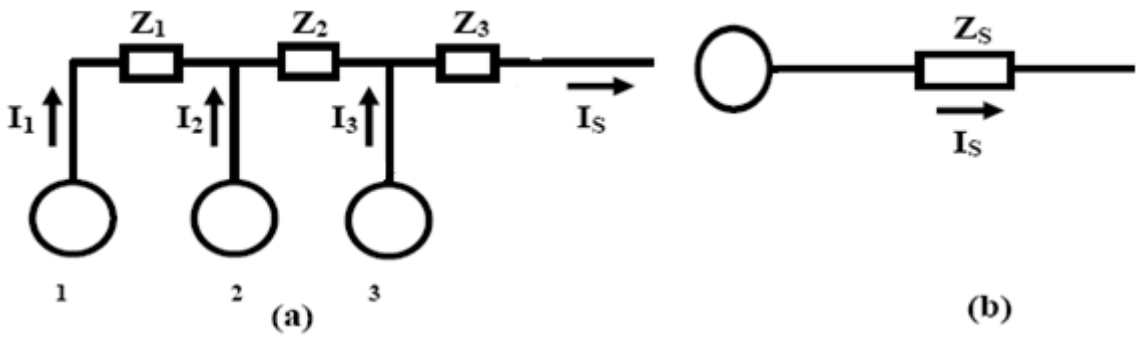

Figure 3.3. A) Wind turbines generators with collector impedance; B) Equivalent circuit representation

The power flow on the line segment Zi be P_{Zi} (i=1, 2, 3) then the total power flow in the line segment will be

$$S_{LOSS\_Z1} = \Delta V_{Z1} I_1^* = \left(\frac{P_1}{V}\right)\left(\frac{P_1}{V}\right)^* Z_1 = \frac{P_1^2 Z_1}{V^2} = \frac{P_{Z1}^2 Z_1}{V^2} \quad 3.33.$$

Similarly, for Z_2 and Z_3

$$S_{LOSS\_Z2} = \Delta V_{Z2} I_2^* = \left(\frac{P_1}{V} + \frac{P_2}{V}\right)\left(\frac{P_1}{V} + \frac{P_2}{V}\right)^* Z_2 = \frac{(P_1 + P_2)^2 Z_2}{V^2} = \frac{P_{Z2}^2 Z_2}{V^2} \quad 3.34.$$

$$S_{LOSS\_Z3} = \Delta V_{Z3} I_3^* = \left(\frac{P_1}{V} + \frac{P_2}{V} + \frac{P_3}{V}\right)\left(\frac{P_1}{V} + \frac{P_2}{V} + \frac{P_3}{V}\right)^* Z_3 \quad 3.35.$$

$$S_{LOSS\_Z3} = \frac{(P_1 + P_2 + P_3)^2 Z_3}{V^2} = \frac{P_{Z3}^2 Z_3}{V^2} \quad 3.36.$$

Note that Z_3 is the last line segment in the daisy chain branch. The total loss can be computed as:

$$S_{LOSS} = \frac{P_{Z1}^2 Z_1}{V^2} + \frac{P_{Z2}^2 Z_2}{V^2} + \frac{P_{Z3}^2 Z_3}{V^2} \quad 3.37.$$

From figure 3.3 (b), we can compute the voltage drop across the equivalent impedance as:

$$\Delta V_{ZS} = V_{ZS} I_S \quad 3.38.$$

Where

$$I_S = \left(\frac{P_1}{V} + \frac{P_2}{V} + \frac{P_3}{V}\right) \quad 3.39.$$

The total loss in the equivalent impedance can be computed as:

$$S_{LOSS\_ZS} = \Delta V_{ZS} I_S^* = \left(\frac{P_1}{V} + \frac{P_2}{V} + \frac{P_3}{V}\right)\left(\frac{P_1}{V} + \frac{P_2}{V} + \frac{P_3}{V}\right)^* Z_{ZS} = \frac{P_{Z3}^2 Z_S}{V^2} \quad 3.40.$$

Equating the two loss equation

$$S_{LOSS} = S_{LOSS\_ZS}$$

Or

$$\frac{P_{Z3}^2 Z_S}{V^2} = \frac{P_{Z1}^2 Z_1}{V^2} + \frac{P_{Z2}^2 Z_2}{V^2} + \frac{P_{Z3}^2 Z_3}{V^2} \quad 3.41.$$

The general expression can be written as:

$$Z_S = \frac{\sum_{m=1}^{n} P_{Zm}^2 Z_m}{P_{Zm}^2} \quad 3.42.$$

This expression can be used to calculate the equivalence collector circuit impedance

3.4.3. Equivalence of Shunt Impedances

A transmission line is represented using an equivalent circuit. In a transmissions line, the line inductive reactance consumes the reactive power and the line capacitive reactances generate reactive power. The generated reactive power by the line capacitance is proportional to the square of the voltage across them. Considering that the bus voltage is close to unity under normal conditions, the representation of the shunt can be considered as the sum of all the shunts in the wind farm networks. With the assumption presented above, we can compute the total shunt capacitance within the wind farm as follows [14],

$$B_{tot} = \sum_{m=1}^{n} B_m \quad 3.43.$$

3.4.4. Equivalence of Pad -Mount Transformers

The equivalence of the pad-mounted transformer connected to turbine generator is made using the loss formula. Each branch has unique impedance and is connected to a wind turbine.

i. Each turbine has its own transformer with the same ratings.

ii. All turbines are producing rated power.

iii. The transformer impedances for each turbine are Z_{T1}, Z_{T2}, and Z_{T3} respectively.

The voltage drops across the impedance Z_{T1} can be found with I_1 is substituted with S_1/V, (where S_1 is the apparent power of wind turbine one) and multiplying by the impedance Z_{T1}.

Based on the assumption that each turbine generates equal current in magnitude and phase angle and each wind turbines are compensated to have a very close unity power factor, the apparent power (S_1) can be substituted by the rated power of wind turbine one(P_1).Then the voltage drop across the impedance of each transformer is given as follows;

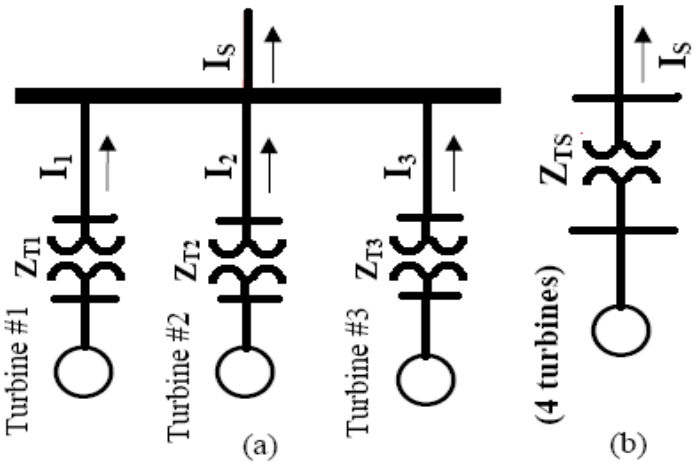

Figure 3.4.Pad mounted transformer and turbine.

From figure 3.4(a), we have,

$$\Delta V_{ZT1} = I_1 Z_{T1} = \left(\frac{S_1}{V}\right) Z_{T1} = \left(\frac{P_1}{V}\right) Z_{T1} \quad 3.44.$$

$$\Delta V_{T2} = I_2 Z_{T2} = \left(\frac{S_2}{V}\right) Z_{T2} = \left(\frac{P_2}{V}\right) Z_{T2} \quad 3.45.$$

$$\Delta V_{T3} = I_3 Z_{T3} = \left(\frac{S_3}{V}\right) Z_{T3} = \left(\frac{P_3}{V}\right) Z_{T3} \quad 3.46.$$

Losses in individual transformer:

$$S_{ZT1} = \Delta V_{ZT1} I_1^* = \left(\frac{P_1 Z_{T1}}{V}\right)\left(\frac{P_1}{V}\right)^* = \frac{P_1^2 Z_{T1}}{V^2} \quad 3.47.$$

$$S_{ZT2} = \Delta V_{ZT2} I_2^* = \left(\frac{P_2 Z_{T2}}{V}\right)\left(\frac{P_2}{V}\right)^* = \frac{P_2^2 Z_{T2}}{V^2} \quad 3.48.$$

$$S_{ZT3} = \Delta V_{ZT3} I_3^* = \left(\frac{P_3 Z_{T3}}{V}\right)\left(\frac{P_3}{V}\right)^* = \frac{P_3^2 Z_{T3}}{V^2} \quad 3.49.$$

The voltage drop across the equivalent impendence

$$\Delta V_{ZTS} = Z_{TS} I_S = \left(\frac{P_1}{V} + \frac{P_2}{V} + \frac{P_3}{V}\right) Z_{TS} = \frac{P_{total}}{V} Z_{TS} \quad 3.50.$$

The total loss is

$$\frac{P_{total}^2}{V^2} Z_{TS} = \frac{P_1^2 Z_{T1}}{V^2} + \frac{P_2^2 Z_{T2}}{V^2} + \frac{P_3^2 Z_{T3}}{V^2} \quad 3.51.$$

The general expression can be written as [17][18],

$$Z_{TS} = \frac{\sum_{m=1}^{n} P_m^2 Z_{Tm}}{[\sum_{m=1}^{n} P_m]^2} \quad 3.52.$$

3.4.5. Wind Turbine Grouping

For a very large wind farm, the area within the wind farm is very large. Hence, the number of turbines within the wind farm can be a very high in number and sometimes it is not easy to get the same types of turbines.

For wind turbine dynamic study, the model has to be represented correctly and it has to be properly initialized using power flow study. For a wind farm which is constitute of different rating, the group has to be represented by one single turbine which has a dominating characteristic compared to the other wind turbine within the group.

One of the criterions for grouping of a wind turbine is short circuit current contribution for the grid.Generally, wind turbine grouping can be made in either of the following criteria's [14],

i. Grouping based on the diversity of the wind farm
ii. Grouping based on the transformer size
iii. Grouping based on the short circuit capacity

3.5. Voltage Stability Analysis

Wind generators can have a significant impact on the voltage profile and the power quality depending on the level of penetration to the system as explained previously. As size of wind farm increases, a large amount of wind power is integrated into the power system. Consequently, the influence on the system is becoming more and more significant and, therefore, it needs to be addressed carefully during impact studies.

A system experiences a state of voltage instability when there is a progressive or uncontrollable drop in voltage magnitude after a disturbance, increase in load demand or change in operating condition. The main factor, which causes these unacceptable voltage profiles, is the inability of the system to meet the demand for reactive power. Reactive power is essential for the stable operation of the power system. It facilitates flow of active power from generation sources to load centers and keep an acceptable voltage limits [15],[16].

Stable operation of power system requires the availability of sufficient amount of reactive power generation on the system. Under normal operating conditions, magnitude of the bus voltage increases as the reactive power injected at the same bus is increased. However, when the voltage of any one of the system buses decreases with the increase in reactive power injection, the system is said to be unstable.

Voltage stability is commonly analyzed by employing two techniques, namely time domain (dynamic) simulation and steady-state analysis. Depending on the stability phenomenon or phenomena under investigation, one or both of these techniques may be applied.

Static analysis (also referred to as load-flow or steady-state analysis) reveals equilibrium points of a system under study. The power flow equations employed in static analysis assume constant system frequency; in other words, generation output equals load demand plus losses. Voltage stability studies are frequently undertaken with static analysis. A common use of this study is the development of curves that shows incremental active power transfer against voltage (that is, a PV curve).

Dynamic analysis (also referred to as time-domain analysis) is commonly employed in the study of power system stability to reveal system trajectory after a disturbance. In contrast to static analysis in which equilibrium points of a PV curve are not time dependent, dynamic analysis method reveals the transient and/or the longer-term stability of a power system under study.

3.6. PV Curves

When considering voltage stability, the relationship between transmitted power and receiving end voltage is a primary interest. The voltage stability analysis involves the transfer of power from one region of a system to another and monitoring the effects to the system voltages. This type of analysis is commonly referred to as a PV study [15].

The PV curve is obtained in power-flow simulation by monitoring a voltage at a bus of interest and varying the power in small increments until power-flow divergence is encountered. Each equilibrium point shown represents a steady-state operating condition.
The effect of transmitted active power on terminal voltage demonstrated using two bus systems as shown in figure 11 in [14] and [15] as follows,

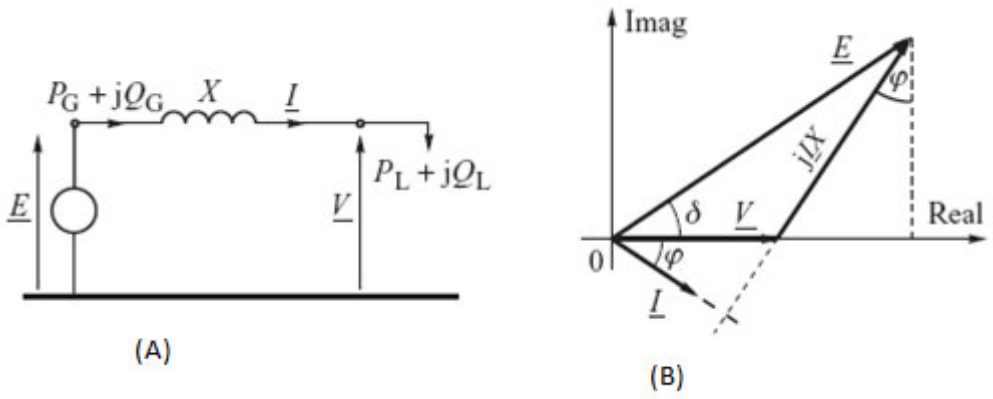

Figure 3.5. Figure (A) shows equivalent circuit of the transmission line and figure (B) shows its phaser diagram [3].

The real and reactive power absorbed by the load, P_L (V) and Q_L (V), can be calculated from;

$$P_L(V) = VI\cos\varphi = V\frac{IX\cos\varphi}{X} = \frac{EV}{X}\sin\delta \qquad 3.53.$$

$$Q_L(V) = VI\sin\varphi = V\frac{IX\sin\varphi}{X} = \frac{EV}{X}\cos\delta - \frac{V^2}{X} \qquad 3.54.$$

Where X is transmissions reactance

E is sending voltage and V is receiving end voltage.

The angle between V and E can be eliminated using identity trigonometric relation, $\sin^2\delta + \cos^2\delta = 1$.thus, equation 3.53 and 3.54 can be simplified as

$$\left(\frac{EV}{X}\right)^2 = [P_L(V)]^2 + \left[P_L(V) + \frac{V^2}{X}\right]^2 \qquad 3.55.$$

For an ideally stiff load the load is independent of voltage and is constant [13].

$$P_L(V) = P_n \quad \text{and} \quad Q_L(V) = Q_n$$

Where Pn and Qn are the real and reactive power demand of the load at the rated voltage Vn. Equation 3.55 can now be rewritten as

$$\left(\frac{EV}{X}\right)^2 = [P_n]^2 + \left[Q_n + \frac{V^2}{X}\right]^2 \quad 3.56.$$

Expressing Qn interms on Pn(Qn = Pn tanφ) we obtain;

$$P_n^2 + P_n^2\tan^2\varphi + 2P_n\tan\varphi\frac{V^2}{X} = \left(\frac{EV}{X}\right)^2 - \left(\frac{V^2}{X}\right)^2 \quad 3.57.$$

Substituting for (tan φ = sin φ/ cos φ) in equation 3.57 we get

$$P_n^2 + P_n^2\frac{\sin^2\varphi}{\cos^2\varphi} + 2P_n\frac{\sin\varphi}{\cos\varphi}\frac{V^2}{X} = \left(\frac{EV}{X}\right)^2 - \left(\frac{V^2}{X}\right)^2 \quad 3.58.$$

Or

$$P_n^2\cos^2\varphi + P_n^2\sin^2\varphi + 2P_n\cos\varphi\sin\varphi\frac{V^2}{X} = \left(\left(\frac{EV}{X}\right)^2 - \left(\frac{V^2}{X}\right)^2\right)\cos^2\varphi \quad 3.59.$$

Substituting ($\sin^2\varphi + \cos^2\varphi = 1$) in equation 3.59 and simplifying

$$P_n^2 + P_n^2\sin\varphi\cos\varphi = \frac{V^2}{X}(E^2 - V^2)\cos^2\varphi \quad 3.60.$$

The left hand side of this equation is an incomplete square of a sum. Hence, the equation can be transformed to the following form,

$$\left(P_n + \frac{V^2}{X}\sin\varphi\cos\varphi\right)^2 - \left(\frac{V^2}{X}\right)^2\sin^2\varphi\cos^2\varphi = \frac{V^2}{X^2}(E^2 - V^2)\cos^2\varphi \quad 3.61.$$

Or

$$P_n + \frac{V^2}{X}\sin\varphi\cos\varphi = \frac{V}{X}\cos\sqrt{E^2 - V^2\cos^2\varphi} \quad 3.62.$$

The voltage at the load bus can be expressed per unit as V/E. The above equation can be expressed as

$$P_n = -\frac{E^2}{X}\left(\frac{V}{E}\right)^2\sin\varphi\cos\varphi + \frac{E^2}{X}\frac{V}{E}\cos\varphi\sqrt{1 - \left(\frac{V}{E}\right)^2\cos^2\varphi} \quad 3.63.$$

Or

$$P = -v^2\sin\varphi\cos\varphi + v\cos\varphi\sqrt{1 - V^2\cos^2\varphi} \quad 3.64.$$

Where

$$v = \frac{V}{E}, P = \frac{P_n}{\frac{E^2}{X}}$$

Equation 3.64 describes a P-V of curve with ϕ as a parameter.

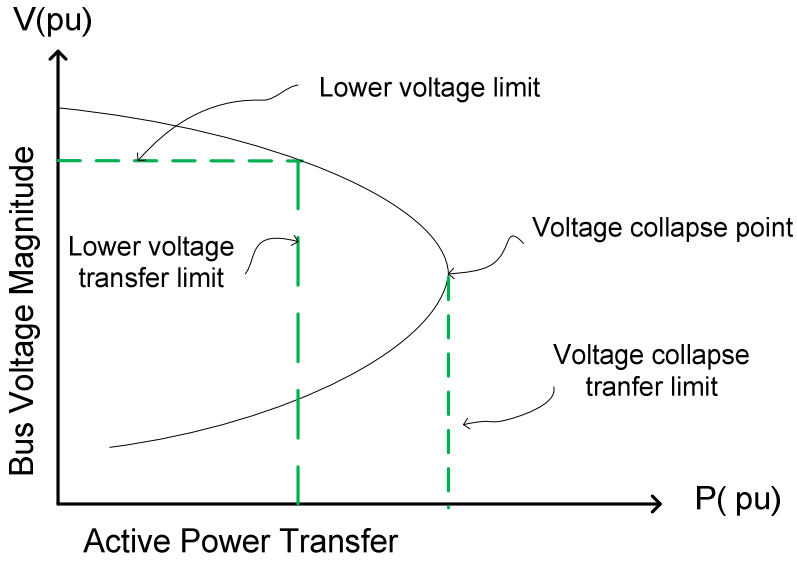

Figure 3.6. P-V curves

It represents the variation in voltage at a particular bus as a function of the total active power supplied to loads or sinking areas. It can be seen that at the "knee" of the PV curve, the voltage drops rapidly when there is an increase in the load demand. Load flow solutions do not converge beyond this point, which indicates that the system has become unstable. This point is called the 'Critical point". Hence, the curve can be used to determine the system's critical operating voltage and collapse margin. Generally, operating points above the critical point signifies a stable system. If the operating points are below the critical point, the system diagnosed is to be in an unstable condition.

3.7. QV Curves

Voltage stability depends on how the variations in Q and P affect the voltages at the load buses. The influence of reactive power characteristics of devices at the receiving end is

more apparent in a QV relationship. It shows the sensitivity and variation of bus voltages with respect to reactive power injections or absorptions. Figure 3.7 shows a typical QV curve, which is usually generated by a series of load-flow solutions.

A voltage stability limit is at the point where the derivative dQ/dV is zero. This point also defines the minimum reactive power requirement for a stable operation. An increase in Q will result an increase in voltage during normal operating conditions. Hence, if the operating point is on the right side of the curve, the system is said to be stable. Conversely, operating points in the left side of the graph are deemed unstable [13].

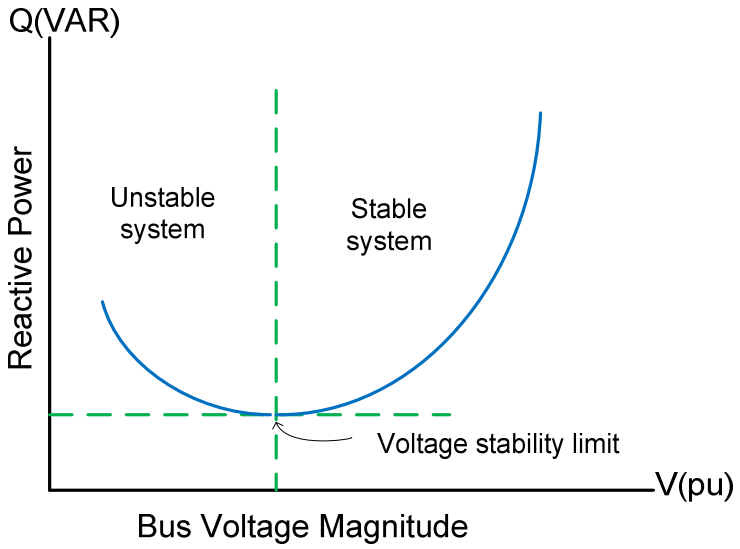

Figure 3.7. QV curve

Chapter 4. Results, Discussion and Analysis

4.1. Statistical analysis of wind and system load variability

The wind distribution is changing from day to day; hour to hours and minute to minute. Variation of wind will have an additive effect on the variable nature of the power system load characteristic.

For power system operation, the following characteristics are relevant: the knowledge of wind power variability and predictability; the knowledge of wind turbine capabilities in providing ancillary services. It is very important to take the variability of wind farm output power into account in a right way in power system studies.

The aim of this section is determining the extent of variability nature of wind output from AWF and system load variability with and without wind farm connected using statistical method based on past historical data.

4.1.1. System load variability.

An hourly and thirty minute system load data has been prepared and the change in system load between successive hours and thirty minute is calculated. The variability is sorted into equal bins and plotted as shown in figure 4.1. The y-axis is the frequency of load hourly variability.

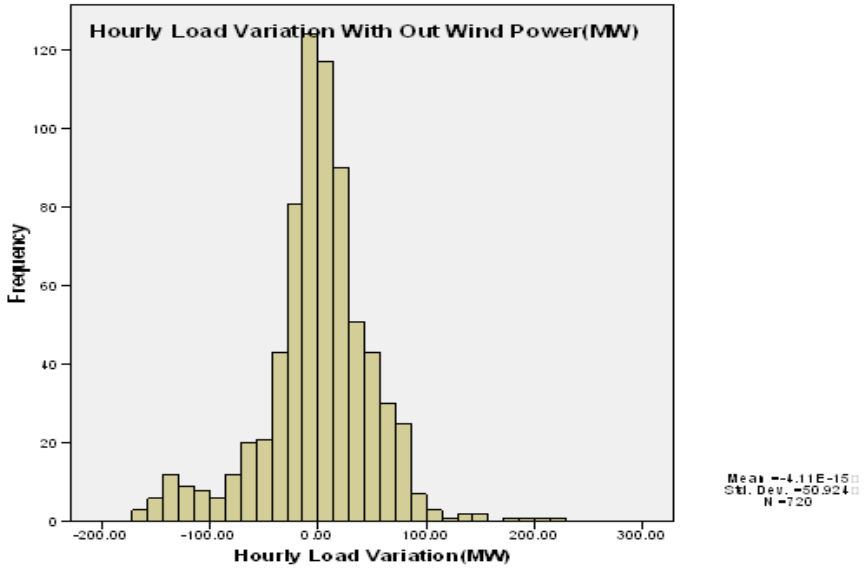

Figure 4.1. Hourly load variation without wind connection

From the graph, what we can observe that it has a normal distribution. From central limit theory, the maximum amount of load variation in terms of MW is 3σ MW or the major load changes (that is, 98.78% of values) are within the range of 3σ MW/h which is equivalently 155.7 MW/hr.

Table 4. 1.The statistical summary of hourly load variability

Mean(MW)	Minimum(MW)	Maximum(MW)	3σ(MW)	Points>3σ	Points<-3σ
0	-168	221.7	150	12	8

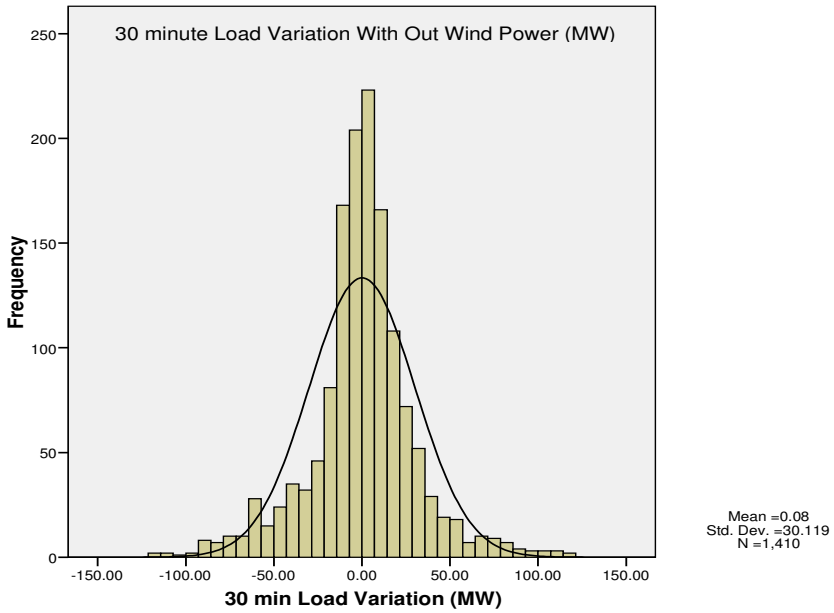

Figure 4.2.Half hour load variation

Table 4.2.The statistical summary of half - hourly load variability

Mean(MW)	Minimum(MW)	Maximum(MW)	3σ (MW)	Points> 3σ	Points < -3σ
0.08	-117	181.29	90.36	11	11

As we can see from table 4.1 and table 4.2), the variability of system load is higher in case of hour to hour as compared to 30min-to-30min.

The maximum amount of hourly load variability that has to accommodate by dispatch able generation in unit commitment period is 150 MW (3σ MW). The system must guarantee at least 150 MW of unit commitment requirement every hour to ensure the secure operation. This can be considered as spinning reserve on hourly basis of operation as a minimum requirement for power system operation. There are a time in which the load drops below or above (3σ)/h. In case of hourly (30 min-to-30min) load variability, the load rise above or drop below (3σ)/h occurs for 20 (22) hours. These hours represent the most severe hours. However, the majority of load changes (99.78 % of the total time) are within the range of -/+ 3σ MW/h.

4.1.2. Wind Power Variability.

Wind power output from the wind farm is prepared for year 2007 for hourly and thirty minute for a single turbine using manufacturer power curve and rescaled to wind farm output multiplying by the number of wind turbines assuming there is equal wind distribution throughout the wind farm.

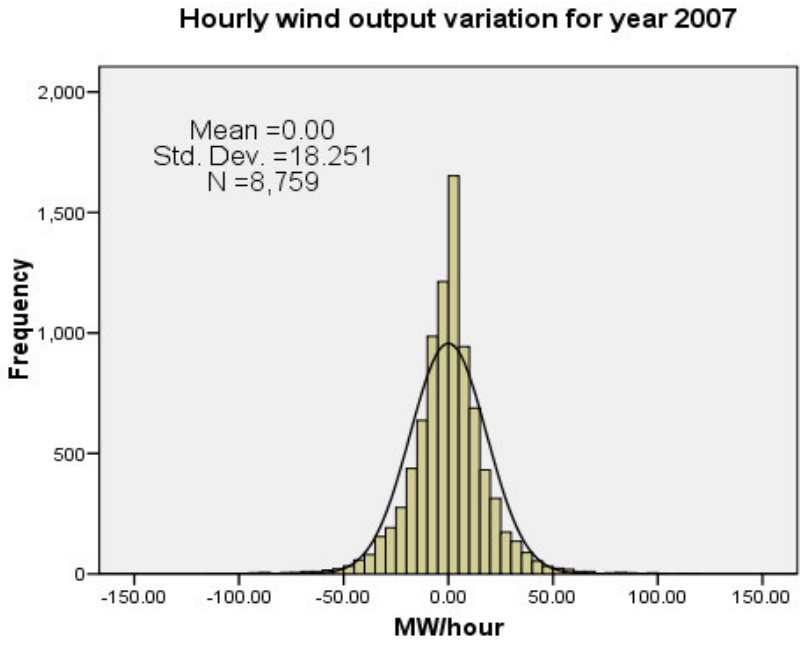

Figure 4.3. Hourly wind power variability

Table 4.3.The statistical summary of hourly wind power variability

Mean(MW)	Minimum(MW)	Maximum(MW)	3σ (MW)	Points > 3σ	Points < - 3σ
0.0045	-114.5	118.79	54.8	12	12

In case of thirty minute, the variability of system load is smaller than the hourly variability.

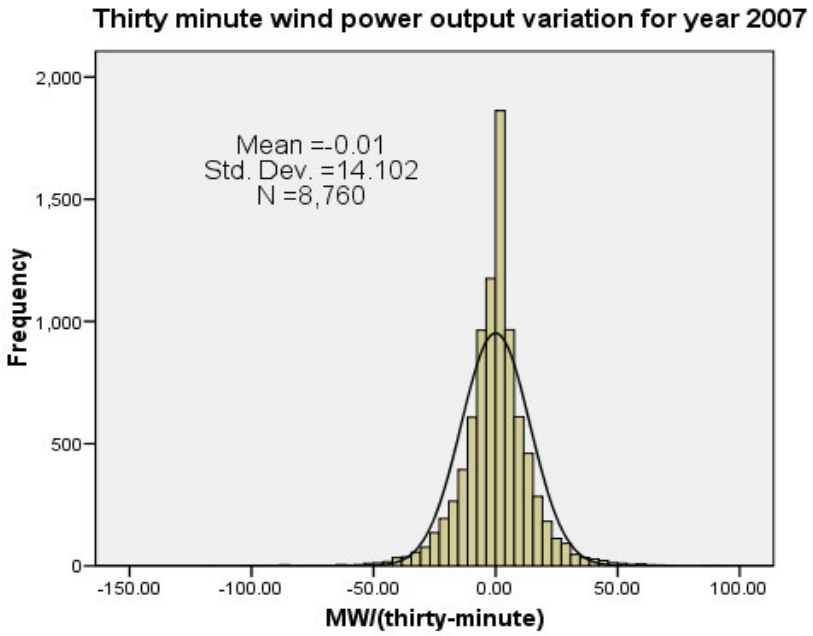

Figure 4.4. Thirty minute wind power variability

Table 4.4.The statistical summary of thirty minute wind power variability

Mean(MW)	Minimum(MW)	Maximum(MW)	3σ (MW)	Points > 3σ	Values < -3σ
-0.0102	-116.7	92.81	42.31	12	12

4.1.3. Combined Load and Wind Power Variability

Most frequent method of analyzing the impacts of integration of wind farm on grid system is comparing the variability of system load variability with wind and without wind farm connection.

To observe the variability impact two different sample data prepared, output from the wind farm and corresponding system load data without wind connection, that is system load alone.

To integrate the wind with the system the wind output is considered as a variable negative load and it is added with the corresponding system load data to find net-load for each hour.

The net-load or load-wind data variability is then plotted as a histogram as shown in figure 4.5.

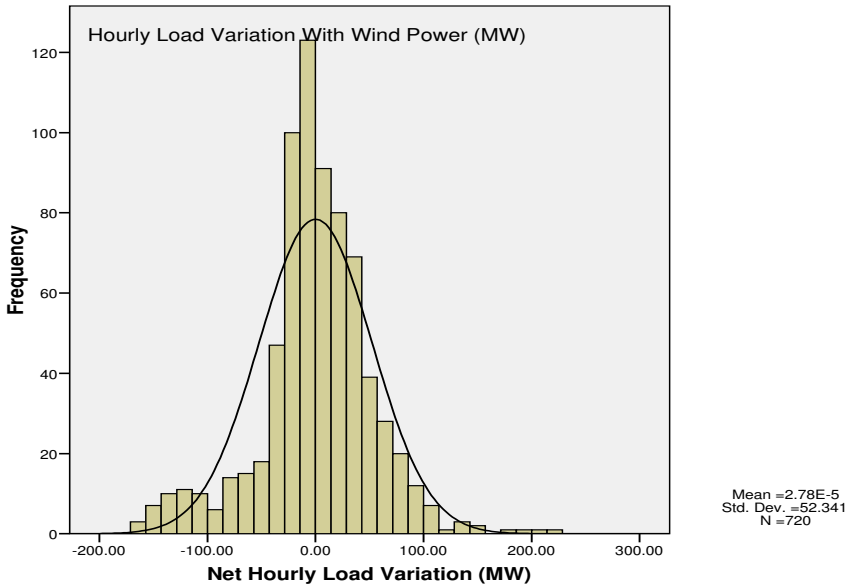

Figure 4.5.Hourly combined load and wind power variability

Table 4.5. Statistical summary of Hourly Combined Load and Wind Power Variability

Mean(MW)	Minimum(MW)	Maximum (MW)	3σ (MW)	Points > 3σ	Values < -3σ
0.0	-170.42	221.29	157	11	7

In case of thirty minute, the net-load variation when the wind farm connected to the system is shown in figure 4.6. As can be seen that it is less than hourly net-load variation.

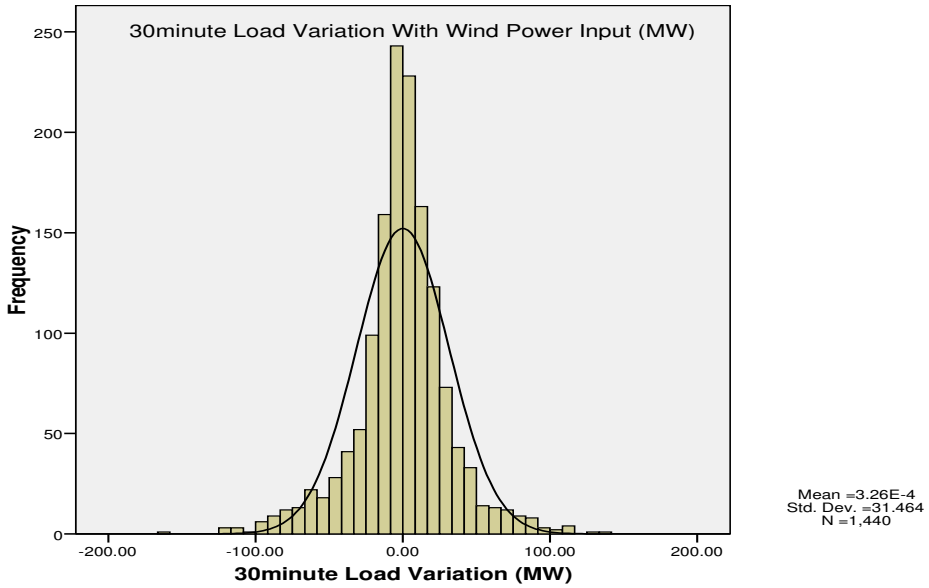

Figure 4.6. Half hourly combined load and wind power variability

Table 4.6. Statistical summary of half hourly combined load and wind power variability

Mean(MW)	Minimum (MW)	Maximum(MW)	3σ(MW)	Points > 3σ	Points < -3σ
0.0003	-159.8	140.54	94.4	12	12

Compared combine load wind variation with the system load-only variation, combined load wind variation distribution is wider. The negative tail of combined wind load has increased by a small value than the load distribution. This indicates that the total variability is increasing after wind power is integrated in the system.

The value of 3σ MW increases from 150 MW to 157 MW in case of hourly load and from 90.36 MW to 94.36 MW incase of thirty minute load after wind power integrated. The incremental or additional hourly (30 min) load-wind variability is 5.8% (3.3%) of the rated capacity of the wind farm .Hence; it needs additional reserve requirement to respond for incremental load variation caused by integration of AWF wind farm.

4.2. Estimation of Energy Output of Ashegoda Wind Farm

The aim of this section is estimating annual energy output of Ashegoda wind farm using statistical method on the basis of sample data taken at year 2007/08 and calculating system

capacity with wind farm connected to check that integrating Ashegoda wind farm avoids the energy shortage occurs during year 2007/08.

The methodology followed is

1. First shape and scale factors of Weibull distribution determined.

2. Cumulative frequency generated using estimated factors and actual cumulative frequency distribution prepared from the sample data are compared

3. Selection of calculations approaches from Weibull and Rayleigh methods

4. Calculating annual energy output

5. Finally determining system capacity with and without wind for year 2007/08.

4.2.1. Weibull and Rayleigh Approach

The energy output using Weibull approach is calculated as follows using equation 3.27,

$$E_I = T\frac{\rho_a C^3}{2}\frac{3}{K}\Gamma\left(\frac{3}{K}\right)$$

In case of Rayleigh approach it is calculated as follows using equation 3.29,

$$E_I = E_D T = T\frac{\rho_a}{2K^{5/2}}\Gamma\left(\frac{5}{2}\right)$$

Where: T is time of period in hours which is equal to 8760 hr for year energy output.

K and C are shape and scale factors respectively.

First, we need to determine shape and scale factor. This has been made using graphical and standard deviation method.

4.2.2. Graphical Method of Scale and Shape Factor Estimation

Using SPSS frequency distribution prepared from the actual sample data and shown in table 4.7.

Table 4.7. CFD of hourly wind speed for year 2007/08

Wind speed class	frequency(fi)	Cumulative frequency distribution F(V)	F(V) in percent	X=ln(V)	Y=ln{-ln[1-F(V)]}
1	3	3	0.0003	0	-7.979
2	39	42	0.0048	0.693	-5.338
3	119	161	0.0184	1.098	-3.987
4	223	384	0.0438	1.386	-3.105
5	360	744	0.0849	1.609	-2.422
6	532	1276	0.1457	1.792	-1.849
7	692	1968	0.2247	1.946	-1.369
8	847	2815	0.3213	2.079	-0.948
9	925	3740	0.4269	2.197	-0.586
10	852	4592	0.5242	2.303	-0.297
11	915	5507	0.6287	2.398	-0.009
12	946	6453	0.7366	2.485	0.288
13	964	7417	0.8467	2.565	0.629
14	697	8114	0.9263	2.639	0.958
15	398	8512	0.9717	2.708	1.271
16	183	8695	0.9926	2.773	1.589
17	49	8744	0.9982	2.833	1.841
18	14	8758	0.9998	2.890	2.126
19	2	8760	1.0000	2.944	None

Two sample data are generated (one as a dependent variable and the other one as independent variable) using equation 3.18 from cumulative frequency distribution of table 4.7 and can be written as first order linear equation as follows,

$$Y = aX + C \quad 4.1.$$

Where, the dependent variable Y is given as

$$Y = \ln\{-\ln[1 - F(V)]\}$$

And the independent variable X is given as

$$X = \ln(V_i)$$

The coefficients of the linear regression equation that relate dependent variable (Y) and independent variable (X) are estimated using SPSS. The form of the linear regression equation using estimated coefficients has the following form;

$$Y = 3.355\ x - 7.848.$$

Therefore, we can easily determine the values of shape factor from the slope of the above equation, that is, k = 3.355. The value of scale factor C is calculated from the intercept of above equation once finding the shape factor as follows,

$$C = \frac{\ln^{-1} 7.848}{K}$$

Substituting the value of K=3.355, we get C=10.37.

4.2.3. Standard Deviation Methods of Scale and Shape Factor Estimation

The standard deviation method uses the standard deviation and mean of the sample data. The standard deviation of the year 2007/08 wind speed is 2.59 and the average value is 8.1 m/s. using equation 3.21, the value of k is determined as follows;

$$K = \left(\frac{\sigma_V}{V_m}\right)^{-1.09}$$

Calculating and substituting the values of mean wind speed velocity and standard deviation from the sample wind speed data of year 2007, we obtain

$$K = \left(\frac{2.59}{8.1}\right)^{-1.09} = 3.46$$

And the value of C is found using equation 3.23,

$$C = \frac{V_m K^{2.6674}}{0.184 + 0.816K^{2.73855}}$$

Substituting the value of K

$$C = \frac{8.1x3.46^{2.6674}}{0.184 + 0.816x3.46^{2.73855}} = 9.02$$

Now generating the cumulative frequency distribution table using the calculated values of shape and scale factors for methods, standard deviation and graphical method, it is compared with actual frequency distribution and plotted as shown in figure 4.7. From the plot what we can see that the standard deviation method give a more accurate distribution than graphical method. Therefore, shape and scale factor estimated form standard deviation method, has been used during energy output estimation.

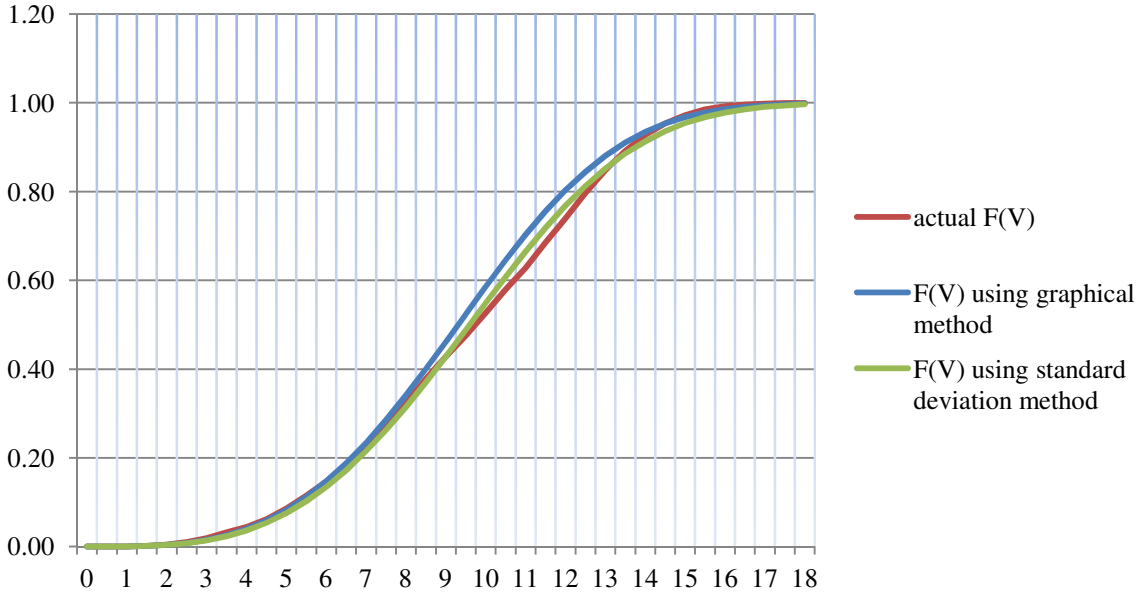

Figure 4.7.CFD of wind velocity using the estimated value K and C by Weibull approach

In case of Rayleigh approach using equation 3.16, F (V) is calculated and plotted against the actual cumulative frequency distribution as shown in figure 4.8.

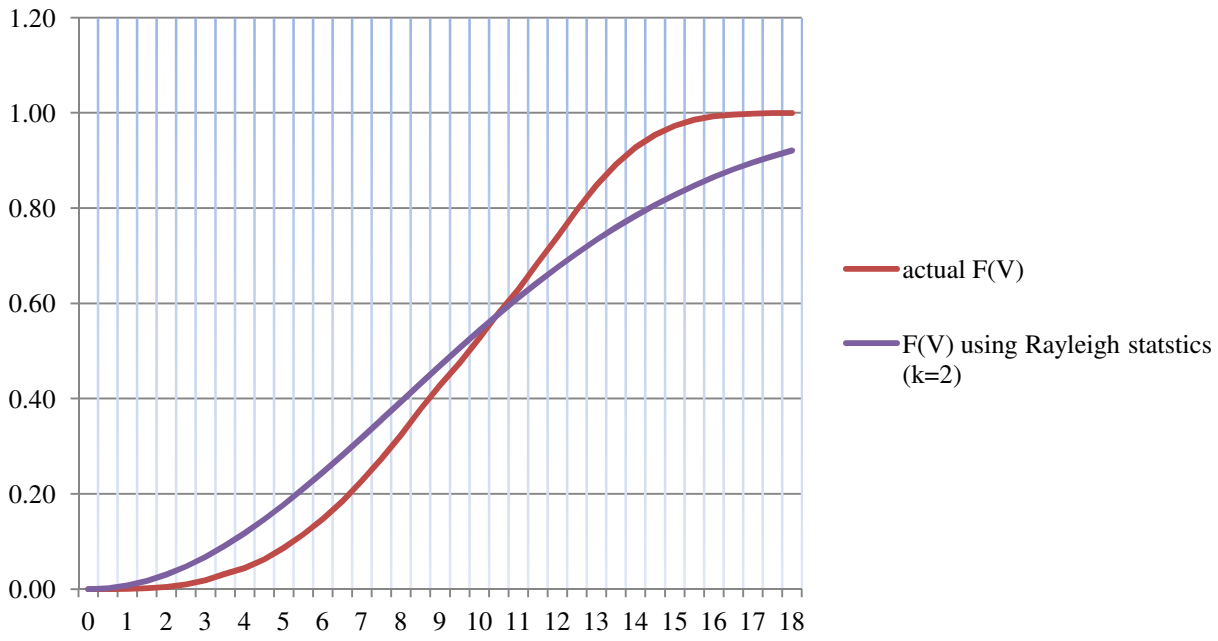

Figure 4.8. CFD of wind velocity using estimated value of K and C using Rayleigh method

Comparing with the actual cumulative frequency and cumulative frequency distribution generated by Rayleigh approach, the Rayleigh approach doesn't fit well. Therefore, Weibull approach is used to estimate annual energy output of Ashegoda wind farm.

4.2.4. Annual Energy Output of Ashegoda Wind Farm

The annual energy estimation is made on the basis of the Vergnet wind turbine manufacturer power curve (supplier of wind turbine for AWF).

First, the number of hours a specific wind speeds throughout the year estimated using equation 3.12. Then, power output of a single wind turbine for a given wind speed estimated from the manufacturer curve and multiplied by the number of hours to get annual energy output.

Table 4.8.Energy output of single wind turbine at AWF

Manufacturer power curve data		Probability f(V)	Hours/year at V (m/s)	Energy (kWH)
wind speed(m/s)	Power(kW)			
1	0	0.002	19.568	0.00
2	0	0.011	98.397	0.00
3	7	0.028	248.885	1742.20
4	7	0.053	467.013	3269.09
5	43	0.083	729.143	31353.14
6	95	0.113	990.875	94133.09
7	168	0.136	1194.108	200610.15
8	269	0.147	1284.120	345428.41
9	399	0.141	1231.758	491471.63
10	560	0.120	1049.292	587603.39
11	731	0.090	788.313	576256.77
12	859	0.059	517.786	444778.38
13	929	0.034	294.387	273485.35
14	969	0.016	143.302	138859.77
15	990	0.007	59.031	58440.38
16	1000	0.002	20.326	20326.13
17	1000	0.001	5.776	5775.96
18	1000	0.000	1.337	1336.72
19	1000	0.000	0.249	248.54
20	1000	0.000	0.037	36.61
21	1000	0.000	0.004	4.21
22	1000	0.000	0.000	0.37
23	1000	0.000	0.000	0.03
24	1000	0.000	0.000	0.00
Total energy output of single wind turbine				3275160.33

To estimate the energy output of AWF, single turbine output rescaled to wind farm level multiplying with the number of wind turbines (N=120).

Finally, to account for power loss, array efficiency and availability of wind turbine, wind farm output multiplied with the following values

- ✓ Array efficiency of 96% (taken from [24])
- ✓ Electrical power loss of 2.83% (found from load flow result)
- ✓ Availability of 98 %(usually it is above 95%)

Therefore, substituting the above factors annual energy output of AWF is calculated as follows

$$\text{Energy}_{\text{anual}} = 0.96 * (1 - 0.283) * 0.98 * 393 = 358\text{G WHr}$$

To appreciate the output of AWF system capacity with wind calculated to check that integration of AWF to system would avoid the energy shortage that had been occurred during year 2007/08. During this year, there was an energy deficiency of 76 GWH.

To determine system capacity with wind first the total amount of energy that can be supplied from the wind farm and the corresponding system energy shortage at each month is calculated. By adding wind farm monthly output and actual energy supplied, the capacity of wind farm with wind has been determined as shown in table 4.9.

Once determining the system capacity with wind it is compared with actual energy supplied during that year. As figure 4.9 shows, the capacity of the system with AWF connected is higher than the total energy demand in the system. Therefore, integration of the wind farm avoids the energy shortage.

Table 4.9. Summary of energy shortage in Ethiopia for year 2007/08.

Month	Actual ICS energy (GWH)	Energy shortage (GWH)	Total system demand (GWH)	Estimated energy production for AWF (GWH)	System capacity with wind (GWH)
Sep_07	288.4	0	288.4	18.4	306.8
Oct_07	295.9	0	295.9	33.2	334.6
Nov_07	298.8	0	298.8	40.9	341.4
Dec_07	303.3	0	303.3	41.5	346.9
Jan_08	308.3	0	308.3	39.6	350.9
Feb_08	304.6	0	304.6	38.5	344.5
Mar_08	293.063	12.412	305.5	43.8	337.7
April_08	281.487	17.4	298.9	41.2	324.2
May_08	252.451	39.1	291.5	23	283.9
June_08	276.696	7.2	283.9	18.4	301.9
July_08	306.112	0.352	306.5	2.8	308.9
Aug_08	312.24	0	312.2	19.5	338.9
Total	3521.394	76.4	3597.8	360.2	3881.6

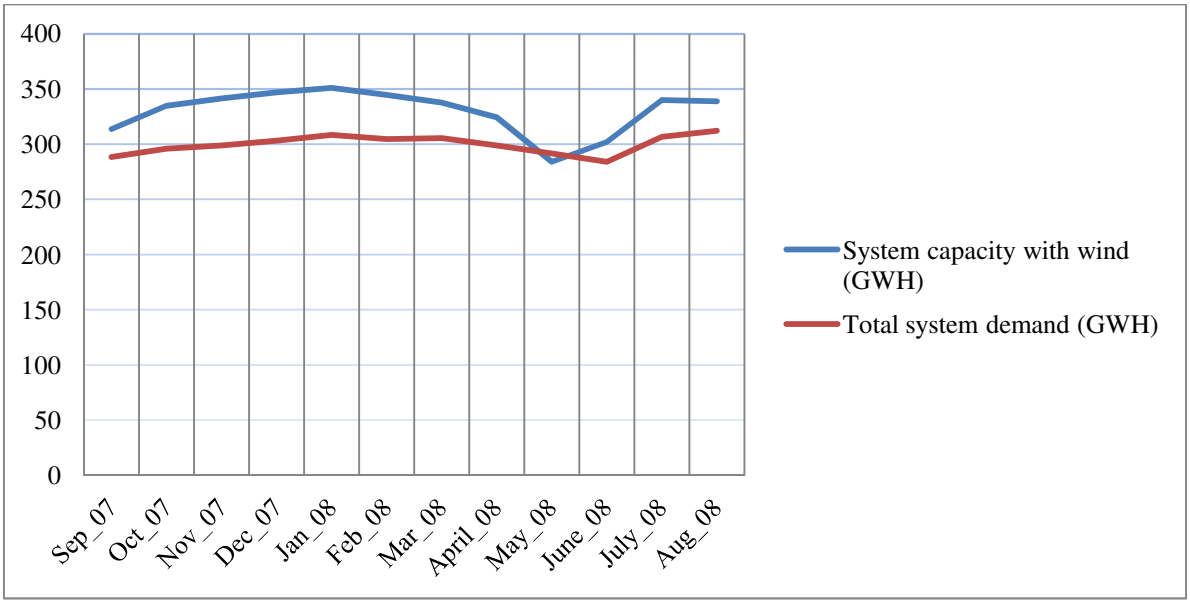

Figure 4.9.System power generating capacity with out and with wind farm

4.3. Wind Power Forecasting

Forecasting model of wind power from AWF that can be used to predict wind power output for a day head using past statistical data of wind output has been developed.

A day head forecast is highly significant during generation planning in order to reduce discrepancy between the schedule generation and actual generation on a daily basis of operation.

In this thesis work, a forecasting model is developed using Box-Jenkins method on the basis of past historical data of wind output power. The procedure followed are during modeling work are

1. Data preparation
2. Model identifications
3. Parameter estimation
4. Model diagnosis, and
5. Forecast evaluation

Each steps followed are discussed step by step in the following sections.

i. Data Preparation

In data preparation stage the sanity of data, that is, outliners, missing data and stationary of the sample data is checked and corrected appropriately. Box-Jenkins bases their theory on the stationarity. Therefore, if the data is not stationary, it has to be converted to stationary. One method of observing either the data is stationary or not is plotting the time sequence of sample data. The other method of checking the stationary is using estimated autocorrelation function of sample data characteristic.

A ten minute wind speed data of year 2007 is taken and the hourly wind speeds are extracted from the sample to have hourly wind speed data. Before calculating corresponding wind power output, the wind speed is transferred to hub height (70 m) using the following equation,

$$\frac{V_o}{V_h} = \left(\frac{H}{H_o}\right)^{\alpha} \quad 4.2.$$

Where: V_h is the wind speed at height H, V_0 is the wind speed at height H_0 (a reference height of 10 m), and α is power law coefficient. The power law coefficient value is taken from [23], which is equal to 0.8114.

Finding the corresponding wind speed at hub height, power output for a single wind turbine is estimated using manufacture power curve and rescaled to wind farm output level assuming that there is similar wind speed distribution in the wind farm.

After calculating the power output for hourly wind speed data, stationarity is checked for wind output power data using time sequence plot and estimated autocorrelation functions. The time sequence plot and autocorrelation function plots are shown in figure 4.10 and figure 4.11 respectively.

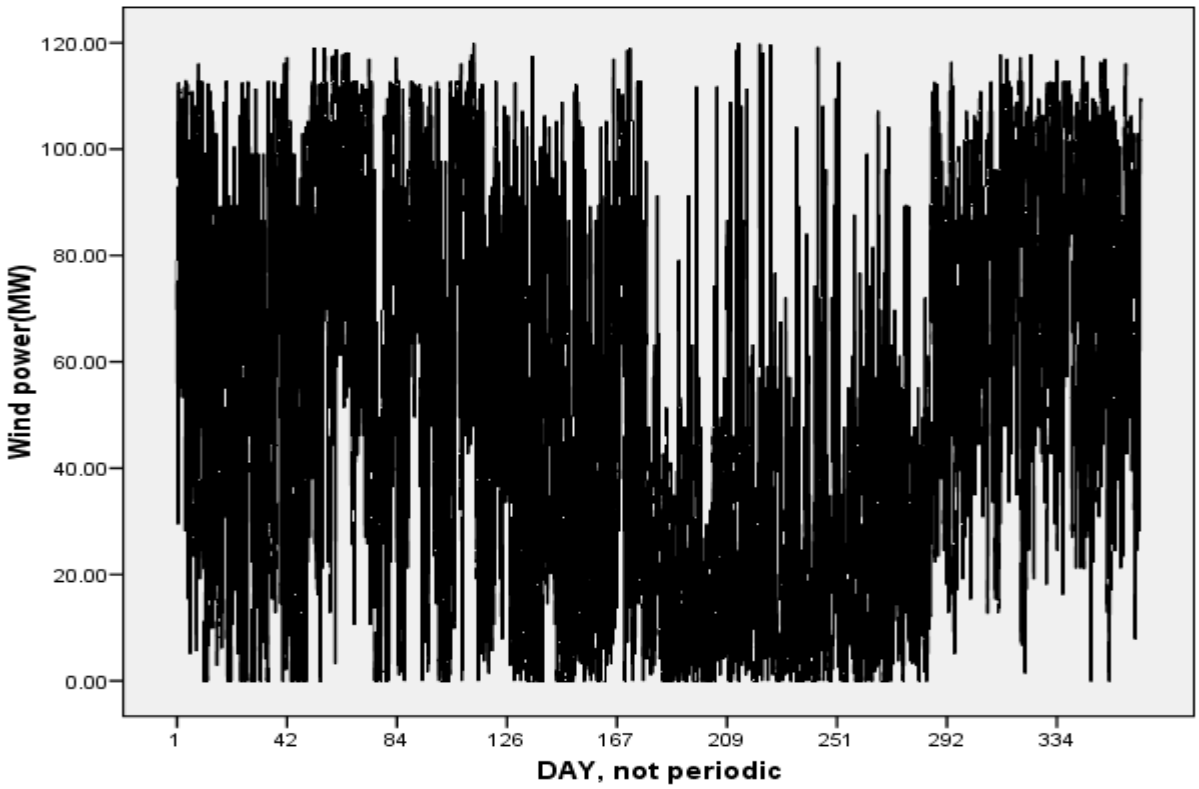

Figure 4.10.Time sequence plot of the sample data

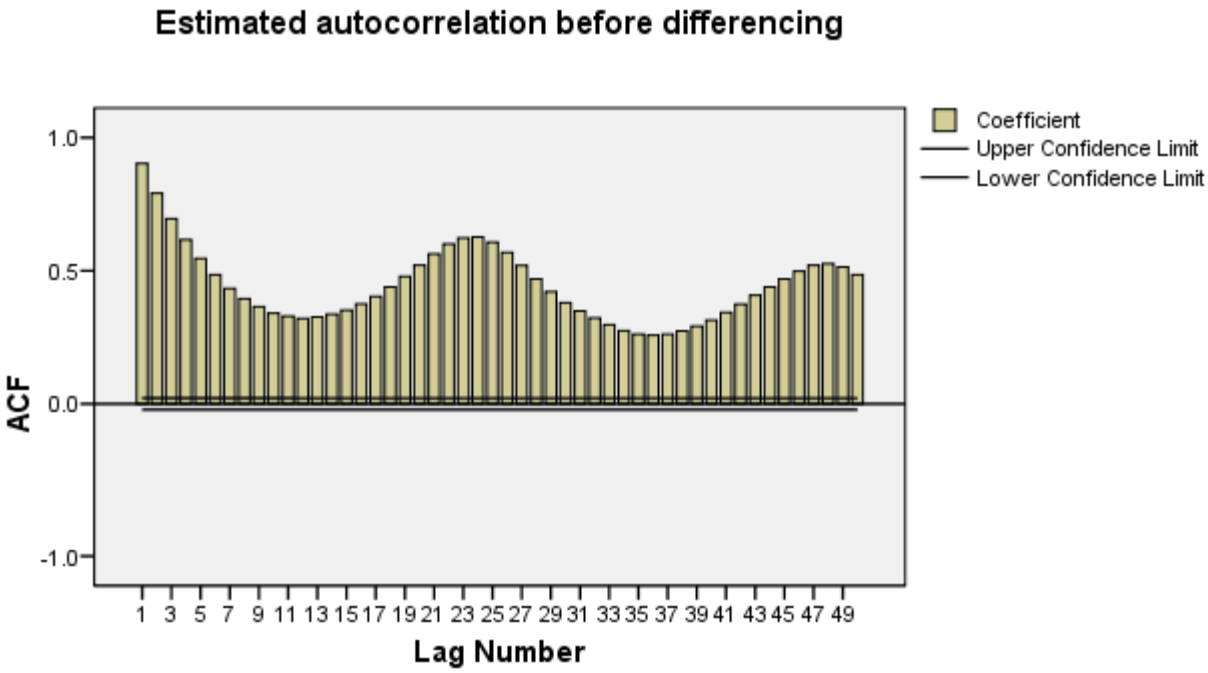

Figure 4.11. ACF of sample data

As we see from the estimated autocorrelation function plots in figure 4.11, the magnitude of the autocorrelation function doesn't decay soon. Such property would suggest us the sample data is not stationary.

The other important information what we can observe is that the type of non stationary. It has a significant magnitude at lag number 1, 24, 48..., with a periodicity of 24. Therefore, there is a strong correlation between sample data 24n (where n is equal to 0, 1, 2...,).

Box-Jenkins suggests that non-stationary data can be converted to stationary using differencing methods. In practice, first order or at most second order seasonal (ordinary) differencing is applied to make stationary. As there is no options available in SPSS to determine the order of differencing, a possible combination of ordinary and seasonal differencing is applied, that is, ordinary differencing only, seasonal differencing only and combination of ordinary and seasonal differencing.

Differencing only ordinary or seasonal will make the sample data stationary as shown in time sequence plot of the time series in figure 4.12 and figure 4.13.The time sequence plot after differencing has a constant mean around zero.

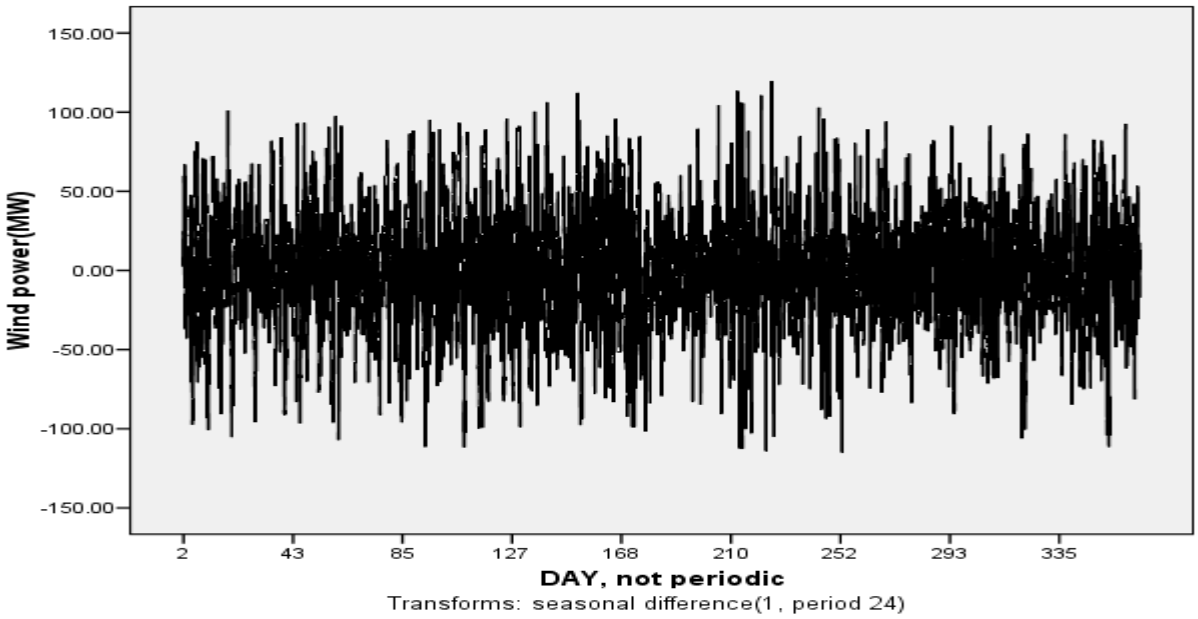

Figure 4.12. Time sequence plot after first order seasonal differencing.

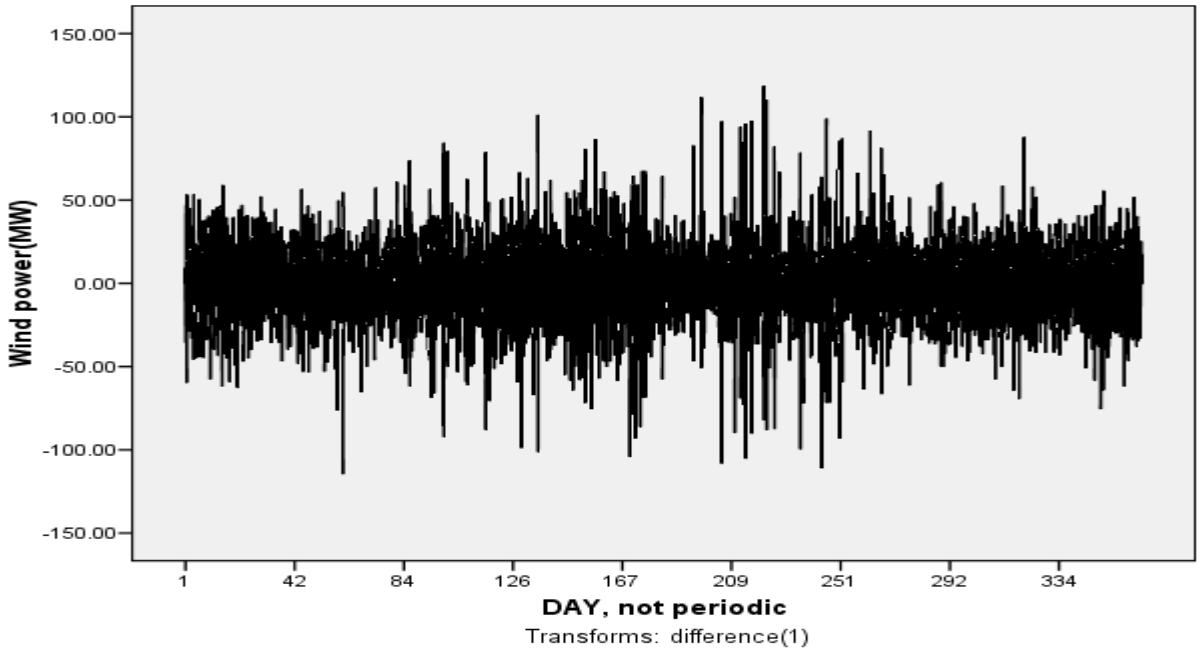

Figure 4.13. Time sequence plot after first order ordinary differencing.

ii. Model Identification

In model identification stage order of the model is identified. As per Box-Jenkins, we can estimate the order of the model using partial correlation function and autocorrelation functions in combination.

First using the above time series found in data preparation stage two models are developed (i.e., one with seasonal differenced and other with ordinary differenced samples). Then, the orders of the models are estimated for both samples independently. Next I will discuss step by step how the order of the model estimation made for each samples.

A. Case one: Seasonally Differenced Time Series Model

The autocorrelation and partial autocorrelation function plot of the seasonally differenced time series has an exponentially decaying autocorrelation function and a partial autocorrelation function that has one significant peak value only at lag number one as shown in figure 4.14 and figure 4.15 respectively.

An exponential decay of autocorrelation function and an oscillating decaying of partial autocorrelation function is a characteristic of mixed model, which means; it is neither only autoregressive nor a moving average process. It is a mixed model of first order autoregressive and a first order of moving average process," SARIMA (1, 0, 1) $(0, 1, 0)_{24}$", which has a first order positive parameter of autoregressive and a negative parameter of moving average model. The form SARIMA $(1, 0, 1)(0,1,0)_{24}$ is given by as follows

$$(1 - \emptyset_1 B)(1 - B^{24})^D Y_t = (1 + \theta_1 B)e_t$$

Where Φ_1 is the parameter of Autoregressive process and θ_1 is the parameter of moving averaged, D is order of seasonal difference.

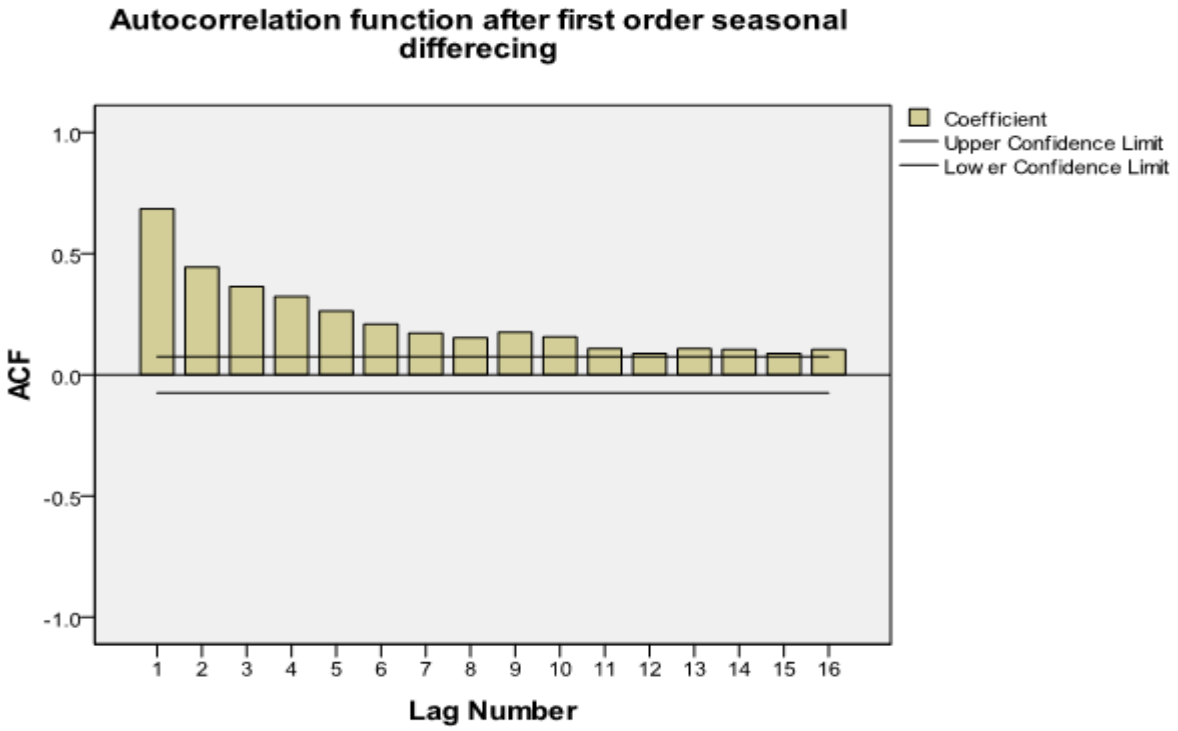

Figure 4.14.ACF first order seasonal differencing

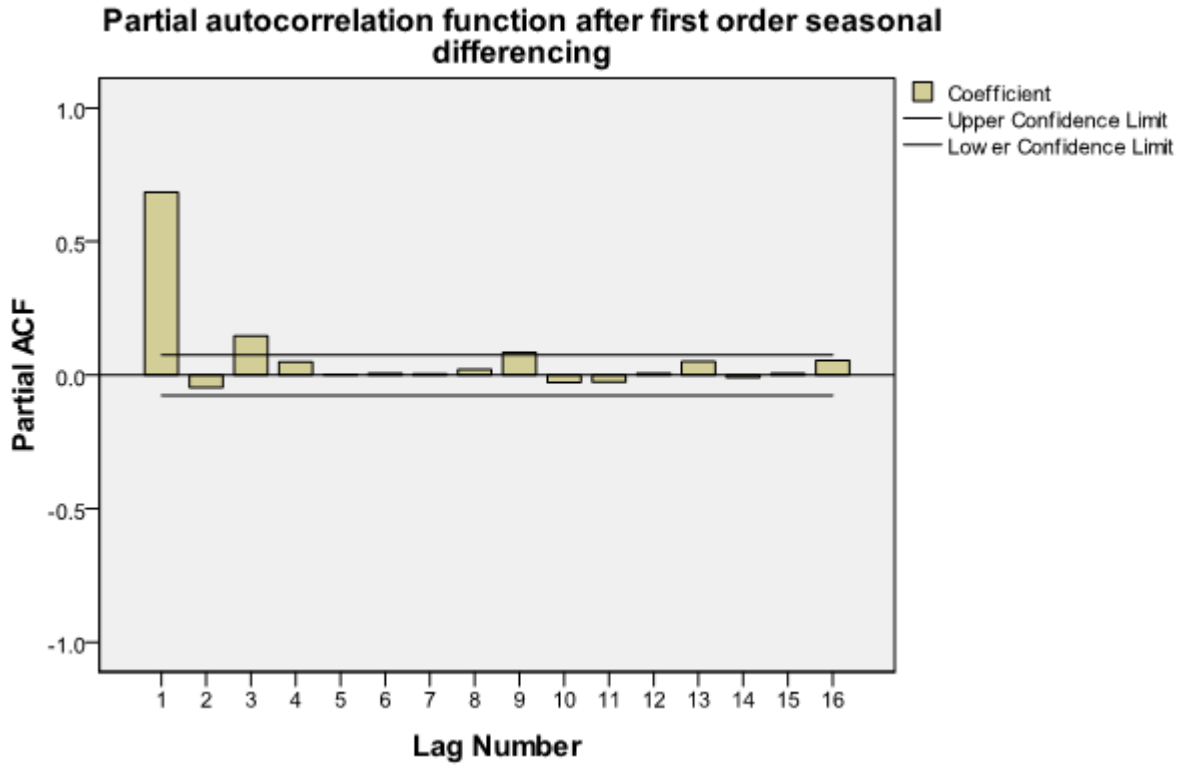

Figure 4.15. PACF after first order seasonal differencing.

B. Case two: Ordinary Differenced Time Series Model

For ordinary differenced case there are two negative spikes of autocorrelation function and exponentially decaying of negative spikes partial autocorrelation function as shown in figure 4.16 and figure 4.17.Such function suggests a second order moving average process only with two positive parameters. A second order moving average is given by as follows

$$(1 - B)^{d}Y_t = (1 + \theta_1 B + \theta_2 B^2)e_t$$

Where θ_1 and θ_2 are the parameters of moving average process.

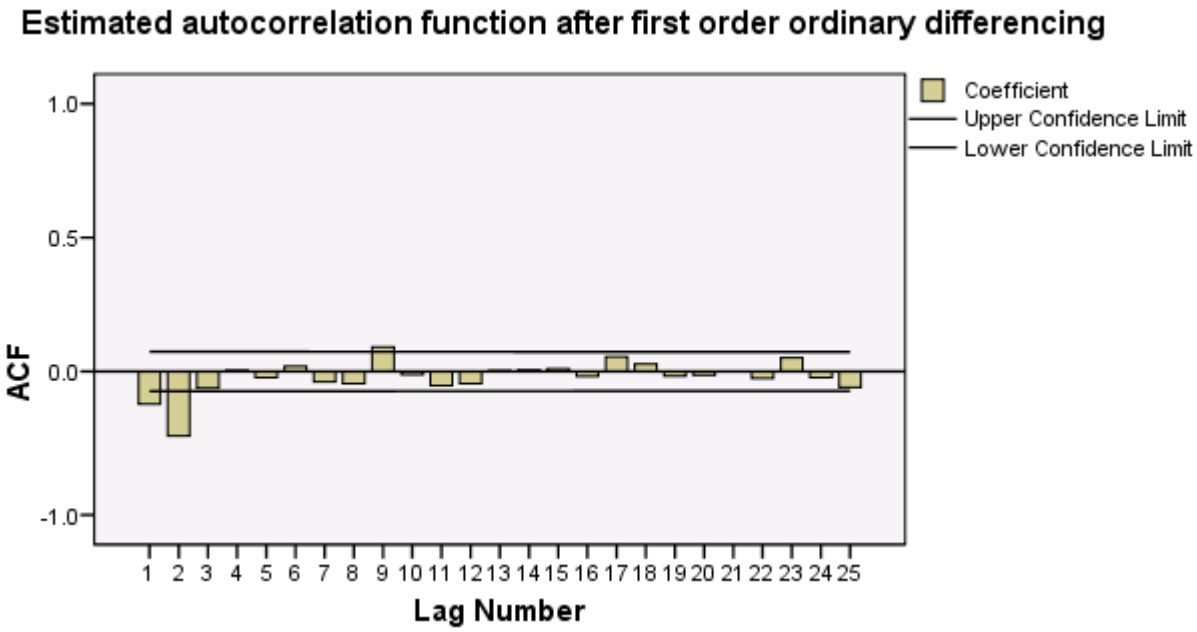

Figure 4.16. ACF after first order ordinary differencing.

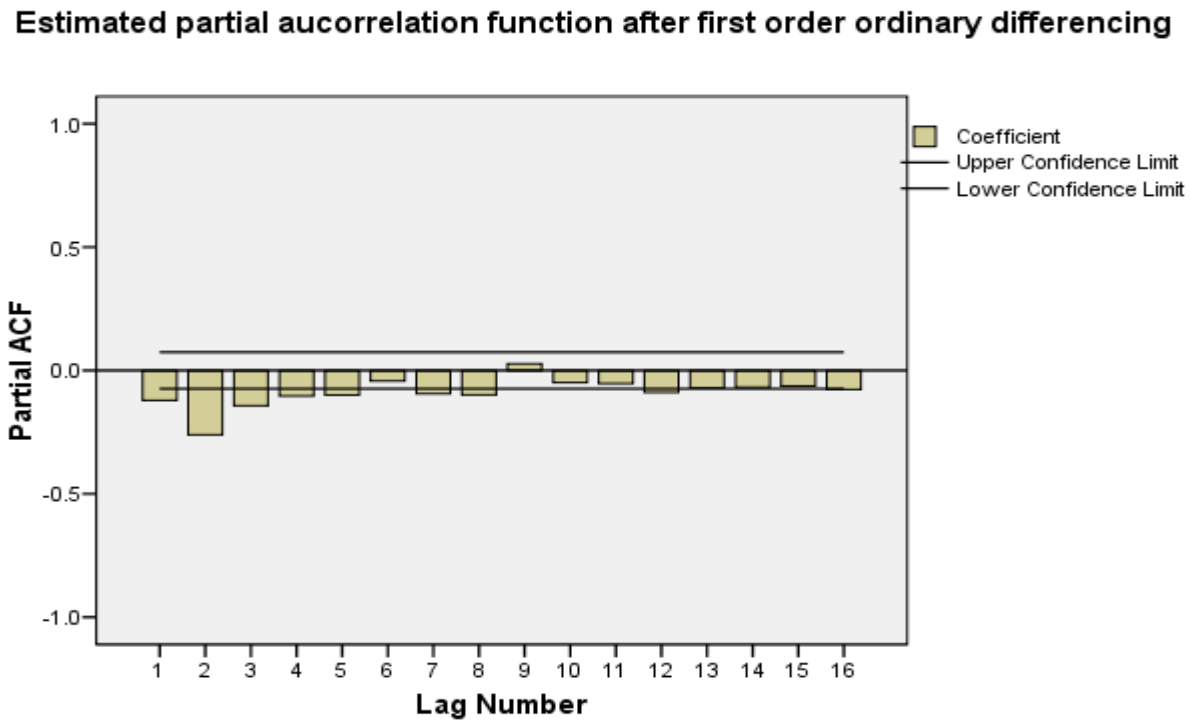

Figure 4.17.PACF after first order ordinary differencing.

Now the order of the model is identified for each case. The next step is estimating the parameters of each model in the next steps.

iii. Parameter Estimation

Under parameter estimation the values of Φ and θ is estimated for the identified models. Estimation of the parameter is made using SPSS software. The estimated values of the parameter for model SARIMA (1, 0, 1) $(0, 1, 0)_{24}$ is given in table 4.10.

Table 4.10. Estimated parameters of SARIMA (1, 0, 1) $(0, 1, 0)_{24}$

Difference	Model type: SARIMA (1, 0, 1) $(0, 1, 0)_{24}$	Estimated Parameter
Seasonal only	Constant	-0.0026
	AR Lag1	0.734
	MA Lag1	0.107

Hence, the SARIMA (1, 0, 1) $(0, 1, 0)_{24}$ will be written as follows;

$$(1 - 0.734B)(1 - B^{24})^{D}Y_t = (1 + 0.107B)e_t \quad ; \text{ where } \{e_t\} \sim WN(0, \sigma^2)$$

$$Y_t - Y_{t-24} = 0.734Y_{t-1} + 0.734Y_{t-25} + e_t + 0.107e_{t-1}$$

The estimated parameters for model IMA (2) is given in table 4.11.

Table 4.11.Estimated parameters of IMA (2)

Difference	Model type : IMA (2)		Estimated Parameter
Ordinary only	Constant		0.004
	MA	Lag1	0.14
		Lag2	0.084

Hence, the MA (2) will be written as follows;

$$(1 - B)Y_t = (1 + 0.14B + 0.084B^2)e_t$$

$$Y_t - Y_{t-1} = e_t + 0.14e_{t-1} + 0.084e_{t-2}$$

Now the parameters of the models are indentified. The next step is diagnosing the models in the next section.

iv. Model Diagnosis

The model selected in the identifications stage now diagnosed using parameter over fitting and residual analysis.

In over fitting analysis the model is fitted by one order extra and the statistical evaluating indexes are observed. If the statically evaluating values are better than the previous model the latter one taken as a temporary model. The process continued iteratively until any further increment doesn't bring improvement on statistical values.

In residual analysis, first the residuals are calculated from predicted and actual values taking their difference. Then, estimating the autocorrelation of the residual it is plotted to see that the residuals are a white noise process. If the model fit well the observed data, the

residual autocorrelation function plot doesn't have any significant spike. Figure 4.18 shows the residual autocorrelation and partial autocorrelation plot from model IMA (2).

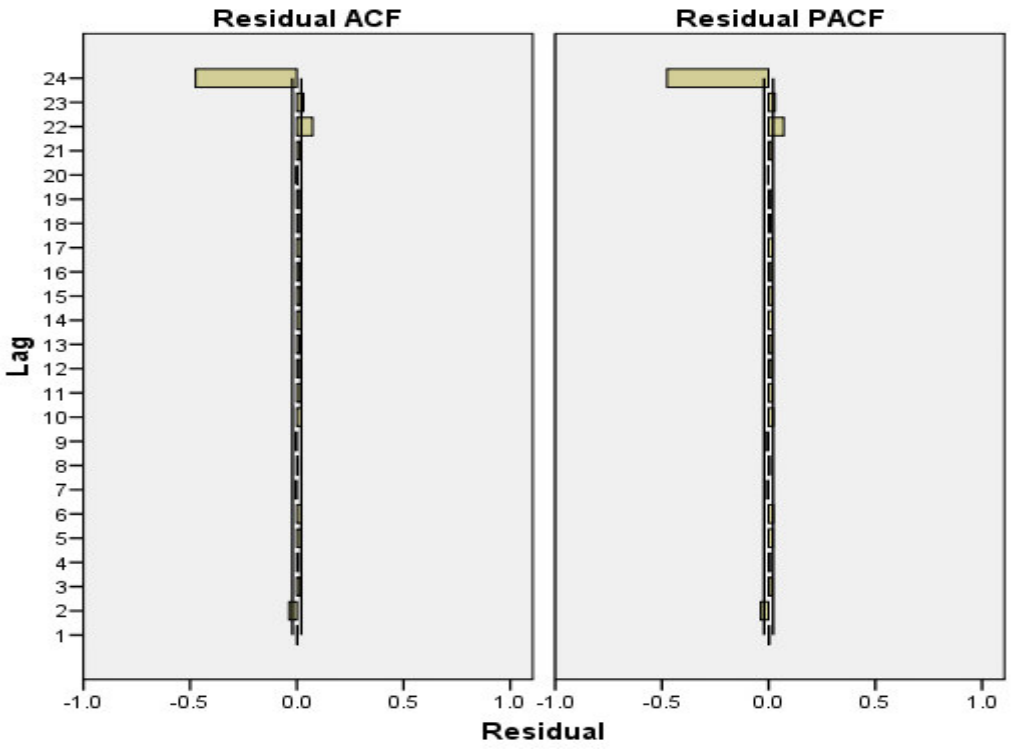

Figure 4.18.Residual ACF of IMA (2)

As we can see from figure 4.18, there is a significant spike at lag number 22 and 24. This significant spike suggests that there is information which is not accounted by the model, especially spike at lag number 24 will indicate that there is a seasonal component which is not accounted by the model. This spike cannot be removed only by increasing non seasonal components i.e. non-seasonal AR or non-seasonal MA process. The better way to remove the spike is increasing the seasonal parameters. Therefore, I terminate model developing process for ordinary differenced sample here. The next discussion is about the model diagnosis of seasonal differenced data only.

In order to avoid the spike at lag 24 the original model of SARIMA (1, 0, 1) $(0, 1, 0)_{24}$ is over fitted by adding seasonal moving process of orders two as shown in figure 4.19.

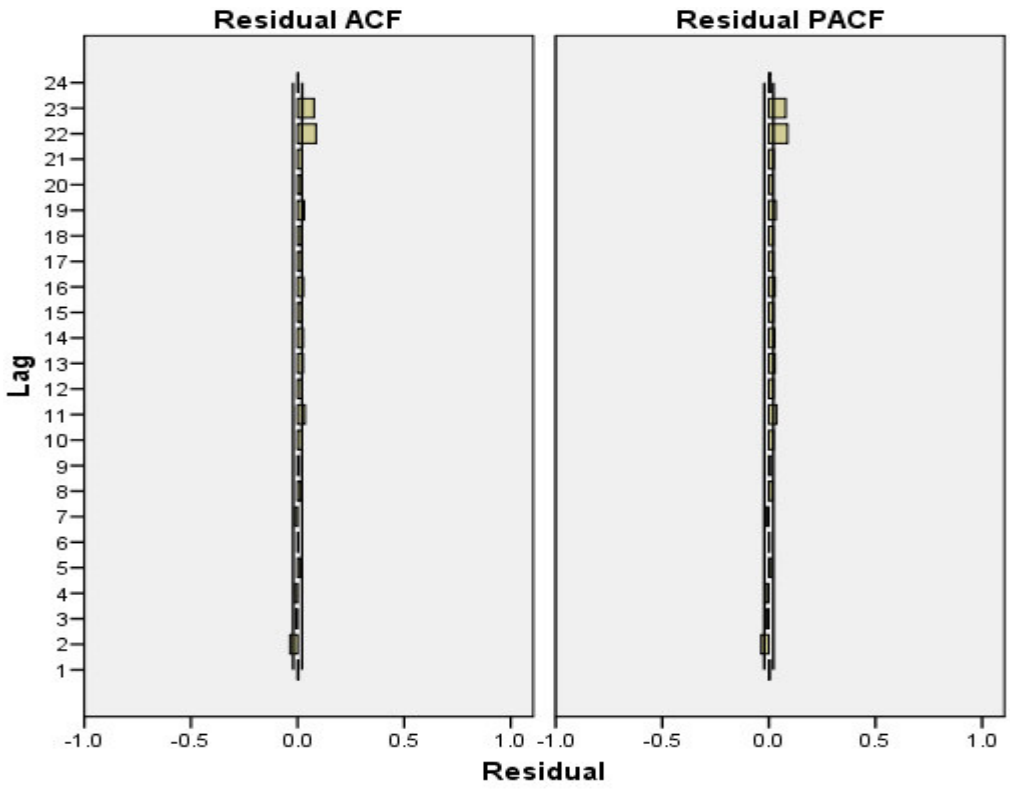

Figure 4.19.Residual ACF of ARIMA (1, 0, 1) $(0, 1, 2)_{24}$

Model SARIMA (1, 0, 1) $(0, 1, 2)_{24}$ has a good performance as compared to model SARIMA (1, 0, 1) $(0, 1, 0)_{24}$ as shown in figure 4.19. Especially it avoids seasonal components. However, still it needs an improvement as there are spikes at lag 22 and 23 as shown in figure 4.19.

To remove spike at lag number 22 and 23, the order of non-seasonal component of AR process increased to order 23 and the autocorrelation function is plotted once again. As can be seen from figure 4.21, the spike at lag number 22 and 23 is removed.

During this modeling work, a number of models are diagnosed by increasing each component step by step and observing the MAE, RMSE and R-squared values. The result which has been diagnosed is summarized in table 4.12.

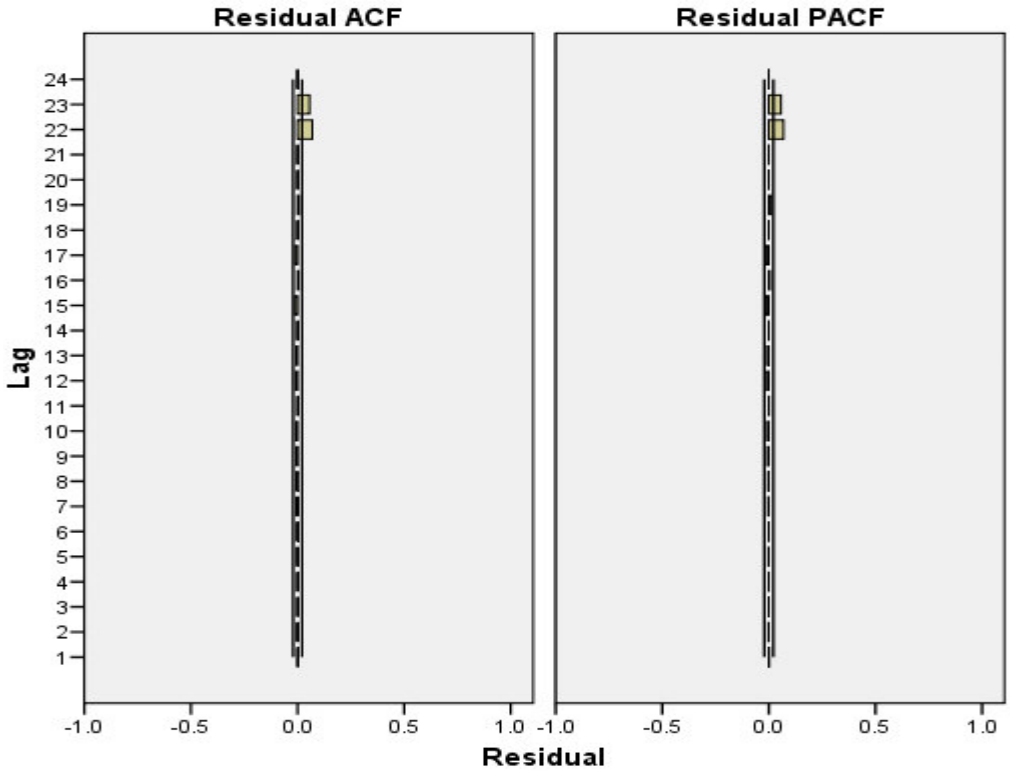

Figure 4.20.Residual ACF and PACF of model ARIMA (2, 0, 7) $(1, 1, 2)_{24}$

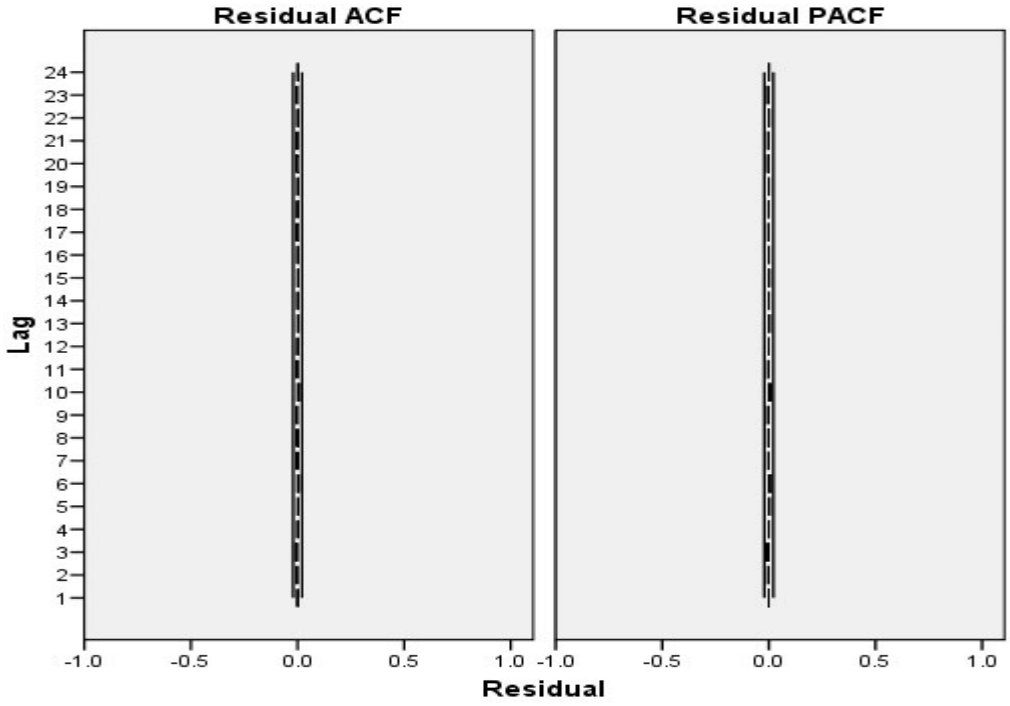

Figure 4.21.Residuals ACF and PACF of model ARIMA (2, 0, 23) $(1, 1, 2)_{24}$

Table 4.12. Diagnosed models

Model No.	ARIMA Model	MAE	RMSE	R-squared
1	p=1,d=0,q=1, P=0,D=1,Q=0	22.532	16.327	0.597
2	p=1,d=0,q=1, P=0,D=1,Q=1	17.019	12.405	0.769
3	p=1,d=0,q=1, p=0,D=1,Q=2	17.002	12.395	0.769
4	p=1,d=0,q=1, P=1,D=1,Q=1	17.001	12.395	0.679
5	p=1,d=0,q=1, P=2,D=1,Q=1	16.996	12.394	0.769
6	p=2,d=0,q=1, P=2,D=1,Q=1	16.822	12.262	0.77
7	p=3,d=0,q=1, P=2,D=1,Q=1	16.822	12.26	0.744
8	p=2,d=0,q=3, P=2,D=1,Q=1	16.821	12.293	0.774
9	p=2,d=0,q=5, P=0,D=1,Q=0	16.822	12.257	0.774
10	P=2,d=0,q=7, P=2,D=1,Q=1	16.751	12.24	0.776
11	P=2,d=0,q=23, P=2,D=1,Q=1	16.774	12.208	0.777

As can be seen from table 4.12, two models (model number 9 and 10) have lower values of MAE, RMSE and R-squared values as compared to other models. Therefore, these two models are selected as a final model to be evaluated their performance in terms of forecast accuracy.

- SARIMA$(2,0,7)(2,1,1)_{24}$
- SARIMA$(1,1,2)\ (2,0,23)(2,1,1)_{24}$

vi. Forecast Evaluation

In the forecasting evaluation stage, future values of the time series will be forecasted based on the selected SARMA model from previous stage and their forecast accuracy evaluated to select the best model out of the two.

First a two month data prepared one from Oct-11-08 to Nov- 09-08 and another from Nov-10-08 to Dec -09 -08.Then using first sample data, Oct 11-08 to Nov- 09-08, as past historical data forecasting of a day head using the developed model is simulated for the

next month, Nov-10-08 to Dec-09-08.During each simulation the first sample is shift forward by one day before making the next simulation; for example to forecast for Nov-10-08 , a data from Oct-11-08 to Nov-09-08 is used. For the next forecast simulation a sample data from Oct-2-08 to Nov -0-08 is used by shifting one day forward as shown in figure 4.22.

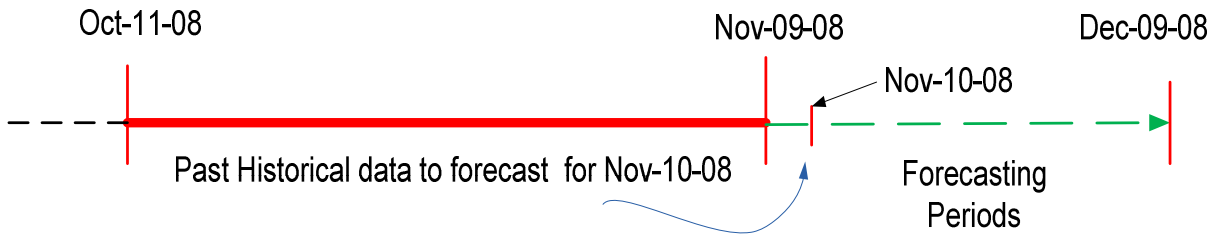

Figure 4.22. Data setup for forecast accuracy evaluation.

Once a forecast data for one month, Nov-09-08 to Dec-09-08, has found from forecast simulation, mean absolute error is calculated using equation 4-3

$$\mathrm{MAE} = \sum_{t=1}^{T} \frac{|e_t|}{T} \qquad 4.3.$$

MAE is plotted for time horizon of 6Hr, 12Hr, 18Hr and 24Hr to see forecast performance of the model when forecast horizon increases; see table 4.13.

Table 4.13. Mean absolute errors of selected models

Forecast Length	Mean absolute error for each model		
	SARIMA(2,0,23)$(2,1,1)_{24}$	SARIMA(2,0,7)$(2,1,1)_{24}$	Persistence Method
6Hr	3.756	3.818	27.88
12Hr	9.159	9.36	32.639
18Hr	13.628	14.197	26.766
24Hr	16.41	17.34	20.688

As can be seen from figure 4.23, as forecast length increases the mean absolute error increases , too.

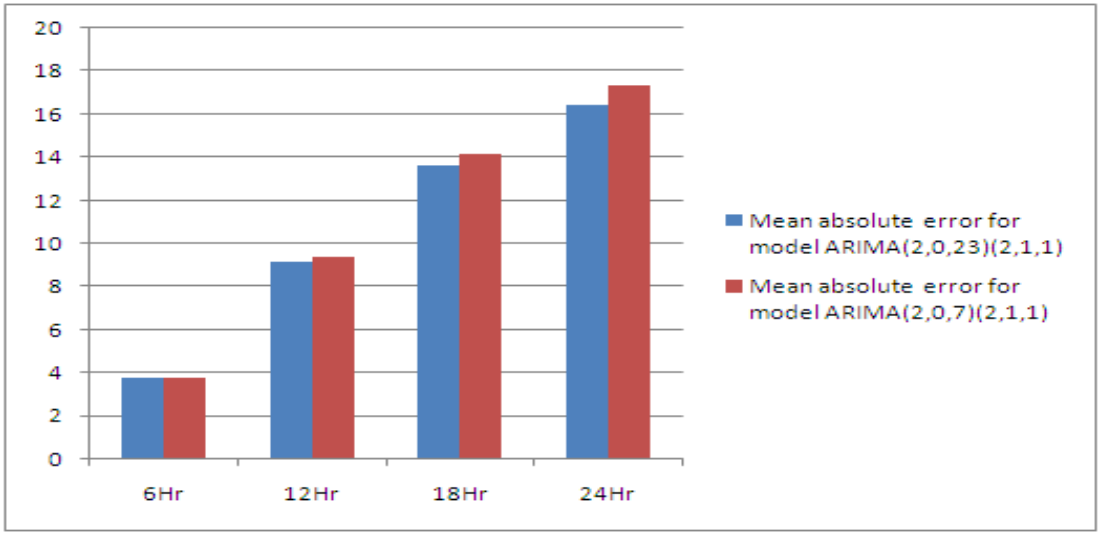

Figure 4.23.Mean absolute error of the models.

The mean absolute error is often normalized as percentage of the rated capacity of the wind farm or the average energy production over the analysis period. In this investigation mean absolute error is normalized by rated capacity using equation (4.4) as follows;

$$\mathrm{MAE} = \frac{\frac{1}{T}\sum_{t=1}^{T}(|\mathrm{Power}_{forcast} - \mathrm{Power}_{Actual}|)}{\text{Rated Power}} x100\% \qquad 4.4.$$

Where rated capacity of the plant is 120MW and T is total number of data point (720). During this time the model also compared with persistence method which is often used as a base model to compared forecast performance of model developed, the values obtained is summarized in table 4.14.

Table 4.14.Percentage Mean absolute errors of selected models

Forecast Length	Mean absolute percentage error (%) for each model		
	$SARIMA(2,0,23)(2,1,1)_{24}$	$SARIMA(2,0,7)(2,1,1)_{24}$	Persistence Method
6Hr	3.13	3.18	23.23
12Hr	7.63	7.8	27.2
18Hr	11.36	11.83	22.31
24Hr	13.68	14.45	17.24

The model can achieve an accuracy of 13.68% MAE for day-ahead forecasting using model SARIMA (2, 0, 23) $(2, 1, 1)_{24}$.

In all cases of forecast horizon, the models developed have a superior performance as compared to persistence method. Forecast accuracy comparison with model of persistence is called skill scores, which is defined as

$$SS = \frac{MAE_{Persistace} - MAE_{Model}}{MAE_{Persistace}} \quad 4.5.$$

Skill scores measures the scatter of the model error compared to the scatter of the persistence model. A skill score close to one indicates very small scatter of the model error, score close to zero indicate that the model does not perform better than the persistence model and scores below zero indicate that the persistence model outperforms the model, that is, the model cannot be used.

Table 4.15. Skill score of selected model

Forecast Length	Skill Score for each model	
	SARIMA(2,0,23)$(2,1,1)_{24}$	SARIMA(2,0,7)$(2,1,1)_{24}$
6Hr	0.865	0.863
12Hr	0.72	0.713
18Hr	0.49	0.47
24Hr	0.207	0.162

Both models have skill score close to one for forecast length of 6Hr and 12Hr and it will be close to zero for forecast length of 18Hr and 24Hr.

4.4. Ashegoda Wind Farm Modeling

Ashegoda wind farm consist of six clusters each contains different number of groups which in turn contains two or more turbines. The project has three phases; first phase will connect 30 MW generations, second and third phase of the project each 45 MW.

As micro - sitting for each wind turbine in cluster number one and two have already finalized. Therefore, the actual distance between each wind turbine is taken to determine the cable length of collector circuit. However, the conductor size and rating is not given. Appropriate cable size has been determined based on the group which contains maximum number of wind turbine.

For second and third phases of the project only the number of clusters, the number of groups in each cluster and the number of wind turbine connected in groups is determined. The spacing between each wind turbine and the rating of cable is not determined. Therefore, to determine the collector impedances a standard value of distance between each wind rotors has been selected.

When several turbines are installed in clusters, the turbulence due to the rotation of blades of one turbine may affect the nearby turbines. In order to minimize the effect of this rotor induced turbulence, a spacing of 3 to 5 times rotor diameter is provided within the rows. Similarly, the spacing between the rows may be around ten time rotor diameter. So that, the wind stream passing through one turbine is restored before it interacts with the next turbine. These spacing may be further increased for better performance, but may be expensive as we require more land and other resources for farther spacing. In this thesis work, a spacing of five times a rotor diameter is assumed. The procedure followed to model the wind farm is demonstrated using cluster two and the final values for the rest of clusters have summarized in tabular form.

i. Cable Modeling

Underground cables are used to take power from each wind turbine. The maximum number of wind turbine connected in the group is not more than fourteen. The cable which carries power from each cluster to the central substation is between 21 MW and 30 MW. The required cable size and rating is determined based on a rating value of 15 MW and 30 MW using;

$$I = \frac{S}{\sqrt{3}V_{LL}} \qquad 4.6.$$

Where the S is the apparent power and V_{LL} is the line voltage of the cable (33 kV).

The cable must be able to handle the maximum active and reactive power that can be generated in the wind farm. The maximum amount of active power generated by cluster wind turbines is 12 MW and the maximum reactive power for rated operation is 2.86 MVAR. For underground cable the current rating is calculated as;

$$I_{underground\_cable} = \frac{15}{\sqrt{3}x33} x10^3 = 262.4A$$

And for overhead cable

$$I_{overhead\_cable} = \frac{30}{\sqrt{3}x33} x10^3 = 525A$$

Appropriate cable size and cable parameter for the above current loading is taken from ABB [24]. Cables with a conducting area of 95 mm^2 and 150 mm^2 is chosen for underground and overhead cables respectively.

The selected for underground cable has 250 A at 65º and 300 A at 90º and the overhead cable has the rating of 430 A at 65º and 580 A at 90º. The resistance, capacitance and resistance of the cables are shown in table 4.16.

Table 4.16. Cable parameters

Cable type	Cross-Section (mm^2)	Current rating of conductor (A)		Capacitance (μ F/ kM)	Inductance (mH/ kM)	Resistance (Ω / kM)
		65º	90º			
Underground	95	250	300	0.17	0.43	0.247
overhead	300	430	580	0.25	0.36	0.0769

.

Once the parameters of the cable determined it has to be modeled as a π-equivalent circuit in order to use PSS/E as simulating software. The π-equivalent value of the cable is summarized in table 4.17.

Table 4.17. Summary of selected cables parameters in per unit

Cable type	Cross-section (mm2)	Xc (p u)	X_L (pu)	R (pu)	B (pu)
Underground	95	1719.38	0.0124	0.247	0.000582
Overhead	300	1169.18	0.01038	0.0769	0.000855

4.4.1. Modelling of Cluster Two of Ashegoda Wind Farm

Cluster two has two groups each with five and seven wind turbine connected in parallel, see figure A.1 in appendix A. The distance between each wind turbine within the group is given in table B.1 in appendix B. The modeling procedure is done in five steps.

1. Equivalency of Pad mounted transformers
2. Equivalency of collector circuit
3. Equivalency of shunt admittance
4. Model verification.

All steps are discussed in the following section step by steps and results for other clusters summarized in tables.

A. Step one (equivalency of pad mounted transformers)

Equivalency of group three pad mounted transformers has been shown and summarized result for the rest of clusters is shown in appendix c.

Equivalence of pad mounted transformer is made using equation 3.52,

$$Z_{TS} = \frac{\sum_{m=1}^{n} p_m^2 z_{Tm}}{[\sum_{m=1}^{n} P_m]^2} \ \Omega$$

The resistive component of pad mounted transformer is determined using equation 4.7 and the reactive component is determined using equation 4.8 as follows.

$$R_{TS} = \frac{U_{Rr} x U_{rt}^2}{100 x S_{rT}} \ \Omega \qquad 4.7.$$

And

$$X_{TS} = \frac{U_{Xr} x U_{rt}^2}{100 x S_{rT}} \ \Omega \qquad 4.8.$$

Where U_{Rr} is rated resistive voltage drop (%)

U_{Xr} is rated reactive voltage drop (%)

U_{rT} is transformer primary voltage (69 kV)

S_{rT} is transformer apparent power (1.25 MVA)

The value of rated resistive voltage drop (U_{Rr} = 1.3 %) is taken from [25]. Then, the value of reactive voltage drop (U_{Xr}) is calculated as follows.

$$U_{Xr} = \sqrt{U_{Kr}^2 - U_{Rr}^2} \qquad 4.9.$$

Where U_{Kr} is the short circuit impedance of pad mounted transformer. The value of U_{Kr} is taken from the manufacturer data (equal to 6%).Substituting the values,

$$U_{Xr} = \sqrt{6^2 - 1.3^2} = 5.86\ \%$$

Hence, the resistance component of pad mounted transformer impedance will be

$$R_{TS} = \frac{1.31 x 0.69^2}{100 x 1.25} = 0.00499\ \Omega$$

The reactance component of pad transformer impedance will be

$$X_{TS} = \frac{5.85 x 0.69^2}{100 x 1.25} = 0.0223\ \Omega$$

i. Group Three Pad Mounted Transformers

Group three pad mounted transformer has five transformers as shown in figure 4.24. Figure 4.24 (A) shows before equivalency and figure 4.7 (B) shows the equivalence circuit of group-three pad mounted transformers.

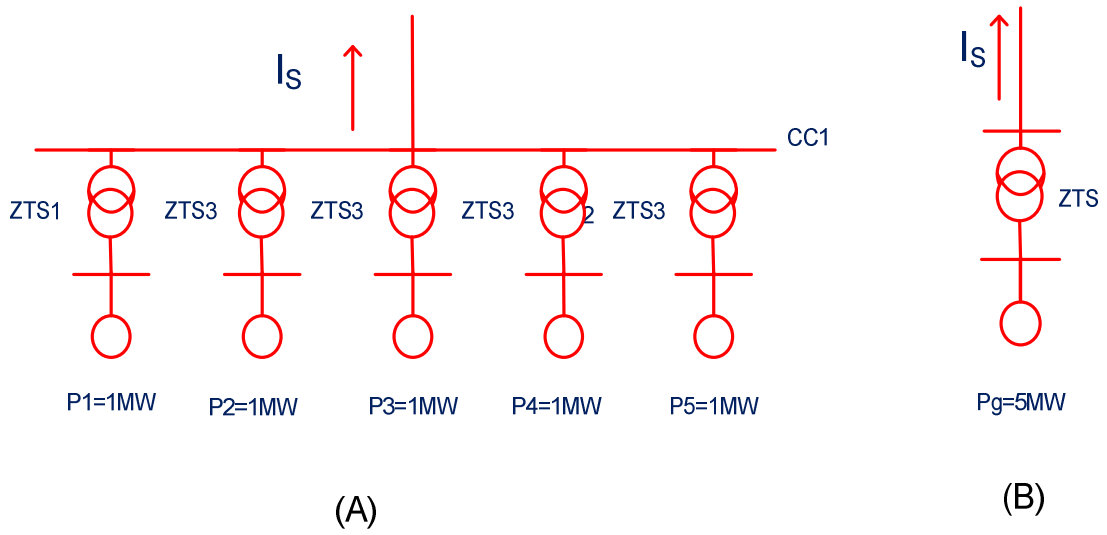

Figure 4.24. (A) full representation and figure, (B) equivalence of full transformer representation

Applying equation 3.52,

$$Z_{TS} = \frac{P_{01}^2 Z_{TS1} + P_{02}^2 Z_{TS2} + P_{03}^2 Z_{TS3} + P_{04}^2 Z_{TS4} + P_{05}^2 Z_{TS5}}{(P_{01} + P_{02} + P_{03} + P_{04} + P_{05})^2}$$

Where $Z_{TS1}=Z_{TS2}= Z_{TS3}= Z_{TS4}=Z_{TS5}$ are transformer leakage reactance, and

$P_{01}=P_{02}= P_{03}= P_{04}=P_{05}$ are the rated power from each wind turbine

Hence, the equation will be reduced to

$$Z_{TS} = \frac{5xZ_{TS1}}{[5xP_1]^2} = \frac{Z_{TS1}}{n}$$

Substituting the value of Z_{TS1} and P_1

$$Z_{TS} = \frac{0.00499 \ + \ j\,0.0233}{5} \ = \ 0.001 \ + \ j\,0.00446 \ pu$$

In per unit,

$$Z_{TS} = \frac{1.25}{0.69^2}(0.001 \ + \ j\,0.00446\,) = \ 0.002625 \ + \ j\,0.0117 \ pu$$

ii. Group Three Pad Mounted Transformers

Similarly for group four, equivalence impedance will be;

$$Z_{TS} = \frac{0.00499 \ + \ j\,0.0233}{7} \ = \ 0.000713 \ + \ j\,0.00319 \ \ pu$$

In per unit,

$$Z_{TS} = \frac{1.25}{0.69^2}(0.00713 \ + \ j\,0.00319\,) = \ 0.00187 \ + \ j\,0.00836 \ \ pu$$

B. Step Two (equivalency of shunt impedances)

Equivalency of shunt impedances is calculated using equation 3.52.

$$B = \sum_{i=1}^{n} B_i$$

i. Group Three Shunt Impedance

$$B_{G3}=5x7.212=36.06\ \mu S$$

ii. Group Four Shunt Impedance

$$B_{G4}=7x7.212=50.484\ \mu S$$

C. Step three (equivalency of collector circuit)

Here the collector circuit of group three and four is equivalence using equation 3.42, as follows.

$$Z_S = \frac{\sum_{m=1}^{n} p_{Zm}^2 z_m}{[\sum_{m=1}^{n} P_m]^2} \ \ \Omega$$

i. Group Three Collector Circuits

Since in group three we have five we wind turbine, the equation will be

$$Z_{CCG3} \ = \frac{P_{01}^2 Z_{01} + P_{02}^2 Z_{02} + P_{03}^2 Z_{03} + P_{04}^2 Z_{04} + P_{05}^2 Z_{05}}{(P_{01} + P_{02} + P_{03} + P_{04} + P_{05})^2}$$

Where Z_{01}, Z_{02}, Z_{03} and Z_{04} are the branch impedance between each wind turbines (W_{T19}-W_{T20}, W_{T20}-W_{T21}, W_{T21}-W_{T22} and W_{T22}-W_{T23} respectively) and Z_{05} are branch impedance between wind turbine 23 and end point C_{2A3} as shown in figure 36, and $P_{01}(W_{T19})$,P_{02}(sum of (W_{T19} and W_{T20}), P_{03}(sum of W_{T19},W_{T20} and W_{T21}), $P_{04}(W_{T19},W_{T20},W_{T21}$and W_{T22}) and P_{05}(sum of power from all wind turbines) are branch flow.

Substituting the values of the power flow and branch impedance in equation 3.42 from table B.1 in appendix B,

$$\mathrm{Re}(Z_{CCG3}) = \frac{1^2x0.009 + 2^2x0.009 + 3^2x0.009 + 4^2x0.009 + 5^2x0.049}{(1+2+3+4+5)^2} = 0.02718$$

$$\mathrm{Img}(Z_{CCG3}) = \frac{1^2x0.008 + 2^2x0.008 + 3^2x0.008 + 4^2x0.008 + 5^2x0.026}{(1+2+3+4+5)^2} = 0.01604$$

Hence, Z_{CCG3} given as

$$Z_{CCG3} = 0.02718 + j\ 0.01604\ \text{pu}$$

ii. Group Four Collector Circuits.

Similarly substituting the values of branch impedances we obtain

$$Z_{CCG4} = \frac{P_{01}^2 Z_{01} + P_{02}^2 Z_{02} + P_{03}^2 Z_{03} + \cdots + P_{07}^2 Z_{07}}{(P_{01} + P_{02} + P_{03} + \cdots + P_{07})^2}$$

$$X = \mathrm{Img}(Z_{CCG4})$$

$$= \frac{1^2x0.01 + 2^2x0.025 + 3^2x0.008 + 4^2x0.008 + 5^2x0.007 + 6^2x0.008 + 7^2x0.026}{(1+2+3+4+5+6+7)^2}$$

$$\mathrm{Img}(Z_{CCG4}) = 0.0026$$

And the resistive component

$$R = \mathrm{Re}(Z_{CCG4})$$

$$= \frac{1^2x0.012 + 2^2x0.031 + 3^2x0.01 + 4^2x0.009 + 5^2x0.009 + 6^2x0.009 + 7^2x0.049}{(1+2+3+4+5+6+7)^2}$$

$$\mathrm{Re}(Z_{CCG4}) = 0.0042 \text{ pu}$$

Hence, ZCCG4 given as

$$Z_{CCG4} = 0.026 + j\ 0.0042 \text{ pu}$$

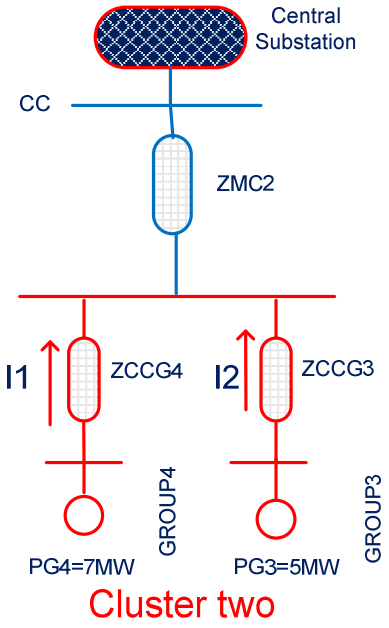

Figure 4.25. Reduced collector circuit impedance of cluster two collectors.

Now again applying equation 3.42 to reduce group three and four collector circuit impedance shown in figure 4.25 to single equivalence impedance. Hence,

$$Z_{S2} = \frac{P_{G3}^2 Z_{CCG3} + P_{G4}^2 Z_{CCG4}}{(P_{03} + P_{04})^2}$$

Substituting the values

$$\mathrm{Img}(Z_{S2}) = \frac{5^2x0.02718 + 7^2x0.0026}{(5+7)^2} = 0.0056 \text{ pu}$$

The real part

$$\mathrm{Re}(Z_{S2}) = \frac{5^2 x 0.01604 + 7^2 x 0.0042}{(5+7)^2} = 0.0042 \text{ pu}$$

Therefore,

$$Z_{S2} = 0.0056 + j\,0.0042 \text{ pu}$$

Hence, the final equivalence impedance of cluster two collector circuit is given by Z_{S2} and the pad mounted transformer equivalence impedance is given by Z_{TS} . Combining these two impedances and rescaling the output of a single generator (1 MW) by the number of wind turbine in cluster two (N=12), we can represent cluster using single turbine representation shown in figure 4.26.

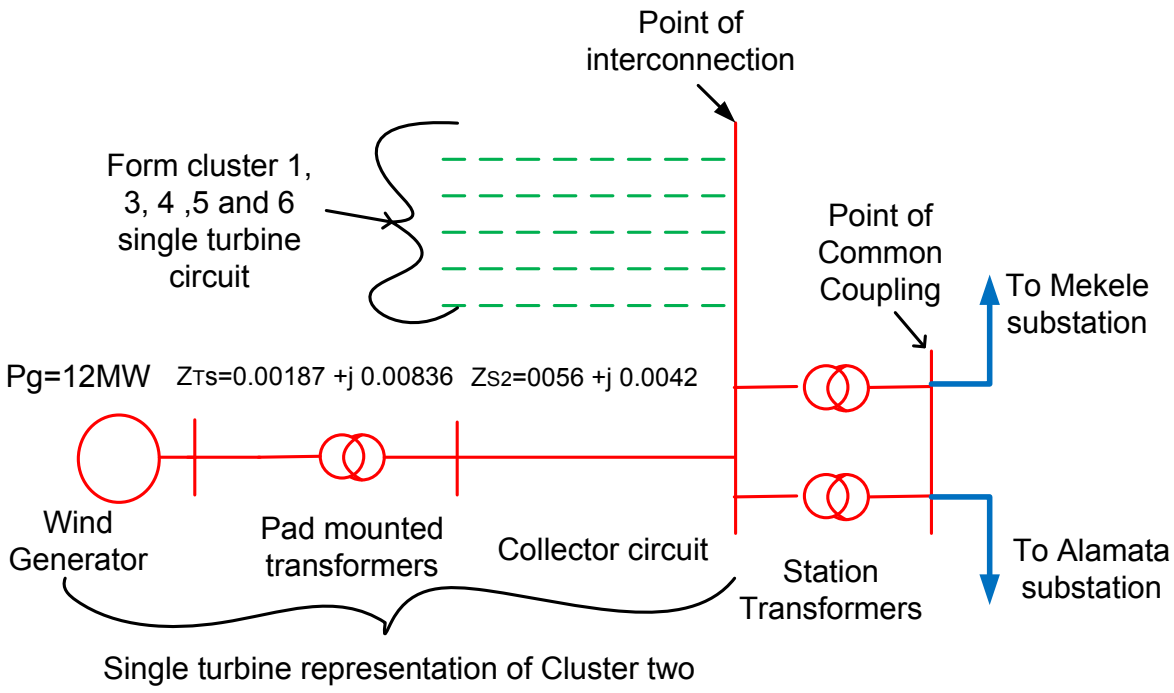

Figure 4.26.Single turbine representation of cluster two

4.4.2. Model Verification for Cluster Two

The full turbine representation of cluster two is applied in PSS/E to calculate the total active power loss within cluster two by running load flow analysis and observe the

terminal power outputs. The single turbine representation of cluster two is shown in figure 4.27 enclosed by circle and full turbine representation enclosed by rectangular.

For clarity purpose only the terminal flow redrawn as shown in 4.28. Bus number 151 is connected from the equivalent circuit and bus number 133 is connected from the full turbine representation. The active power flow is represented by the green color and the reactive power flow shown by yellow color toward the swing bus 140.

As can be seen from figure 4.28, the active power flow to ward bus bar 140 from equivalent circuit is 11.9 MW and reactive power is 0.3 MVAR. Whereas, the active power flows to ward bus 140 from full turbine representation is 11.9 MW and reactive power flow is 0.4 MVAR. The active power flow in both cases is the same. However, there is a difference of 0.1 MVAR in reactive power flow.

In practice, there is a total power loss less than 3 % of the rated capacity of the wind farm. The model developed for cluster two has a total active power loss of 0.1 MW which is 0.83% of the rated capacity of cluster two (12 MW). Therefore, the model developed is acceptable.

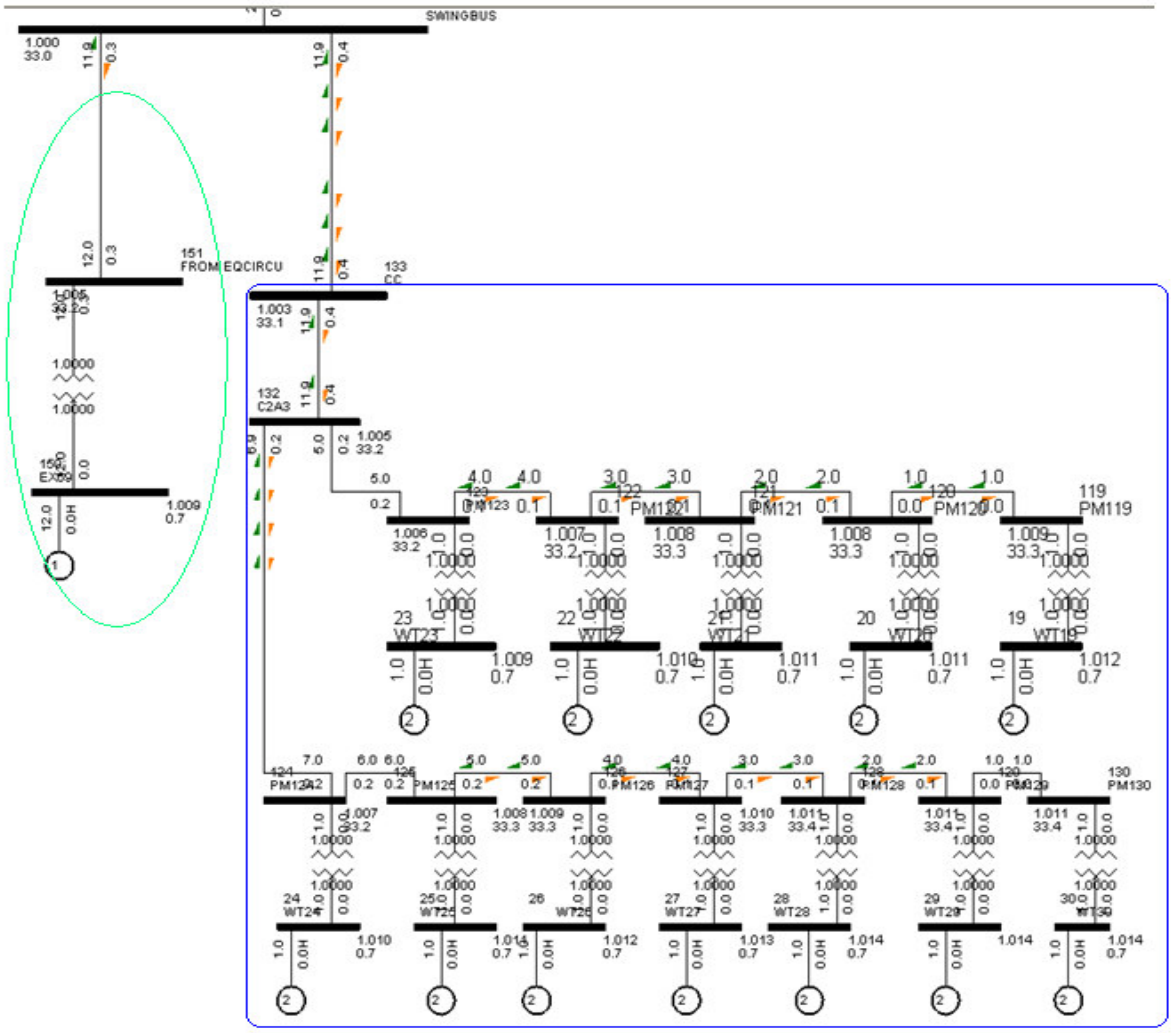

Figure 4.27.Model verification set up in PSS/E for cluster two.

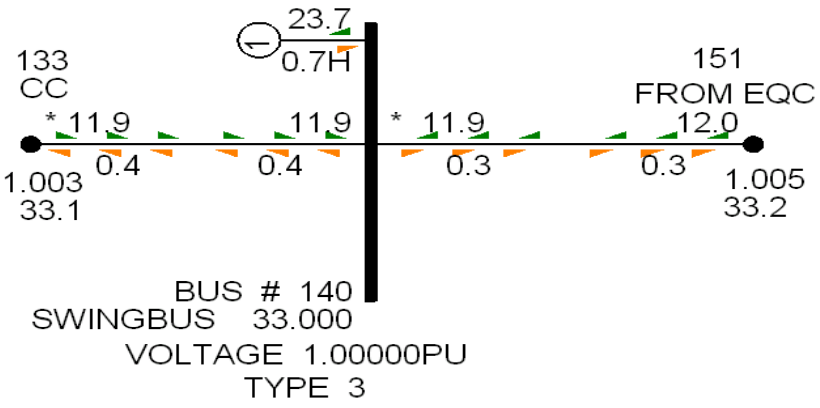

Figure 4.28.Terminal flows from single turbine and full turbine representation

4.5. Steady Stated Voltage Stability Impact of Ashegoda Wind Farm

Wind power integration has an impact on steady state and transient stability of the power system depending on their penetration level. In this thesis work, steady state stability impact assessment is made using PV and QV analysis.

4.5.1. Power System Description

The Ashegoda wind farm is connected at the northern parts of the grid system tapping the 230 kV existing line from Alamata to Mekele substation. The northern region contains four main hydro-power plants.

The project is finalized in two years period. According to "EEPCO load forecast study ", the total system demand at peak hour will be 1430 MW by year 2012.So, to be more realistic, I took as base case forecasted system loading of year 2012 by EEPCO.

4.5.2. PV Analysis

The objective of a PV curves is to determine the ability of a power system to maintain voltage stability at all the buses in the system under normal and abnormal (disconnection of any branch element from network) steady state operating conditions. Therefore, it helps to study the maximum transfer of power between AWF and buses (PCC as well as on local buses) before voltage collapse point. The local buses observed during PV analysis are Alamata 230 kV, Mekele 230 kV, Gashena Tap point, Combolcha II 230 kV and Bahir Dar 230 kV.

In large systems with many possible contingencies, especially single branch outages, it is often useful to minimize the computational and subsequent analyses by identifying the most severe contingencies prior to performing the contingency analysis.

PSS/E facilitates the "ranking" of designated single branch outage contingencies and builds a Contingency Description Data File (CDDF) with contingencies specified in decreasing order of their estimated severities using two different performance criteria of:

1. An overload criteria measuring branch loadings relative to their ratings.

2. A voltage depression criteria which indicates increased reactive power consumption by estimating increases in reactive losses due to increased line loadings.

In the overload ranker, the performance index, PI, is defined as [21],

$$PI = \sum_{i=1}^{L} \left(\frac{P_i}{P_{MAXi}} \right)^2 \quad 4.10.$$

Where:

Pi = the active power flow on branch "i".

P_{MAXi} = the rating of branch "i".

L = the set of monitored branches contributing to PI.

Clearly, PI has a small value for system conditions when branch loadings are light and a large value when lines exceed their limits. An increase in PI following a contingency indicates that overall loading on the branches contributing to PI has increased.

In the voltage ranker, the performance index is defined as:

$$PI = \sum_{i=1}^{L} X_i P_i^2 \quad 4.11.$$

Where:

X_i = the reactance of branch "i".

P_i = the active power flow on branch "i".

L = the set of monitored branches contributing to PI.

PI gives an indication of reactive power losses under different system conditions. As line loadings increase, their I^2X losses also increase. This increase in reactive demand generally results in a depression of system voltages.

The process of ranking contingencies in order of severity involves the following:

1. Establish the criteria to be considered in formulating the ranking. The criteria formulated are voltage collapse at busses of less than 0.9 pu.

2. For each criterion established in (1), calculating the performance index for each contingency.

The most sever list of contingencies of single outage, i.e., disconnection of any element (it could be transformer, generating unit or transmission line) at a time, created is summarized in table 4.18.

Table 4.18. List of contingency created

No	CONTINGENCY	CONTINGENCY DESCRIPTION	PI
1	OPEN LINE FROM BUS 4001 TO BUS 4003 CKT 1	G-GIBE-240' TO 'SEBETA-2 400'	6.527
2	OPEN LINE FROM BUS 2320 TO BUS 2321 CKT 1	ALAMATA 230' TO 'MEKELE 230'	6.4085
3	OPEN LINE FROM BUS 2320 TO BUS 2323 CKT 1	ALAMATA 230' TO 'COMBOLCHA II 230'	5.9616
4	OPEN LINE FROM BUS 2320 TO BUS 2346 CKT 1	ALAMATAA 230' TO 'GASHE-TA 230'	5.8605
5	OPEN LINE FROM BUS 2320 TO BUS 2402 CKT 1	ALAMATA 230' TO 'CS230 230'	5.7859
6	OPEN LINE FROM BUS 2321 TO BUS 2402 CKT 1	B.DAR2 230' TO 'N.MEW TP 230'	5.736
7	OPEN LINE FROM BUS 2318 TO BUS 2346 CKT 1	D-MARKOS 400' TO 'GEBRE-GURACH400'	5.7269
8	OPEN LINE FROM BUS 4010 TO BUS 4014 CKT 1	ALAMATA 230' TO 'MEKELE 230'	5.7114
9	OPEN LINE FROM BUS 2317 TO BUS 2318 CKT 1	COMBOL-II 230' TO 'COTOBI-II 230'	5.5841
10	OPEN LINE FROM BUS 2323 TO BUS 2325 CKT 1	'D-MARKOS 400' TO 'BAHIRDAR-II 400'	5.5713

The PV analysis made in under base cases and taking into consideration the above list of contingency cases.

i. PV Analysis in Base Case (without considering contingency cases)

Under base case, simulation there is no any drop in voltage at the point of coupling until the incremental transfer reaches the full load rating of the wind farm, which is, 120 MW. The voltage at full load is above the steady state limiting voltage level of 0.90 pu, see

figure 4.29. However, the voltage magnitude at "Alamata 230 kV Bus Bar" is near to the steady stability limit when the incremental transfer reaches to full load. Therefore, under base case there is no any steady state voltage stability impact on the system.

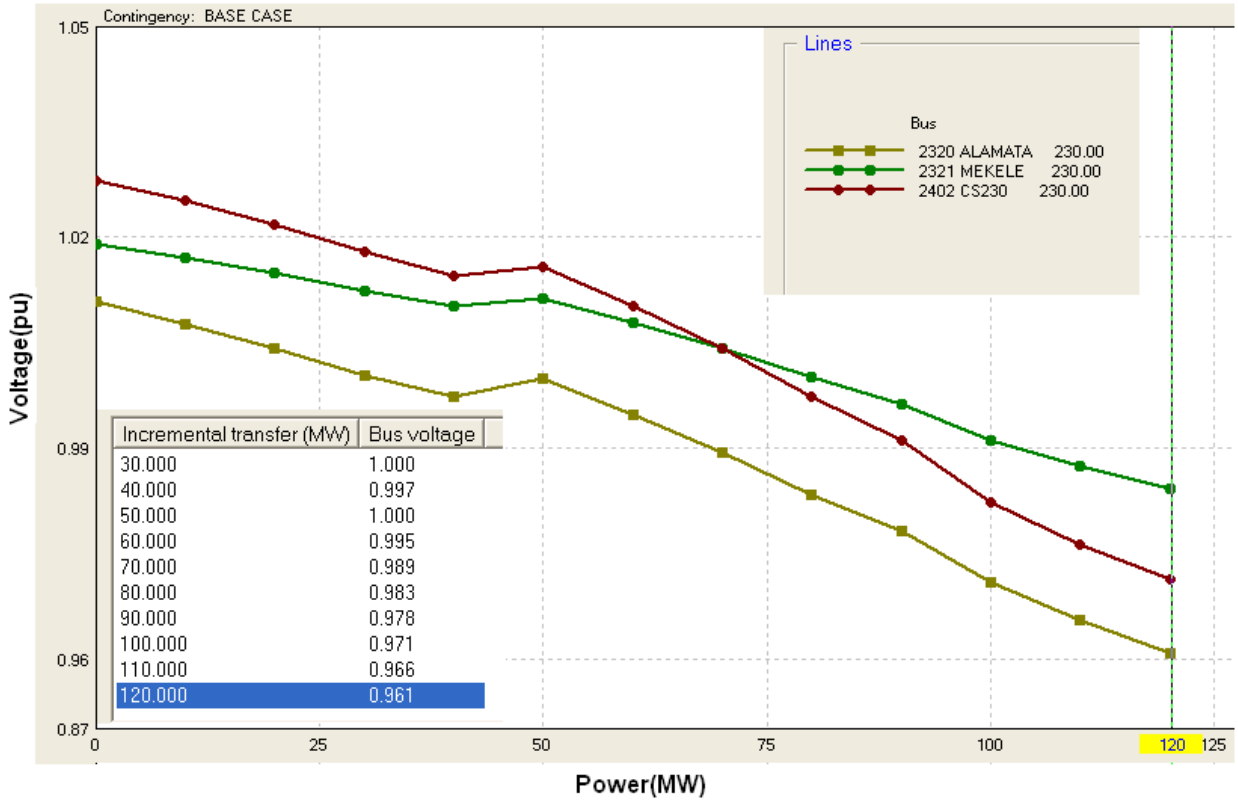

Figure 4.29.voltage profile at Alamata, mekele and PCC under base case.

ii. PV Analysis in Contingency Cases

Under contingency cases, the maximum amount of power that can be injected to the system reduced from the rated capacity. For example, disconnection of 230 kV line outgoing from "Alamata" to "Combolcha II" reduces the output power of the wind farm to 70 MW, if we consider the voltage magnitude at PCC as shown in figure 4.30.

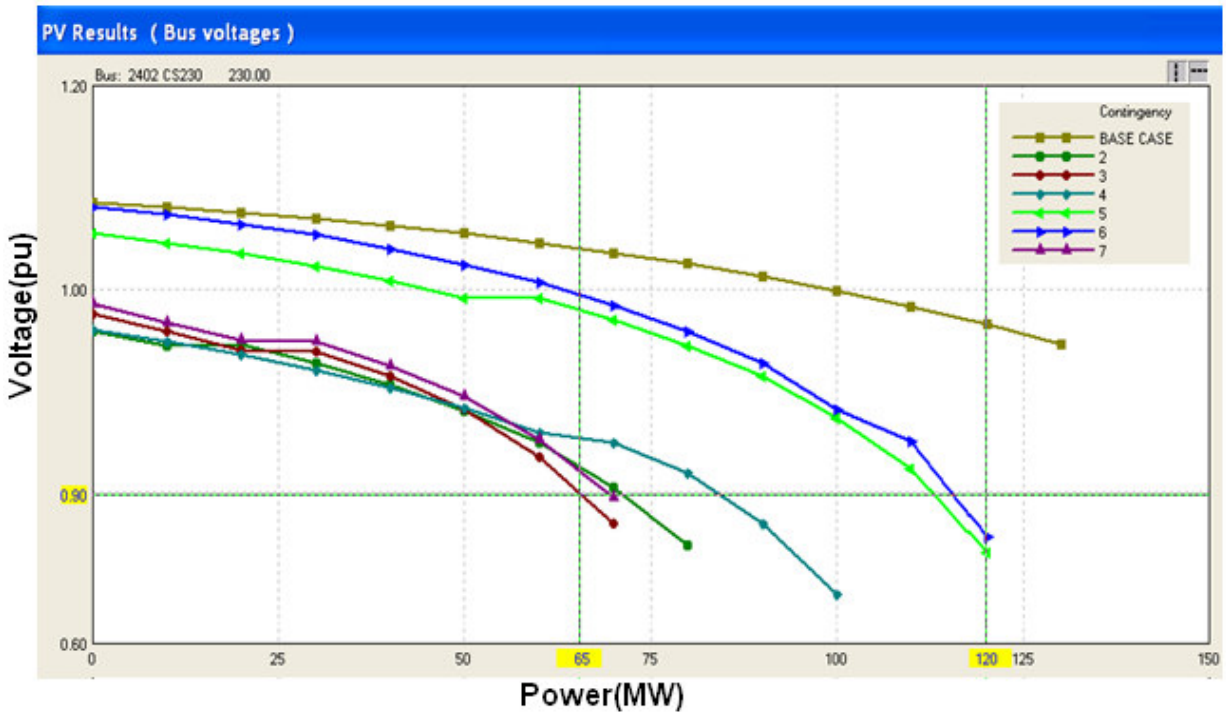

Figure 4.30. Voltage profile at Point of coupling under contingency cases.

However, the voltage magnitude at Alamata 230 kV substation reaches to the steady state limits soon at 40 MW as shown in figure 4.31.

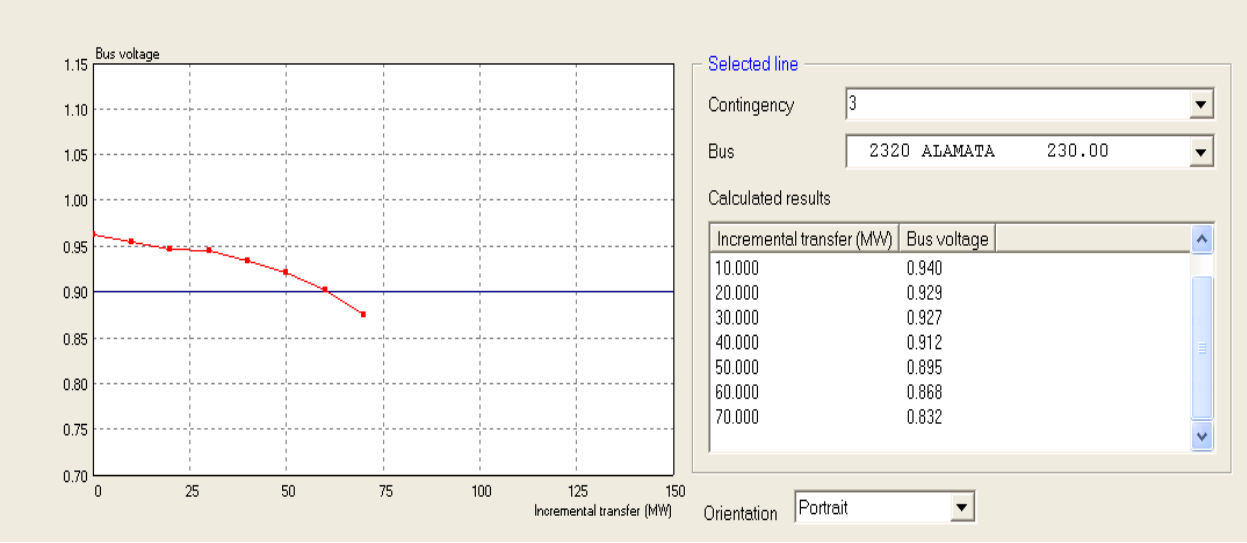

Figure 4.31.Voltage profile at Alamata 230 kV bus under contingency case 3.

Therefore, the maximum amount of active power transfer from wind farm has to be limited to 50 MW in order to avoid voltage collapse in the system.

4.5.3. QV Analysis

The aim of QV analysis is to determine under steady state condition what amount of reactive power can be injected or absorbed without causing voltage stability problem at point of coupling and local buses. In this section, the QV analysis has been made with base case and contingency cases to determine the required reactive power injection or absorption at Alamata and point of coupling.

i. Case One-Base Case

Under base case condition the amount of reactive power that is absorbed by wind generator is shown in figure 4.32.

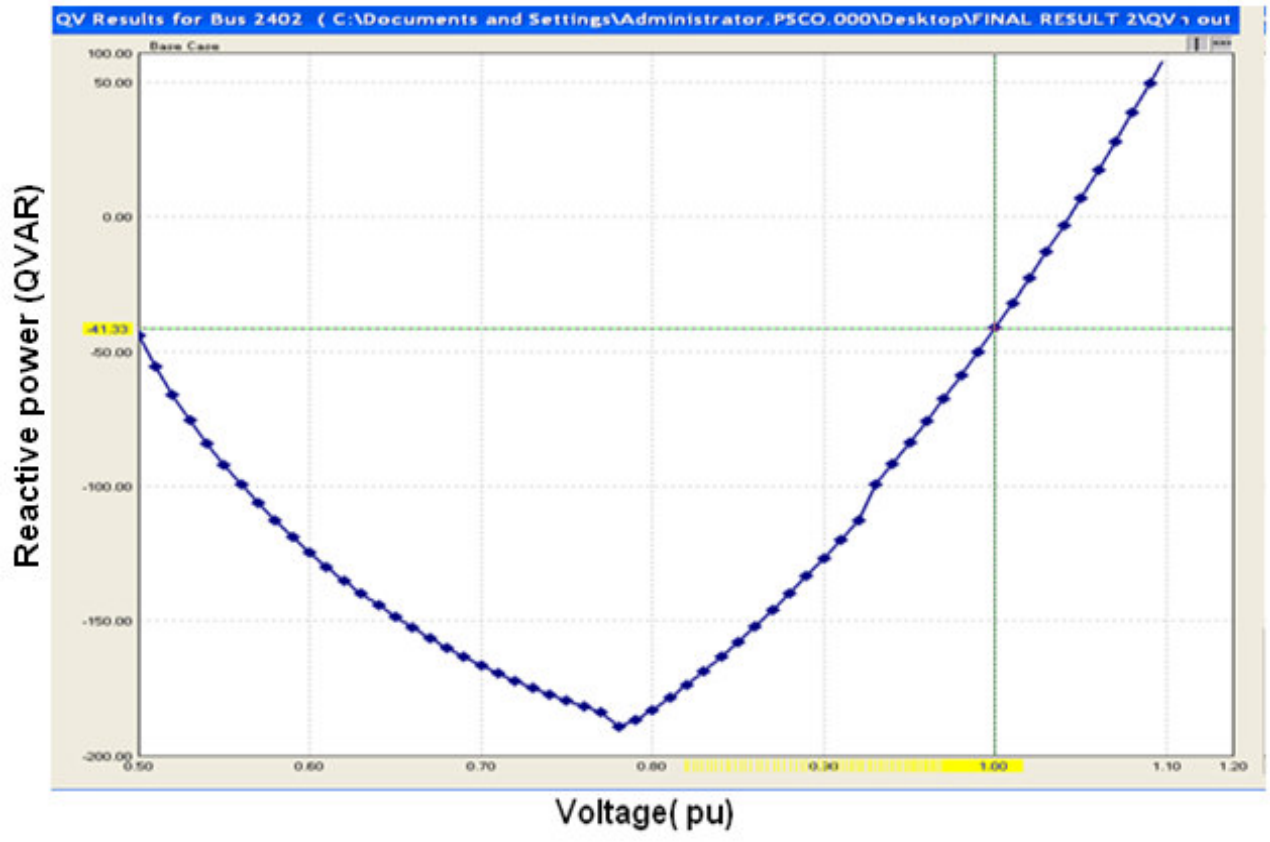

Figure 4. 32.QV result under base case at point of coupling.

As can be seen from figure 4.32, the voltage magnitude to be 1pu at point of coupling with grid, the wind farm has to absorb -41.33 MVAR from the system.

ii. Case two-Under Contingency Cases

Under contingency cases, a minimum of 11 MVAR and a maximum of 52.53 MVAR injections are needed to keep voltage magnitude at 1pu at point of coupling as shown in figure 4.33. Most of contingency cases require reactive power injection.

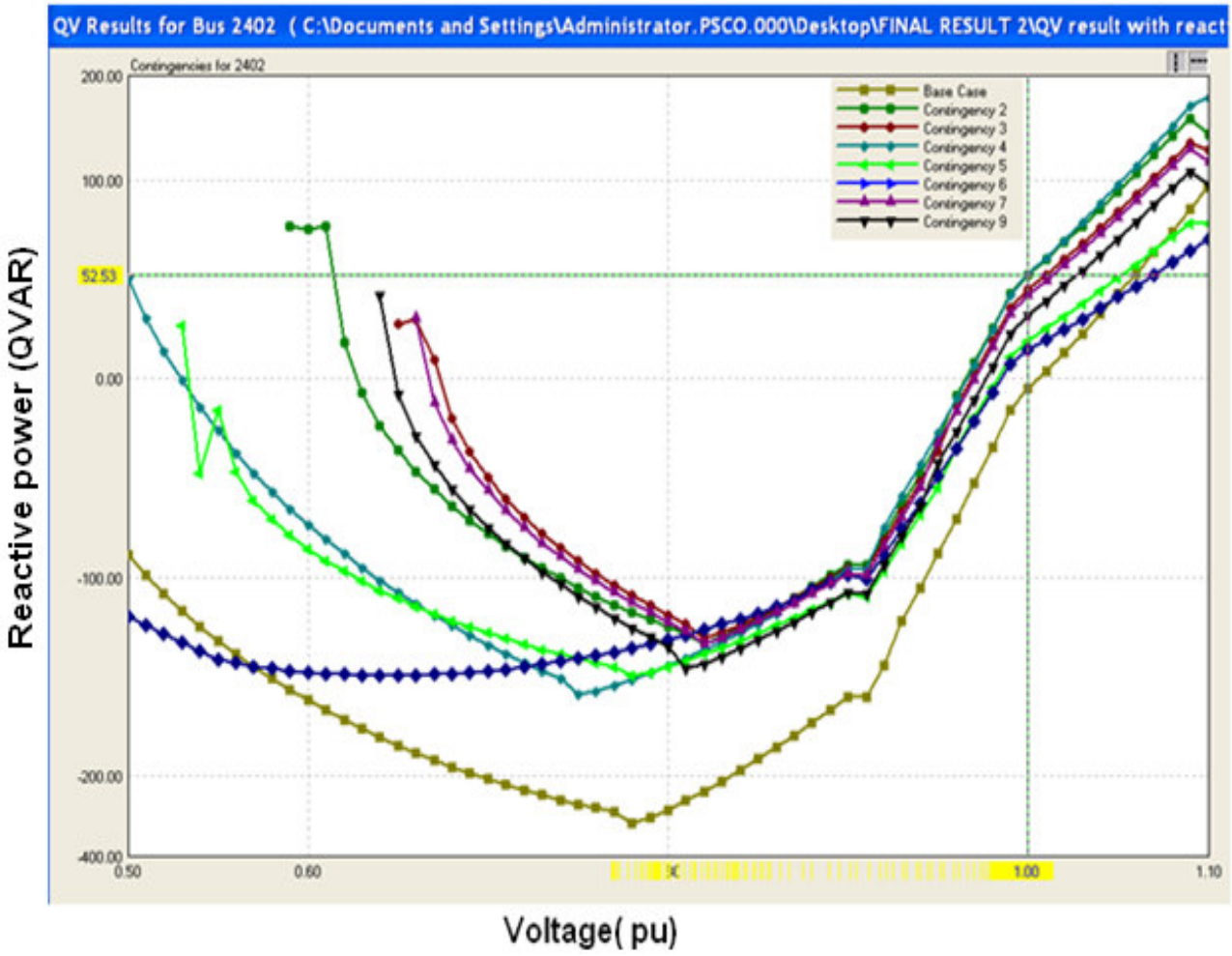

Figure 4.33.QV result under contingency cases

In case of Alamata substation under all contingency cases there must be a reactive power injection to make the voltage magnitude at 1pu as shown in figure 4.34.

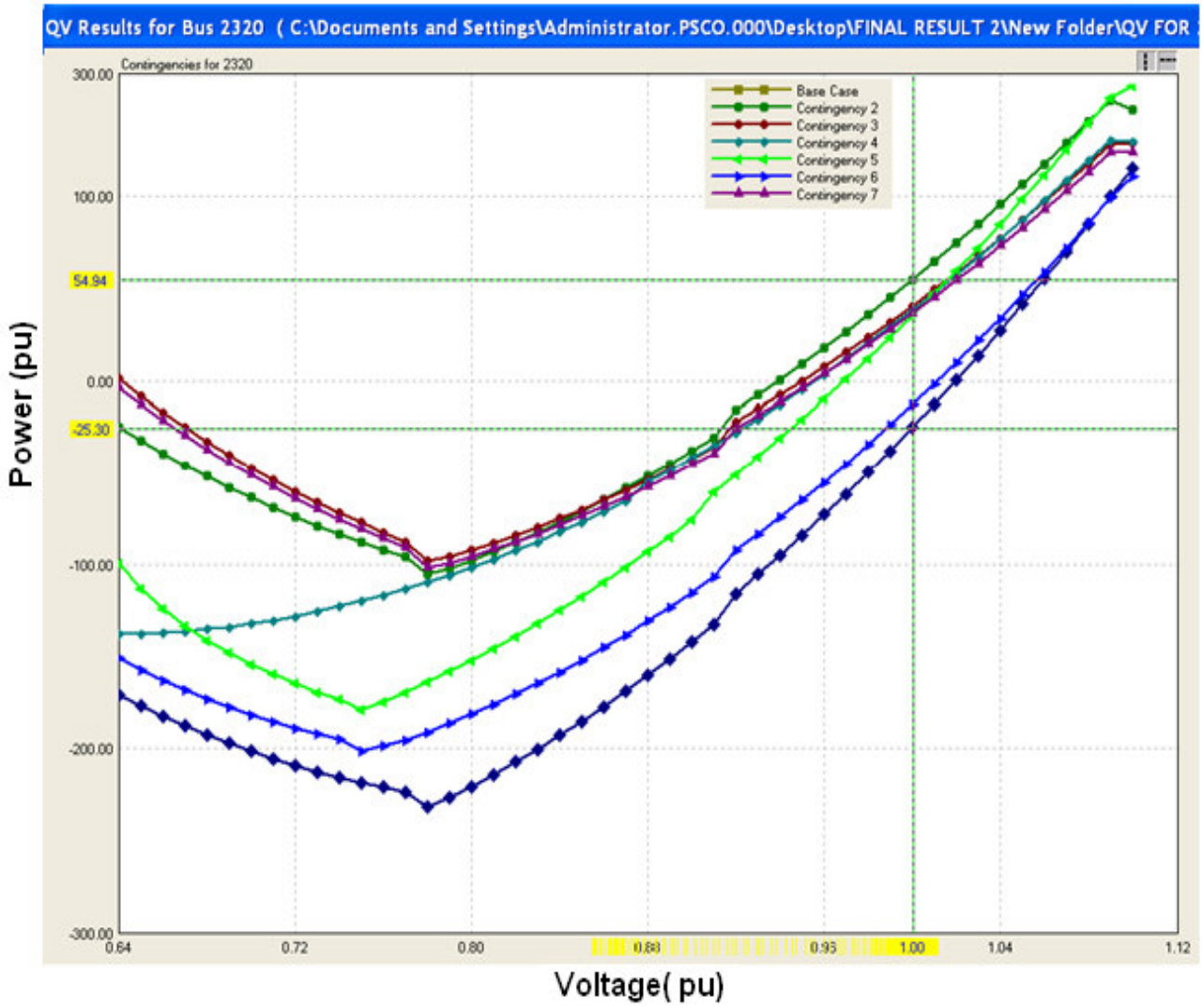

Figure 4.34.QV result under contingency cases at Alamata 230KV bus bar

As we have seen from the PV and QV analysis the wind farm has to participate in the voltage regulation to satisfy grid connection requirement during contingency and base cases to make integration of wind farm with system smooth.

In order to determine whether the needed reactive power injection or absorption can be satisfied or not by wind farm only, voltage control capability of the wind farm is assessed in the next section by determining the reactive power capability curve of the wind.

4.6. Voltage Control Capability of Ashegoda Wind Farm

One of operational challenges faced by the wind operator is managing system voltage magnitude at point of connection. AWF is connected at northern region of Ethiopia where the network is affected by overvoltage under both network loading, that is, light load and peak load conditions. To regulate the voltage magnitude either injection or absorption of reactive power from the wind farm is needed. Such operation can be performed respecting the reactive limits of wind generator that mainly depend on the grid side converter current and voltage ratings limits.

The aim of this section is to analyze reactive power ancillary services that can be provided by wind farm to support the grid operation under two operation conditions and observing reactive power capability curves of the wind farm.

i. Unity power factor operation and

ii. Operated at +/- 0.95 power factor

In each case, the required reactive power capability of the wind farm is determined and compared with actual reactive capability limits of the generator. Finally reactive capability of the wind farm is checked whether it satisfies or not the required reactive power, what is determined previously in QV analysis.

4.6.1. Reactive Capability Curve of the Wind Farm

The reactive power capability curve of the wind farm is limited by the grid side converter current carrying capacity. In a PQ plane, it is a circle similar to that of armature current of synchronous generator. The relationship between active power and reactive power at converter current limit is given as follows [18];

$$P^2 + Q^2 = \left(V_g I_C\right)^2 \qquad 4.12.$$

Where Ic is converter current.

Converter voltage will also impose a limit on P and Q capability of wind turbine, which is similar to that of the field current limit of a synchronous generator [18]. The relationship between P and Q at converter voltage limit is given as follows;

$$P^2 + \left(Q + \frac{V_g^2}{X}\right)^2 = \left(\frac{V_g V_C}{X}\right)^2 \quad 4.13.$$

Where X is the total equivalent reactance up to point of coupling with grid system. Therefore, it is a circle whose center and radius is given by

$$C = \left(0, \frac{V_g^2}{X}\right) \quad 4.14.$$

And radius r at;

$$r = \frac{V_g V_C}{X} \quad 4.15.$$

The reactive power capability of a wind turbine installed at AWF is shown in figure E.1 of appendix E. The reactive power capability of the wind farm is given by;

$$Q = \min\left(Q_g; Q_V\right) \quad 4.16.$$

Where Qc and Qv are the limiting factors of reactive power injection due to converter maximum voltage and maximum current limitation of grid side converter and given by;

$$Q_C = \sqrt{\left(V_g I_{cmax}\right)^2 - P^2} \quad 4.17.$$

$$Q_V = \sqrt{\left(\frac{V_{cmax} V_g}{X}\right)^2 - P^2} - \frac{V_g^2}{X} \quad 4.18.$$

Where Icmax and Vcmax is given by

$$I_{cmax} = \frac{\sqrt{1 + \tan^2\theta_R}}{V_{gmin}} \quad 4.19.$$

And

$$V_{Cmax} = \frac{f_{max}X}{V_{gmax}}\sqrt{1+\left(\tan\theta_R + \frac{V_{gmax}^2}{f_{max}X}\right)^2} \quad 4.20.$$

V_{gmin} and V_{gmax} are the minimum and maximum network voltage at point of connection, X is total reactance up to coupling point and f_{max} is the maximum network frequency. The reactive power capability curve of the wind farm is constructed for two cases, unit power factor operation and a power factor operation of +/- 0.95.

4.6.2. Unity Power Factor Operation

For unity power factor operation, the wind farm doesn't supply or absorb a reactive power to or from the grid system at point of common coupling. The current and voltage limit curves of the wind farm should intersect the real axis of the P-Q plane at point (1, 0) .for Unit PF operation the maximum value of converter currents are calculated using equation 4.19 as follows;

$$I_{cmax} = \frac{\sqrt{1+\tan^2\theta_R}}{V_{gmin}}$$

Substituting the values of V_{gmin}=0.9 and θ=0;

$$I_{cmax} = \frac{1}{0.9} = 1.11 \text{ pu}$$

The value of converter voltage is calculated from equation 4.21;

$$V_{Cmax} = \frac{f_{max}X}{V_{gmax}}\sqrt{1+\left(\tan\theta_R + \frac{V_{gmax}^2}{f_{max}X}\right)^2}$$

Where f_{max}=1.01pu, X=0.25616pu, V_{gmax}=1.05 and θ_R=0. Substituting the values

$$V_{Cmax} = \frac{1.01x0.148}{1.05}\sqrt{1+\left(0+\frac{1.05^2}{1.01x0.148}\right)^2} = 1.06 \text{ pu}$$

The reactive power capability of the wind farm , at converter current and voltage limits , when the terminal voltage(V_g) be 1pu is calculated as follows using equation 4.17 and 4.18;

$$Q_C = \sqrt{(1x1.11)^2 - 1^2} = 0.4812 \text{ pu}$$

And

$$Q_V = \sqrt{\left(\frac{1.06x1}{0.148}\right)^2 - 1^2} - \frac{1^2}{0.148} = 0.333 \text{ pu}$$

As per equation 4.16, the minimum limiting factor is the converter voltage. Therefore, the reactive power capability of the wind farm at rated power output is 0.333 pu (39.96 MVA). The reactive power capability of the wind farm, at converter current and voltage limits, when the terminal voltage (Vg) be 0.95 pu will be

$$Q_C = \sqrt{(0.95x1.11)^2 - 1^2} = 0.335 \text{ pu}$$

And

$$Q_V = \sqrt{\left(\frac{1.06x0.95}{0.148}\right)^2 - 1^2} - \frac{0.95^2}{0.148} = 0.630 \text{ pu}$$

Therefore, the reactive power capability of the wind farm at rated power output with 0.95 pu magnitude of voltage is limited by converter current limit at 0.335 pu (40.2MVAR).

By supper imposing wind farm and the generator the reactive power capability it is checked the required ancillary services can be satisfied by the wind farm at connection point. As shown in figure 4.35, reactive power injection capability of wind generator is limited by the wind farm in case of leading power factor operation of wind generator for rated power output. However, for lagging power factor operation wind generator reactive capability will limit reactive power absorption capability.

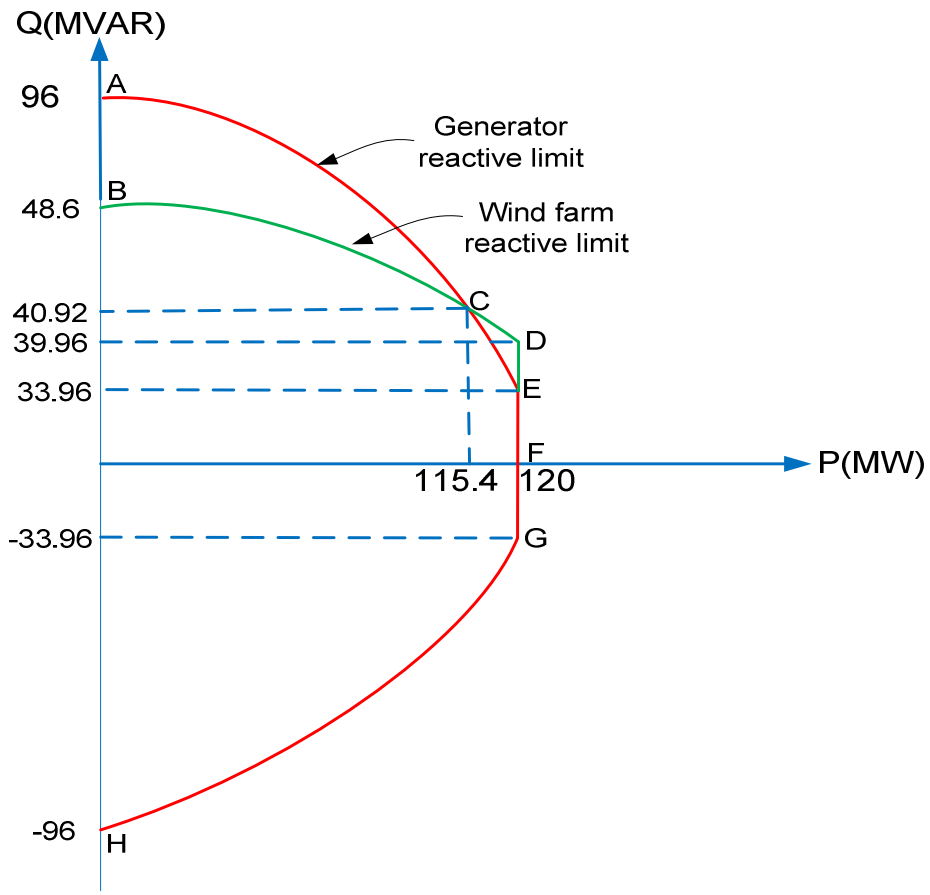

Figure 4.35.Reactive power capability curve of AWF with unity power factor operation.

For rated power operation, the maximum amount of reactive injection would be 39.96 MVAR as long as 1pu voltage magnitude and unity power factor operation with the grid system is needed. However, the maximum reactive limit of the wind farm, as shown above, is 33.96 MVAR.

4.6.3. Operation for Power Factor of 0.95 (both lead or lagging)

In this case, the wind farm can operate at leading and lagging of 0.95. Therefore, it can absorb or inject a reactive power to the grid.

In order to fulfill this requirement, the maximum converter voltage (V_{cmax}) and the maximum current-carrying capacity of the converter (I_{cmax}) should be larger compared to unity power factor [18]. The maximum converter voltage and current is given as follows;

$$I_{cmax} = \frac{\sqrt{1 + \tan^2 18.2}}{0.9} = 1.17 \text{ pu}$$

And converter voltage

$$V_{Cmax} = \frac{1.01x0.148}{1.05}\sqrt{1 + \left(\tan 18.2 + \frac{1.05^2}{1.01x0.148}\right)^2} = 1.106 \text{ pu}$$

The reactive power capability of the wind farm, at converter current and voltage limits, when the terminal voltage (Vg) be 1pu will be

$$Q_C = \sqrt{(1x1.17)^2 - 1^2} = 0.607$$

And

$$Q_V = \sqrt{\left(\frac{1.106x1}{0.148}\right)^2 - 1^2} - \frac{1^2}{0.148} = 0.649 \text{ pu}$$

The reactive power capability of the wind farm at rated power output with 1pu magnitude of voltage is 0.607 pu (72.84 MVAR).

The reactive power capability of the wind farm, at converter current and voltage limits, when the terminal voltage (Vg) be 0.95 pu will be

$$Q_C = \sqrt{(0.95x1.17)^2 - 1^2} = 0.484 \text{ pu}$$

And

$$Q_V = \sqrt{\left(\frac{1.106x0.95}{0.148}\right)^2 - 1^2} - \frac{0.95^2}{0.148} = 0.931 \text{ pu}$$

The reactive power capability of the wind farm at rated power output with 0.95 pu magnitude of voltage is 0.484 pu (58.1 MVAR).

Similarly for power factor operation of +/- 0.96, the reactive capability of the wind farm is constructed by supper imposing wind farm and the generator the reactive power capability as shown in figure 4.36.

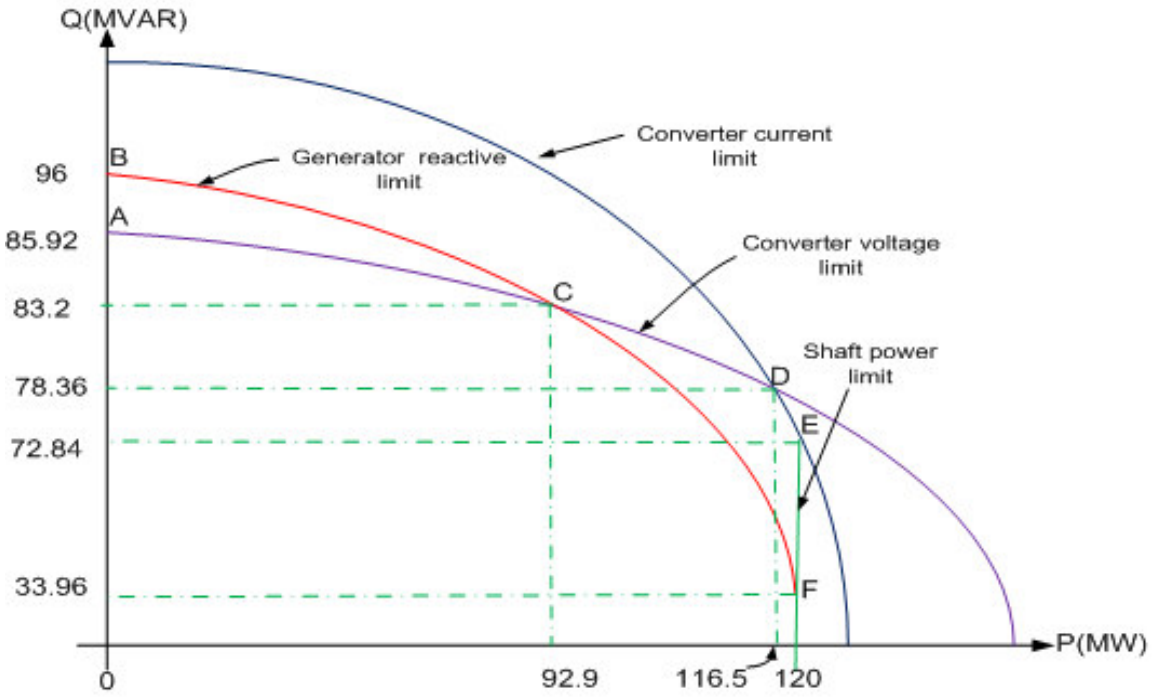

Figure 4.36. Reactive power capability curve of AWF with +/- 0.95 power factor operation.

As can be seen easily from the numerical analysis, the amount of reactive power that is supposed to be provided by wind generator increases in +/ - 0.95 power factor operation than unit power factor as shown in figure 4.36. Hence, in all operating conditions, the required reactive power at rated active power output is above the rating of wind generator reactive limits. Hence, in order to provide the required reactive power it is needed reduce active power output of wind farm. For example, as you remember form QV analysis of previous section under contingency case four, we need 52 MVAR to keep the voltage magnitude at rated value (1 pu). However, as the maximum amount of reactive power limit of wind generator is 48.6 MVAR, this amount of reactive power cannot be provided with unity power factor operation and rated power output (120 MW).

For 0.95 leading power factor operation, it is needed to reduce active power output to 113 MW (94.2% of installed capacity) to provide the required reactive power. Otherwise, we need to take other measures to increase reactive power output of wind farm. Therefore, under contingency cases due to limited capacity of transmission line, there is a limitation to

inject the generated power to grid without causing voltage stability problems. The limitation in transmission capacity can be avoided taking additional measures. Generally, measures taken to increase transmission capacity can be summarized in two groups as soft and reinforcement measures [22], [23].

Soft measure can be provided by extensive use of system protection schemes, especially of automatic control actions following critical line outages, may help to relax transmission congestions without substantial investments. These measures include:

i. Shedding of preselected generators;

ii. Shedding of preselected loads;

iii. Network splitting to avoid cascading events.

EEPCO most frequently uses shedding of selected loads and generation. Some time it implement splitting the northern part and the rest of the network into two whenever there is transmission fault on the major transmission lines (eg. Line between Bahir Dar to Mota, line between Bahir Dar to Alamata). Even if it is a temporary solution, such schemes are practiced by EEPCO primarily to reducing the consequences of disturbances.

The reinforcement measures to increase transmission capacity takes into consideration thermal current and voltage stability limit as critical factors. In case of thermal limit as a critical factor, reinforce measure can either be aimed to increase the current limits of individual lines and associated equipment (eg. Breakers, voltage and current transformers, etc) or to optimize the distribution of load flows to decrease loading of the critical lines.

If voltage limits or voltage stability are the determining factor for the transmission capacity, additional sources of reactive power (i.e., FACTS elements) can be installed at critical locations in order to smoothen the steady state voltage profile and to increase reserves against the loss of voltage stability.

As per the result of PV analysis in previous section, there is steady state voltage stability problem during contingency case that needs reinforcement measures. In this thesis work reactive power compensation, managing transmission line capacity been considered in the following sections.

4.7. Managing Transmission Line Bottlenecks

Increasing of transmission capacity using reinforcement measure is time-consuming. Therefore, other measure is necessary like managing transmission congestion. Such measure includes reducing the power production in conventional generation units and curtailing excess wind energy, when the transmission system is congested.

The transmission capacity of the line under contingency case is affected when ever generation from AWF or Tekeze hydropower plant is increased. Unless transmission line capacity managed by coordinating generation of AWF farm and Tekeze hydropower plant, the system operation can be affected during contingency cases.

If we consider a particular case ,for example contingency case four, either the output of the wind farm or Tekeze has to be limited to 50 MW before voltage collapse happening on the system as per PV analysis of previous section. Such problems will be more serious if it happens during peak hours. This is because of the load duration curve of AWF has similar shape as system load duration curve. This can be observed from average daily power output of AWF for year 2007. It has average power generation more than 50 MW starting from 6 pm in afternoon to 3 pm in the evening as shown in figure 4.37.

During this time, generation from the Tekeze hydropower plant has to be increased to balance system demand that may cause system operation difficult. In fact, if this happens there is maximum output from the wind farm and there is line outage, especially disconnection of any line from Alamata 230 kV bus bar.

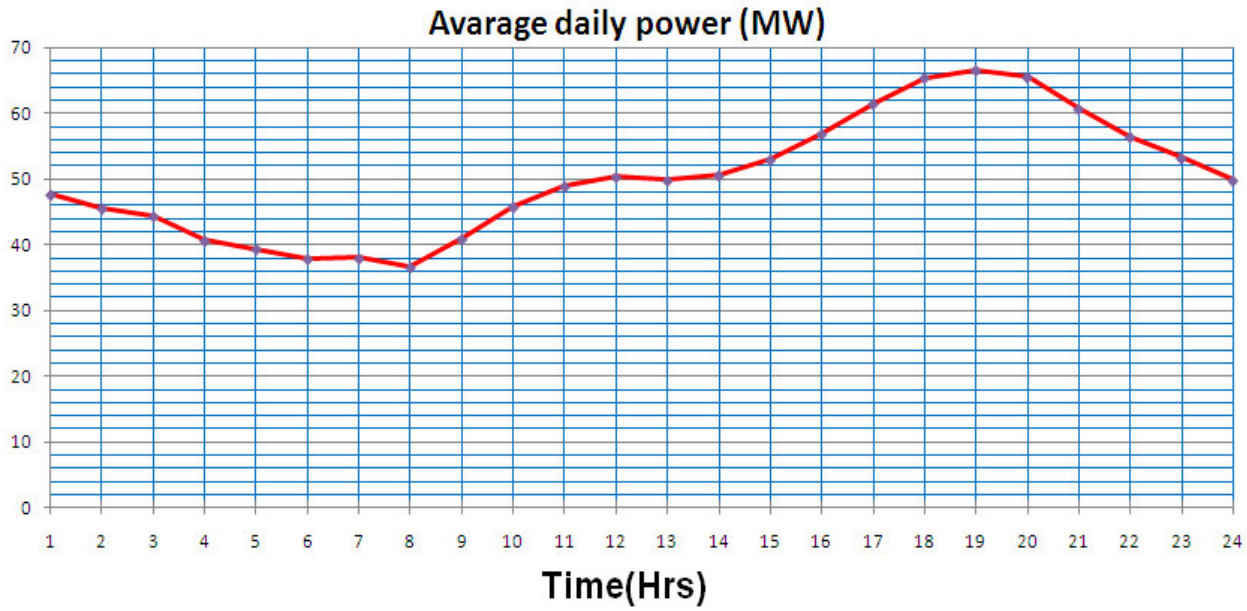

Figure 4. 37.Average daily power of AWF in year 2007/08

Even if there is similarity in shape of daily load duration curve, there is no correlation between average inflow and wind energy distribution. This important thing needs to be checked before implementing coordination of generation output from wind farm and hydropower plant. Otherwise, the capacity of the hydro reservoirs will put additional limitations on the regulating capability if there is correlation.

This is checked taking yearly average water inflow of Tekeze reservoir and wind distribution of AWF. As can be seen in figure 4.38, average inflows and wind speeds are not correlated.

During dry seasons (Jan to May), the wind speed distribution is higher than average inflow and then it will be lower during wet seasons (June to September). During high wind power production (dry seasons) and simultaneous congestion problems in the transmission system, Tekeze power production can be reduced and water can be saved in Tekeze hydro reservoirs.

Thus, wind power production would not be affected by the congestion problem and it would not be necessary to curtail the production of wind energy. The saved water can then

be optimally used by Tekeze hydro power plant when the bottleneck is relieved. Methods have to be developed for estimating the amounts of spilled energy at various wind power penetration levels.

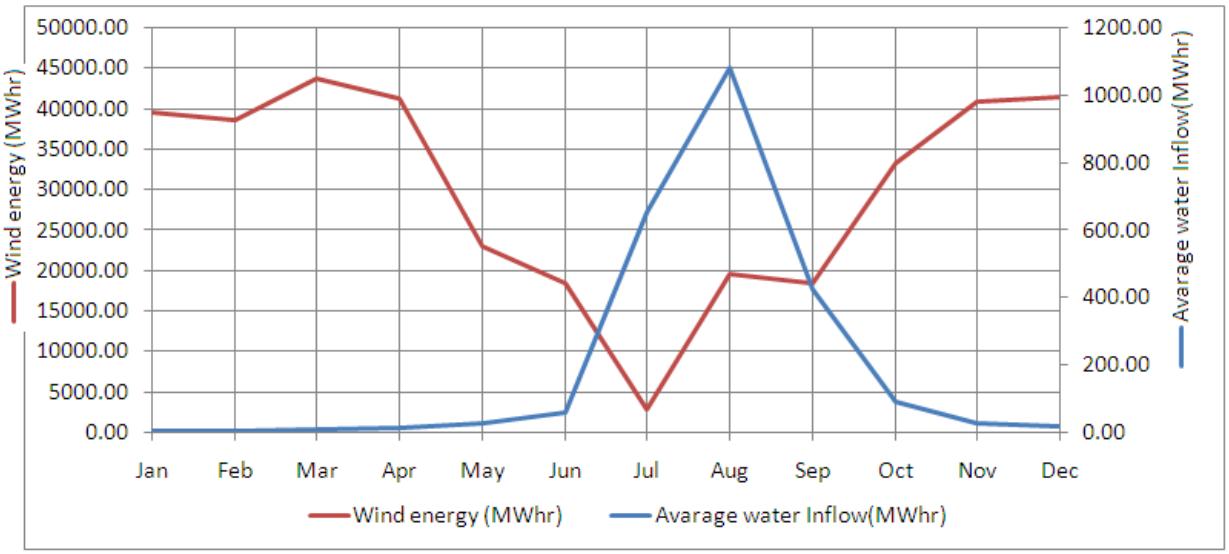

Figure 4.38.Seasonal wind and water distribution in year 2007

This operation needs a proper unit scheduling or production planning as redispatching of Tekeze and other hydropower plants affect their efficiency.

In addition forecast errors has to be accounted for by frequent updates of the wind power production forecasts, and hydro power production planning is changed accordingly so that transmission limits will not be exceeded.

4.8. Reactive Power Compensation

The purpose of this section is to estimate the reactive power compensation that is needed to compensate the system for maximum penetration of wind output. In order to get the rating of the compensator two different worst case scenarios are formulated as follows;

- ✓ Maximum generation ,at rated speed, from the wind in peak hour loading
- ✓ Minimum generation, at cut in speed, from the wind in light system loading condition.

From the first scenario, at rated wind speed and peak hour operation, we can get the maximum voltage drop as the system is heavily loaded and there is high reactive power loss in the system.

From the second scenario, at cut in wind speed and light system loading, we can get the maximum voltage raise, especially at night time and holiday, the voltage in the system raised above the rated value in the northern region of the country due to low system loading.

The result of load flow analysis using PSS/E simulation software under base cases (light system loading and peak loading) and contingency cases is summarized in table 4.19.The procedures followed to determine the rating the reactive compensation is;

- ✓ Making the load flow analysis for both scenarios.
- ✓ Selecting the bus which is severely affected buses.
- ✓ Determining the reactive power needed analytically based on the data obtained from load flow analysis.
- ✓ Determining line parameters and modeling to be compensated.
- ✓ Finally, modeling and applying the reactive compensation device with determined values of rating and checking if there is any violation of voltage magnitude using a load flow run.

Table 4.19. Voltage profile at base and selected contingency cases.

contingency	Substation name	Voltage magnitude(kV)	Angle (deg)
Base case in peak hour loading	Alamata	234.562	7.58
	Mekele	236.1	14.02
	Wind PCC	239.9	13.28
	Combolcha	235.7	-0.57
	Gasheta TP	236.5	3.63
Base case in light system loading	Alamata	242.3	-0.75
	Mekele	240.84	-0.08
	Wind PCC	244.87	-0.63
	Combolcha	245.2	-1.54
	Gasheta TP	243.1	-0.93
Contingency two	Alamata	219.865	7.94
	Mekele	disconnected	
	Wind PCC	225.3	21.33
	Combolcha	225.4	-0.97
	Gasheta TP	225	3.59
Contingency three	Alamata	216.11	27.74
	Mekele	225.6	34.5
	Wind PCC	225.1	34.02
	Combolcha	disconnected	
	Gasheta TP	213.8	17.67
Contingency four	Alamata	218.6	29.5
	Mekele	227	36.25
	Wind PCC	227.1	35.7
	Combolcha	215.1	13.07
	Gasheta TP	disconnected	

As can be seen from table 4.19, Alamata bus bar is affected more as compared to other bus bars in case of contingency and base case. Therefore, Alamata 230 kV bus bar is considered as a weak bus where compensation is applied taking the line parameters between Alamata 230 kV bus bar and PCC with AWF.

4.8.1. Modelling of Alamata to PCC Transmission Line Modelling

Transmission line in PSS/E is modeled using Pi-equivalent circuit as shown in figure 4.39[21].

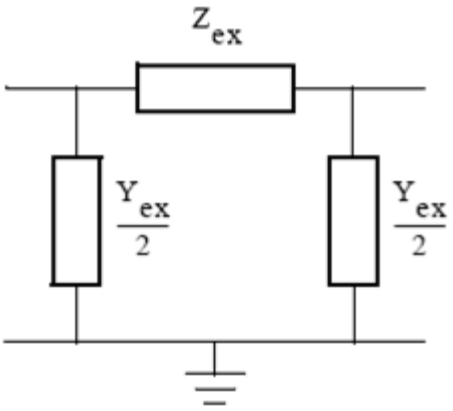

Figure 4.39. Pi- equivalent circuit of a transmission line.

Z_{ex} is the series impedance and Y_{ex} is the shunt impedance and calculated as follows

$$\frac{Y_{ex}}{2} = \frac{1}{Z_C}\tanh\left(\frac{\gamma L}{2}\right) \quad 4.21.$$

$$Z_{ex} = Z_C \sinh \gamma L \quad 4.22.$$

Where:

Z_C is surge or characteristic impedance of the transmission line (Ω).

γ is the propagation constant of the line(rad / kM)

L is transmission line length (kM)

Transmission line between Alamata to PCC has the following line impedance

$$Z = R + j\,X = 0.0918 + j\,0.3193\ \Omega/\ kM$$

And capacitance

$$C = 11.4\ \text{nF/ kM}$$

The length of the line is 120.7 kM from Alamata to PCC. Therefore, the surge impedance of the line is calculated as follows

$$Z_C = \sqrt{\frac{L}{C}} \qquad 4.23.$$

Substituting the values in equation (3-26),

$$Z_C = \sqrt{\frac{1.016x10^{-3}}{11.4x10^{-9}}} = 298.5\Omega$$

The propagation constant of the line is

$$\gamma = \omega\sqrt{LC} = 2x\pi x50\sqrt{1.016x11.4x10^{6}} = 1.07x10^{-3}\ \text{rad/ kM}$$

The electrical length of the line is

$$\theta = \beta l = 1.07x10^{-3}x120.7 = 0.129\ \text{rad}$$

Or

$$\theta = 0.129\ x\frac{120}{\pi} = 7.39\ \text{deg}$$

Z_{ex}, the series impedance of the line is found substituting the values in equation 4.22,

$$Z_{ex} = 298.5\ x\ \sinh(0.129) = 38.61\ \Omega$$

Y_{ex}, the shunt admittance of the line is found substituting the values in equation 4.21,

$$\frac{Y_{ex}}{2} = \frac{1}{298.5}\tanh(\frac{0.129}{2}) = 2.15x10^{-4}\ \text{mho}$$

The surge impedance loading of the is

$$SIL = \frac{V_{L-L}{}^2}{Z_C} \qquad 4.24.$$

Substituting the values,

$$SIL = \frac{230^2}{298.5} = 177.2\ \text{MW}$$

4.8.2. Required Reactive Power

The reactive requirement of the transmission line with a function of terminal end voltages, i.e. receiving and sending end voltage, is given by [2];

$$Q_R = \frac{V_R(V_S\cos\delta - V_R\cos\theta)}{Z_C\sin\theta} \quad 4.25.$$

And sending end reactive power is give by

$$Q_S = \frac{-V_S(V_R\cos\delta - V_S\cos\theta)}{Z_C\sin\theta} \quad 4.26.$$

4.8.3. Required Reactive Power under Contingency Cases

The aim of this case is to find out the maximum reactive injection needed by the compensation device. The high amount of reactive power loss in the system occurs during maximum system load demand. This may even worsen if there is outage of transmission line or generation units, i.e. under contingency cases. For this analysis generation from wind farm is considered to be maximum (120 MW) and generation from Tekeze hydropower plant limited to peak hour loading (160 MW).the contingency case three is selected as it gives maximum voltage drop at PCC. Hence, substituting the values of sending and receiving end voltage and angle form table 4.19 for contingency case three in equation 4.25,the required reactive power at receiving end will be,

$$Q_R = \frac{216.11(225.1\cos(34.02 - 27.74) - 216.11\cos(7.39)}{298.5\sin(7.39)} = 53.1\text{MVAR}$$

Required reactive power compensation at sending end also found substituting the values of sending and receiving end voltage and angle form table 4.19 for contingency case three in equation 4.26,

$$Q_S = \frac{-225.1(216.11\cos(34.02 - 27.74) - 225.1\cos(7.39))}{298.5\sin(7.39)} = 49.32MVAR$$

For existing network there is a shunt reactor of 30 MVAR is installed at Alamata 230 kV bus bar. During load flow analysis, the shunt reactor is disconnected intentionally for contingency cases in order to provide additional reactive power supply and connected in

base cases to absorb excessive reactive generation that occur during light loading. However, there is no any capacitor installed to inject reactive power.

From the calculation, it is needed a shunt compensation of 53.1 MVAR at receiving end and 49.32 MVAR at sending end (PCC). In case of PCC, a reactive power of 33.39 MVAR can be provided by the wind generator. The rest, i.e. 15 MVAR, has to be compensated by shunt capacitor connected at PCC. Otherwise, the voltage drops to 0.98 pu.

4.8.4. Required Reactive Under Base Case

The aim of this case is to find out the maximum reactive absorption needed by the compensation device. The maximum reactive power generation from the system has occurred, if there is no any contingency. Under this condition, the generation from the wind farm is assumed only to have 0.84 MW (at cut in wind speed) and generation of Tekeze hydropower plant is 100 MW. Therefore, base case is selected. Hence, substituting the values form table 4.19 for light loading base case,

$$Q_R = \frac{242.3(244.9\cos(-0.63-(-0.75)) - 242.3\cos(7.39))}{298.5\sin(7.39)} = 24.1 \text{ MVAR}$$

At sending end

$$Q_S = \frac{-244.9(242.3\cos(-0.63-(-0.75)) - 244.9\cos(7.39))}{298.5\sin(7.39)} = 3.6 \text{ MVAR}$$

Therefore, a shunt reactor of rating 24 MVAR is needed in Alamata 230 kV bus bar and a shunt reactor of rating 3.6 MVAR at PCC. Required compensation at Alamat 230 kV bus bar can provide by the existing shunt reactor of rating 30 MVAR. Similarly, in case of PCC, required shunt reactor operation can be provided by the wind farm generator.

Now we have determined the required reactive compensation from above numerical analysis. The next step is verifying the compensation device rating. This made using load flow analysis after modelling and connecting to existing network. The result of the load flow analysis under all contingency and base cases is summarized in table 4.20. As can be seen from table 4.20, there is no any voltage violation at each bus bar.

Table 4.20.Voltage profile after compensation.

contingency	Substation name	Voltage magnitude(kV)	Angle (deg)
Base case in peak hour loading	Alamata	234.562	7.58
	Mekele	236.1	14.02
	Wind POC	239.9	13.28
	Combolcha	235.7	-0.57
	Gasheta TP	236.5	3.63
Base case in light system loading	Alamata	242.3	-0.75
	Mekele	240.84	-0.08
	Wind POC	244.87	-0.63
	Combolcha	245.2	-1.54
	Gasheta TP	243.1	-0.93
Contingency two	Alamata	229.12	6.69
	Mekele	disconnected	
	Wind POC	231.722	19.67
	Combolcha	232.1	-1.26
	Gasheta TP	232.43	3.04
Contingency three	Alamata	231.44	24.67
	Mekele	234.4	31.17
	Wind POC	225.1	34.02
	Combolcha	disconnected	
	Gasheta TP	227.1	15.91
Contingency four	Alamata	232.8	26.43
	Mekele	235.5	32.9
	Wind POC	238.8	32.18
	Combolcha	226.6	11.9
	Gasheta TP	disconnected	

Chapter 5.Conclusions, Recommendations and Future Works

5.1. Conclusion and Recommendation

In this thesis work AWF impacts on EEPCO grid system has been studied. The hourly variability of system load increased by 7 MW and by 4 MW in case of thirty minute when the wind farm connected to the system. The system operator needs to take into account such variability increments in their production scheduling.

In addition to variability impact, predictability impact also studied by developing a wind power forecasting model. Different models have been developed and the one with best forecast accuracy selected on the basis of MAE and compared with persistence model considering as a base model.

SARIM (2, 0, 23) $(1, 1, 2)_{24}$ has MAE of 13.68 % (as percentage of installed capacity of AWF) for day ahead forecast. In practice, MAE of a typical wind farm is between 10 – 15% of installed capacity.

Estimation of energy output using statistical method has been made. Yearly energy output of AWF is 362 GWH. For onshore wind farm, the capacity factor varies from 0.2 to 0.4. The capacity factor of AWF is 0.34 which is near to 0.4.

In final section of this thesis work, the stability impacts of AWF on EEPCO's grid system analyzed under steady state condition performing PV and QV analysis using PSS/E as a simulation software. Before making PV and QV analysis, AWF is modeled and represented by single turbine equivalent circuit. For practical wind farm there is an expected active power loss of less than 3% of installed capacity of the wind farm. Single turbine representation of AWF has a total loss of 2.83% which below the above limit (that is, 3%). Therefore, the model can be used to make steady state voltage stability study as it is gives nearly a similar result with practical system.

As per the result of the stability study, there is a steady state voltage stability impact under contingency cases. However, in base case there is no any stability impact. Along with the stability analysis, possible solutions have been suggested and discussed.

The first solution is reinforcing the network. Here, reactive power compensation at Alamata 230 kV bus bar has been considered. First required reactive power has been determined analytically and reactive power compensation with rating of 62 MVA connected to see that voltage stability due to contingency cases can be avoided. As per the analysis of load flow result voltage stability problem can be avoided.

However, such solutions will take time to be implemented. So that, another alternative solution by managing the bottlenecks of transmission line, has been considered. By coordinating power output of Tekeze hydropower plant and AWF, there is a possibility of controlling voltage stability problems. However, managing transmission line capacity will be more economical; if generation production scheduling process accounts wind power output forecasting.

5.2. Future Work

Some suggestions for further works that can be used as input or idea to formulate new projects for master thesis are dynamic stability and power quality studies. Following this thesis work, dynamic stability studies have to be studied and investigated in detail. Because, it enables us to understand well the performance of the wind farm under transient conditions and verify the work that has been made so far in this thesis work.

References

[1] Thomas Ackermann, "Wind Power in Power Systems", John Wiley & Sons, Ltd, 2005.

[2] Prabha Kundur, "Power System Stability and Control", McGraw-Hill, 1994.

[3] Jonathan D.Cryer, Kung-Sik Chan, "Time series analysis with applications in R", second edition

[4] Robert Yaffee with Monnie McGee," Introduction to time series analysis and forecasting with application of SAS and SPSS", Academic Press, Inc

[5] Chris Chatfield, "The analysis of time series an introduction ", fifth edition.

[6] Piter J.Brockwell, Richard A. Davis," Introduction to time series analysis and forecasting", second edition

[7] John Buglear," Statics Means Business - a guide to business statistics ", Elsevier Butterworth-Heinemann

[8] T.T Soong," fundamentals of probability and statistics for engineers", John Wiley & Sons Ltd

[9] Sanford Bolton; Charles Bon, "Pharmaceutical statistics practical and clinical applications", Marcel Dekker, Inc, fourth editions.

[10] J. F. Manwell, J.G. McGowan,"Wind energy explained theory, design and application", A.L.Rogers, John Wiley & Sons Ltd.

[11] Sathyajith Mathew," wind energy fundamentals, resources analysis and economics", Springer

[12] Gilbert M. Masters," Renewable and efficient electric power system", A John Wiley & Sons, Inc.

[13] "Wind Farm Power System Model Development", E. Muljadi C.P. Butterfield, World Renewable Energy Congress VIII Denver, Colorado August 29 – September 3, 2004.

[14]. E.Muljadi, S.Pasupulati, A.Ellis and D. Kosterov, "Method of Equivalencing for a Large Wind Power Plant with Multiple Turbine representation", IEEE Power Engineering Society General Meeting Pittsburgh, Pennsylvania July 20–24, 2008.

[15] Jan Machowski,Janusz W. Bialek,James R. Bumby ,“ Power system dynamics: stability and control”, John Wiley & Sons Ltd.,second edition

[16] Thierry Van Cutsem, Costas Vournas,” Voltage stability of electrical power system”

[18] Nayeem Rahmat Ullah, Kankar Bhattacharya, Torbj¨orn Thiringer,”Wind farms as reactive power ancillary service providers—Technical and Economic Issues”.

[19] Deutsche Gesellschaft für Technische Zusammenarbeit (GTZ) GmbH,”Feasibility study for wind park development in Ethiopia and capacity building –Ashegoda wind park site final report “

[20] Vergnet group wind generator brochure.

[21] “PSS/E manual, version 31”

[22] J. G. Slootweg,” Wind Power, Modeling and Impact on Power System Dynamics”. PhD thesis, Delft University of Technology, The Netherlands, 2003.

[23] J. Matevosyan,”Wind power integration in power systems with transmission bottlenecks”, PhD thesis, Royal Institute of Technology, Sweden, 2006.

[24] “XLPE User’s guide”, ABB Power Technologies AB, www.abb.com/cables

[25] Günter G. Seip,” Electrical installations hand book (Siemens)”, John Willey & Sons, third edition, 2000.

Appendix A. Micro Sitting of First Phase of AWF Project.

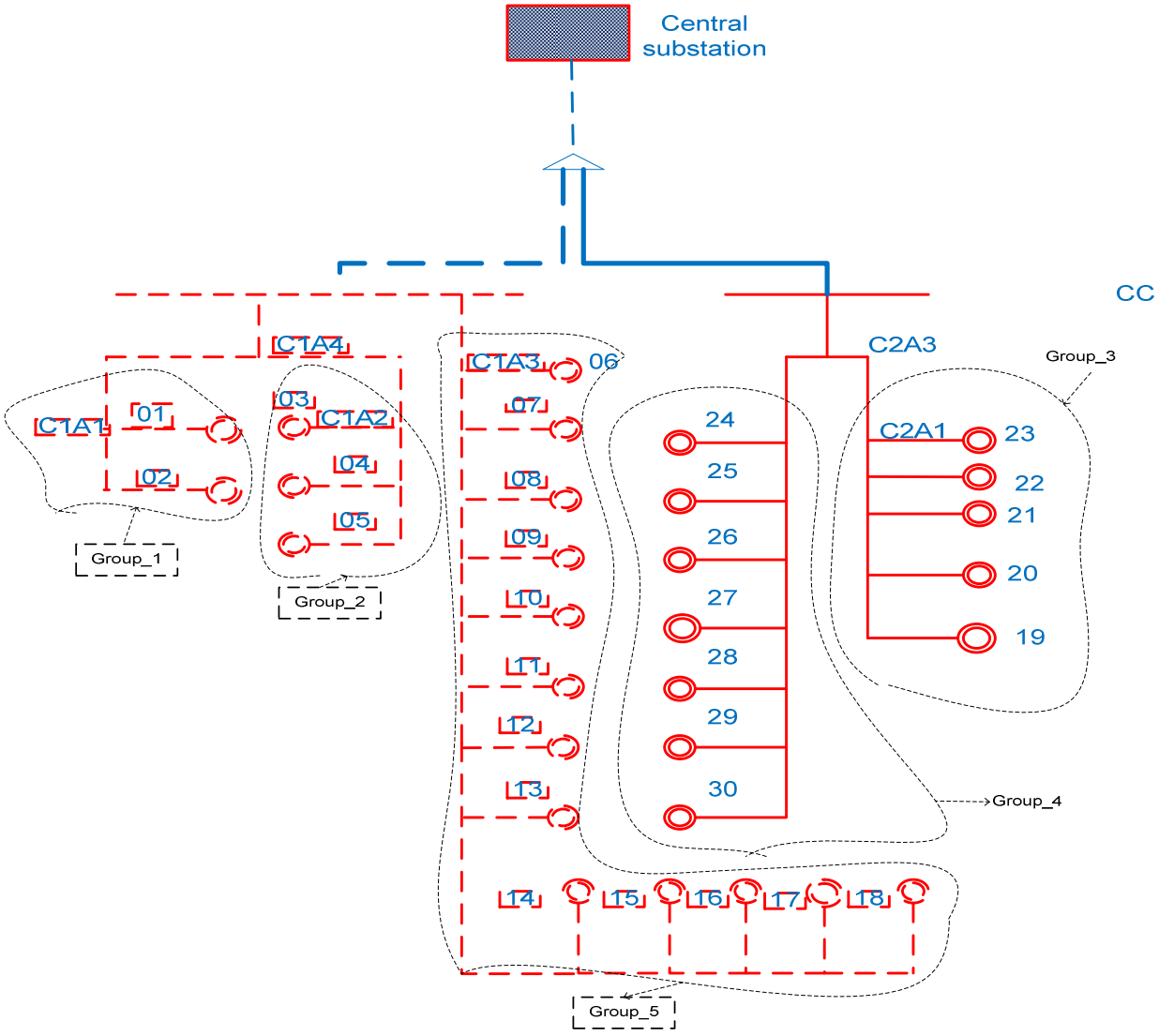

Figure A 1.Micrositting of cluster one and two

Appendix B. AWF Custer Two Parameters.

Table B. 1.Branch impedance of cluster one and two

Branches		Branch flow(MW)	Length(m)	R(pu / kM)	X(pu/ kM)	Z (pu/ kM)
from	To					
1	2	1	265	0.009	0.007	0.012
1	C1A4	2	211	0.049	0.026	0.055
3	4	2	262	0.009	0.007	0.012
3	C1A4	3	179	0.049	0.026	0.055
4	5	1	247	0.009	0.007	0.011
6	CC	13	731	0.049	0.026	0.055
6	7	12	260	0.009	0.007	0.012
7	8	11	259	0.009	0.007	0.011
8	9	10	260	0.009	0.007	0.012
9	10	9	246	0.009	0.007	0.011
10	11	8	258	0.009	0.007	0.011
11	12	7	260	0.009	0.007	0.012
12	13	6	263	0.009	0.007	0.012
13	14	5	651	0.023	0.018	0.029
14	15	4	268	0.009	0.007	0.012
15	16	3	348	0.012	0.010	0.015
16	17	2	271	0.009	0.008	0.012
17	18	1	269	0.009	0.007	0.012
19	20	1	271	0.009	0.008	0.012
20	21	2	271	0.009	0.008	0.012
21	22	3	271	0.009	0.008	0.012
22	23	4	271	0.009	0.008	0.012
23	C2A3	5	843	0.049	0.026	0.055
24	C3	7	1005	0.049	0.026	0.055
24	25	6	271	0.009	0.008	0.012
25	26	5	270	0.009	0.007	0.012
26	27	4	271	0.009	0.008	0.012
7	28	3	284	0.010	0.008	0.013
28	29	2	894	0.031	0.025	0.040
29	30	1	348	0.012	0.010	0.015

Appendix C. Summary of Equivalence Impedance of AWF.

The equivalence impedance of Ashegoda wind farm pad mounted transformer and collector circuit impedance is shown in table C.1 and table C.2 respectively. The values are given in pu at base value of S_B=100 MVA and base voltage of V_B=33 kV.

Table C. 1.Summary of Pad mounted transformer impedance

Cluster	No of transformers	Total power (MW)	Pad mounted transformer	
			Req (pu)	Xeq (pu)
1	12	12	0.0019	0.0084
2	18	18	0.000277	0.00124
3	23	23	0.000217	0.0011
4	21	21	0.00024	0.0011
5	25	25	0.0002	0.0019
6	21	21	0.00024	0.0011

Table C. 2.Summary of all collector circuit impedances AWF

Cluster	No of turbine	Total power(MW)	Collector Impedance	
			Req (pu)	Xeq (pu)
1	12	12	0.0056	0.0042
2	18	18	0.0013	0.0007
3	23	23	0.0023	0.002
4	21	21	0.00062	0.0005
5	25	25	0.00053	0.00042
6	21	21	0.00044	0.00045

Appendix D. Single Turbine Representation of AWF.

The single turbine representation of the wind farm with base power of S_B =100 MVA and base voltage of V_B=33 kV for collector circuit and pad mounted transformer.

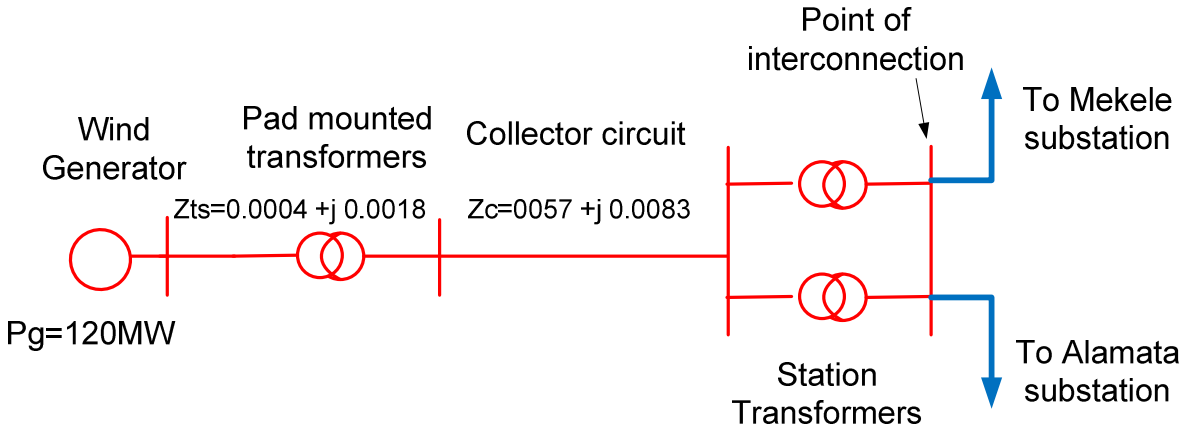

Figure D 1. Single turbine representation of AWF.

Appendix E. Capability curve of AWF Wind Turbine Generator

The reactive power capability curve of wind generator that is going to be installed at Ashegoda wind farm has 0.283 MVAR at rated value (at 1 MW) and power factor of +/- 0.96 as shown below in figure E.1.

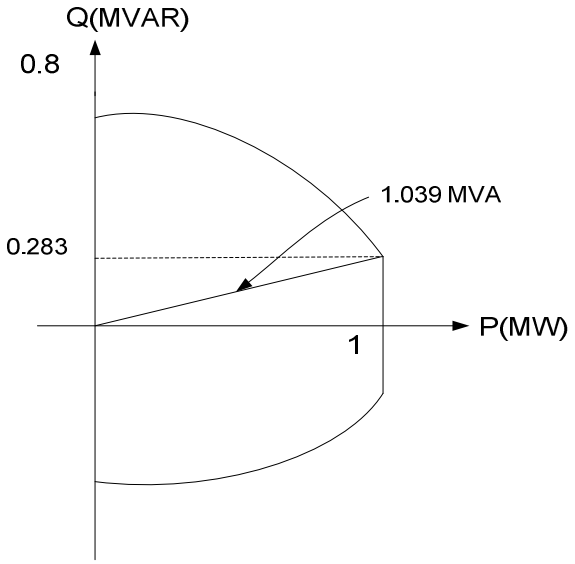

Figure E 1.Capability curve of AWF wind turbine generator [26].

Declaration

I, the undersigned, declare that this thesis work is my original work, has not been presented for a degree in this or any other universities, and all sources of materials used for the thesis work have been fully acknowledged.

Name: Hiwot Eshetu Signature: _____

Place: Addis Ababa

Date of submission:

This thesis has been submitted for examination with my approval as a university advisor.

Dr.-Ing. Getachew Biru Signature: _____
Advisor's Name

Dr.-Ing. Fekadu Shewarega Signature: _____
Advisor's Name